A REVIEW OF GLOBAL TERRESTRIAL EVAPOTRANSPIRATION: OBSERVATION, MODELING, CLIMATOLOGY, AND CLIMATIC VARIABILITY

Kaicun Wang[1] and Robert E. Dickinson[2]

Received 6 September 2011; revised 20 March 2012; accepted 21 March 2012; published 24 May 2012.

[1] This review surveys the basic theories, observational methods, satellite algorithms, and land surface models for terrestrial evapotranspiration, E (or λE, i.e., latent heat flux), including a long-term variability and trends perspective. The basic theories used to estimate E are the Monin-Obukhov similarity theory (MOST), the Bowen ratio method, and the Penman-Monteith equation. The latter two theoretical expressions combine MOST with surface energy balance. Estimates of E can differ substantially between these three approaches because of their use of different input data. Surface and satellite-based measurement systems can provide accurate estimates of diurnal, daily, and annual variability of E. But their estimation of longer time variability is largely not established. A reasonable estimate of E as a global mean can be obtained from a surface water budget method, but its regional distribution is still rather uncertain. Current land surface models provide widely different ratios of the transpiration by vegetation to total E. This source of uncertainty therefore limits the capability of models to provide the sensitivities of E to precipitation deficits and land cover change.

Citation: Wang, K., and R. E. Dickinson (2012), A review of global terrestrial evapotranspiration: Observation, modeling, climatology, and climatic variability, *Rev. Geophys.*, *50*, RG2005, doi:10.1029/2011RG000373.

1. INTRODUCTION

[2] Terrestrial evapotranspiration, E, is the water transferred from the land surface to the atmosphere. This water exchange usually involves a phase change of water from liquid (or ice) to gas, which absorbs energy and cools the land surface. The latent heat accompanying E is λE, where λ is the latent heat of vaporization. This review uses E or λE interchangeably depending on whether water or energy flux is the primary consideration. These terms are required by short-term numerical weather predication models and longer-term climate simulations and for diagnoses of climate change. In such models, E is generally parameterized as a sum of soil evaporation, vegetation evaporation, and vegetation transpiration; the latter is a process that couples with carbon uptake through photosynthesis.

[3] The influence of λE on atmospheric processes [*Pielke et al.*, 1998] has been frequently recognized [*Kanemasu et al.*, 1992; *Rind et al.*, 1992] and has been estimated using land surface models (LSMs) [*Sellers et al.*, 1997]. The increase in heat wave variability in central and eastern Europe has also been attributed to changes in E [*Seneviratne et al.*, 2006]. Summer precipitation (P) over Europe has been linked with local E [*Zveryaev and Allan*, 2010]. Land surface feedbacks have also been found to increase Sahel rainfall variability both on interannual and interdecadal time scales [*Zeng et al.*, 1999].

[4] Provided that the energy storage by the canopy is negligible, λE can be calculated as a residual of the surface net radiation (R_n), the sensible heat flux (H), and ground heat flux (G),

$$\lambda E = R_n - H - G, \quad (1)$$

where R_n is determined from the sum of incident downward and upward shortwave and longwave radiation,

$$R_n = R_s - R_{su} + R_{ld} - R_{lu}, \quad (2)$$

[1]State Key Laboratory of Earth Surface Processes and Resource Ecology, College of Global Change and Earth System Science, Beijing Normal University, Beijing, China.
[2]Department of Geological Sciences, University of Texas at Austin, Austin, Texas, USA.

Corresponding author: K. Wang, State Key Laboratory of Earth Surface Processes and Resource Ecology, College of Global Change and Earth System Science, Beijing Normal University, 19 Xinjiekouwai St., Beijing 86-100875, China. (kcwang@bnu.edu.cn)

8755-1209/12/2011RG000373
Paper number 2011RG000373

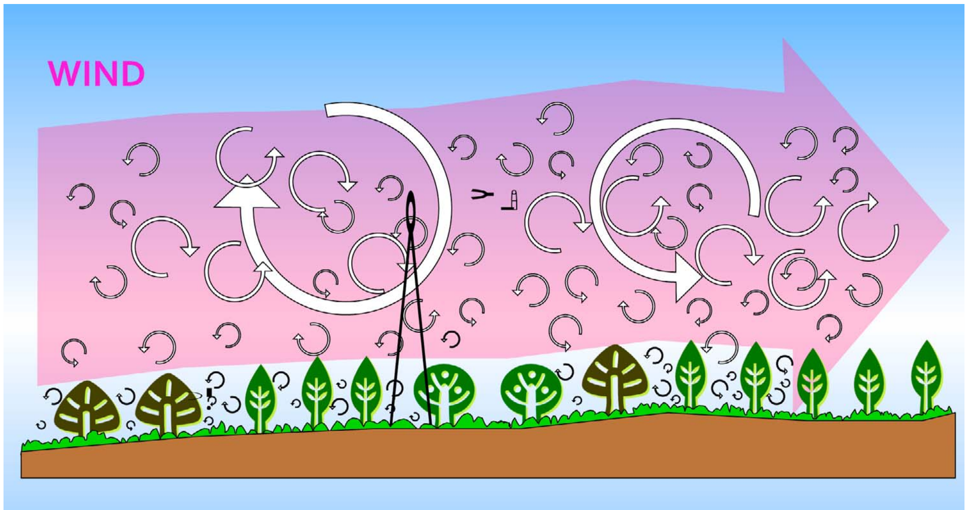

Figure 1. Airflow can be imagined as a horizontal flow of numerous rotating eddies, that is, turbulent vortices of various sizes, with each eddy having horizontal and vertical components. The situation looks chaotic, but vertical movement of the components can be measured from a tower. From http://www.instrumentalia.com.ar/pdf/Invernadero.pdf. Reprinted with permission.

and where R_s is the surface incident solar radiation, R_{su} is the surface reflected solar radiation, and R_{ld} and R_{lu} are the surface downward and upward longwave radiation.

[5] The energy required for evaporating a given mass of liquid water corresponds to approximately 600 times the energy required to increase its temperature by 1 K and to 2400 times the energy required to increase the temperature of a corresponding mass of air by 1 K [*Seneviratne et al.*, 2010]. The cooling effect of λE is so large that the Northern Hemisphere would be 15°–25°C warmer [*Shukla and Mintz*, 1982] if terrestrial λE were assumed to be zero.

[6] On average, terrestrial λE uses approximately three fifths of R_n, with estimates from different models varying from 48% to 88% [*Trenberth et al.*, 2009]. It is a major component not only of the surface energy balance but also of the terrestrial water cycle. From the latter, E can be estimated from surface water balance at basin or continental scale by

$$E = P - Q - dw/dt, \tag{3}$$

where P is precipitation, Q is river discharge, and dw/dt is the change of terrestrial water storage. On annual time scales, the storage term can be neglected so that E can be derived from observation of P and Q [*Hobbins et al.*, 2004; *Teuling et al.*, 2009]. It accounts for about two thirds of the average 700 mm/yr of P that falls over the land [*Chahine*, 1992; *Oki and Kanae*, 2006]. The other one third of P discharges into oceans, compensating for the water vapor transferred from ocean to the land through the atmosphere [*Jackson et al.*, 2001].

[7] Water is transferred from the land surface to the atmosphere through turbulence, which is several orders of magnitude more effective at transporting such quantities than molecular diffusivity. Turbulence can be viewed as consisting of many different size eddies superimposed on each other (Figure 1). Although long recognized, our understanding of turbulence is still advancing [*Lumley and Yaglom*, 2001]. Monin-Obukhov similarity theory (MOST) was developed in the 1950s [*Monin and Obukhov*, 1954]. It estimates λE and sensible heat fluxes (H) from measurements of near-surface winds, temperature, and humidity by relating turbulence fluxes to gradients of mean wind, temperature, and humidity (e.g., as Ohm's law relates current to voltage).

[8] Various aspects of this topic have been reviewed many times. The impact of land cover and land use change on cumulus convective rainfall through λE and H was reviewed [*Pielke*, 2001] and for the West African Sahel region [*Nicholson*, 2000]. The impacts of global warming and the elevated greenhouse gases on hydrological cycle were reviewed [*Gleick*, 1989; *Huntington*, 2006]. Most such review studies depend on model simulations for lack of reliable long-term observations, in particular, of λE. The modeling of λE and H in regional and global models has been summarized [*Brutsaert*, 1999; *Parlange et al.*, 1995; *Sellers et al.*, 1997]. Models on the effects of vegetation and its heterogeneity were reviewed [*Arora*, 2002; *Giorgi and Avissar*, 1997]. The development of λE in the past 30–35 years has been well documented [*Shuttleworth*, 2007]. *Shuttleworth* [2007] reviewed the instruments and techniques to measure the diurnal variation of λE and how to use the understanding of λE for study of land surface processes.

[9] The present review is distinguished from these past reviews by taking a long-term variability and trends perspective to survey the basic theories, observational methods, satellite algorithms, and land surface models of λE. It focuses on the process of water evaporating from land surfaces. What happens to water vapor molecules after they evaporate from the surface and where will they precipitate are addressed elsewhere [*Dominguez and Kumar*, 2008; *Dominguez et al.*, 2008; *Eltahir and Bras*, 1996], as well as the impact of water vapor on convection and dynamics of climate changes [*Held and Soden*, 2000; *Schneider et al.*,

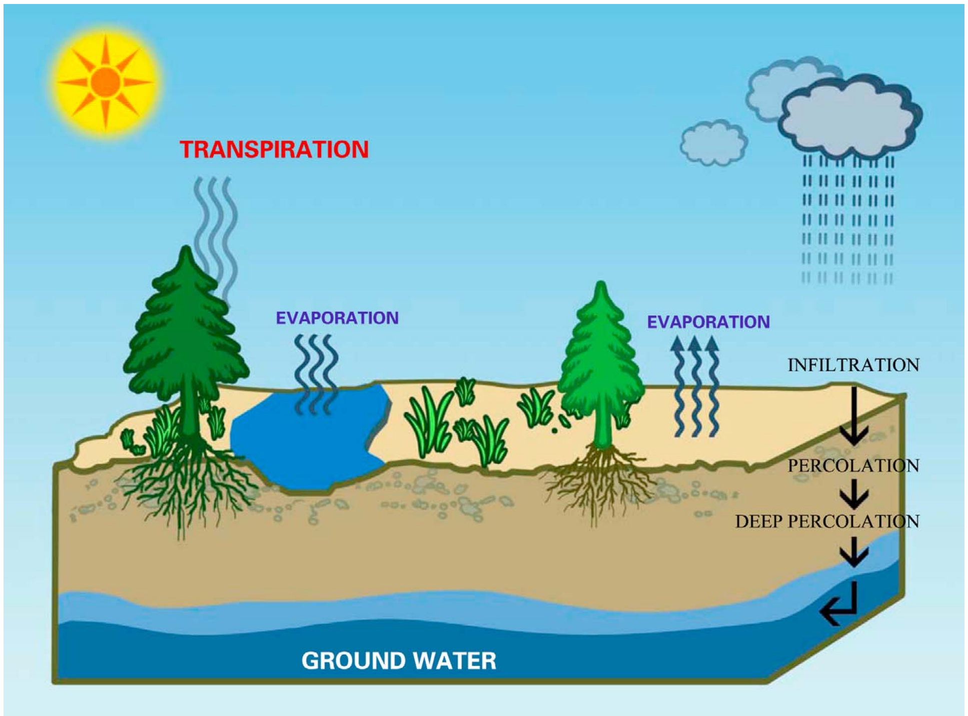

Figure 2. Evapotranspiration includes transpiration from dry leaves and evaporation from water, wet leaves, and soil. Tree transpiration extracts soil water through their root system.

2010; *Sherwood et al.*, 2010], and the monitoring of land surface water and floods from space [*Alsdorf et al.*, 2007; *Schumann et al.*, 2009].

[10] Section 2 examines the basic theories of E and their assumptions. Section 3 discusses the advantages and disadvantages of the current observational methods. The methods to partition total E are also highlighted for their importance in evaluation of the climatic variability of satellite retrievals and LSM simulations. Section 4 provides a survey of current understanding of the factors that control variability of E over different time scales. This understanding and its underlying theory provide a basis for satellite retrieval and land surface modeling of E. Section 5 focuses on how this basic theory and the understanding can be used to relate satellite-derived land surface variables to E. As the development of LSMs has been previously reviewed, section 6 focuses on how they have been evaluated and what the sources are of uncertainty in existing evaluations. The climatology and climatic variability of E from observations, satellite retrievals, and land surface modeling are explored in sections 7 and 8. Section 9 highlights topics that require additional research.

2. BASIC THEORIES OF λE

[11] Turbulence, the gustiness superimposed on mean wind, can be visualized as consisting of irregular swirls of air motion called eddies (Figure 1), which are of many different sizes superimposed on each other. Turbulent eddies have horizontal spatial scales that are up to 1–2 orders of magnitude larger than their vertical dimension [*Brutsaert*, 1999]. Thermals of rising, warmer air caused by solar heating of the ground during sunny days provide large eddies. Boundary layer eddies range in size up to the depth of the boundary layer, i.e., 0.1 km to 3 km in diameter.

[12] Water is transferred both by aerodynamic and by biological processes (Figure 2). Transpiration, the evaporation of water in the vascular system of plants with loss through leaf stomata, is overall the largest contributor to total E [*Dirmeyer et al.*, 2006; *Lawrence et al.*, 2007] and is closely coupled to leaf carbon uptake through leaf conductance [*Niyogi et al.*, 2009]. In addition to stomatal conductance, mesophyll conductance could also contribute to the regulation of photosynthesis and transpiration during periods of water stress [*Keenan et al.*, 2010; *Vesala et al.*, 1996]. This section considers MOST and the Penman-Montheith equation. The Bowen ratio method is discussed in section 3.2 as an observational technique based on MOST.

2.1. Monin-Obukhov Similarity Theory (MOST)

[13] Within the constant-flux layer, turbulent fluxes are assumed to be height-independent (about 10% of the fully developed daytime atmospheric boundary layer, i.e., 100 m above the roughness layer). MOST is designed for use with meteorological data. It relates turbulent fluxes to the differences of mean temperature and humidity at two levels in the constant-flux layer through its universal stability functions [*Businger et al.*, 1971; *Dyer*, 1974]. The estimation of λE and H from time-averaged mean variables in the constant-flux layer is called the flux profile method. MOST was the starting point for modern micrometeorology, including the development of new measuring devices and the execution of

several important experiments [*Foken*, 2006; *Monin and Obukhov*, 1954].

[14] MOST is valid for horizontally homogeneous and stationary surface layers. Under ideal conditions, this theory has errors of about 10–20% [*Foken*, 2006; *Högström and Bergström*, 1996]. It assumes steady, horizontally homogeneous flow for averaging times from 10 min to about an hour [*Monin and Obukhov*, 1954], not always satisfied because of the large ratio of vertical to horizontal gradients of the observed mean scalar concentrations and wind speed (Figure 1).

[15] The gradients of temperature and humidity over the surface can be very small, especially for forest and irrigated croplands and grasslands. After the development of the similarity theory for the constant-flux layer in the 1950s, much experimental effort went into determining its universal functions. Fluxes can be obtained directly by eddy covariance (EC) measurements, i.e., by the average of the product of fluctuating vertical velocity and the transported quantity, e.g., humidity. The widely used universal functions were based on EC observations from the Kansas experiment [*Businger et al.*, 1971]. The value of the von Kármán constant of 0.35 found by the Kansas group [*Businger et al.*, 1971] was questioned because of flow distortion problems from the tower, as well as over-speeding of cup anemometers, and the unstable performance of the phase shift sonic anemometers [*Wieringa*, 1980]. Improved data have resulted in a reformulation of the universal functions [*Högström*, 1988].

[16] Since the late 1980s, it has been realized that the sum of H and λE as measured by the EC method has been generally less than available energy, i.e., the turbulent fluxes have had a closure problem [*Foken*, 2008] (see section 3.1). This difficulty indicates that previous MOST universal functions may underestimate the H and λE in using the profile flux methods by approximately 30% in comparison with the energy balance Bowen ratio (BR) method [*Malek*, 1993] (see section 3.2). The BR method uses equation (1) evaluating the ratio BR to estimate H and λE. The BR is obtained from the MOST theory and measured temperature and moisture differences and with the usual assumption that the MOST coefficients for H and λE are the same.

[17] The universal stability functions are not valid in the roughness sublayer [*Sun et al.*, 1999] of vegetated surfaces so that the profile equations must be modified by using a universal function depending on the thickness of this roughness sublayer [*Garratt et al.*, 1996]. For tall vegetation or an urban area, the roughness sublayer may be tens of meters thick while the constant-flux layer, for which the similarity theory is valid, may be much shallower. Such a difference in scale has important implications for the use of satellite-derived land surface temperature (T_s) to estimate λE because T_s is the temperature of the surface skin in the roughness sublayer (see section 5.1).

2.2. Penman-Monteith Equation

[18] The Penman and Penman-Monteith equations were developed to use surface radiation, temperature, and humidity data to estimate E. The Penman equation describes evaporation from an open water surface or from short vegetation [*Penman*, 1948]. It requires T_a, wind speed (WS), relative humidity (RH), R_n, and G. With canopy resistance as needed for vegetated surfaces, it becomes the Penman-Monteith equation [*Monteith*, 1965]. The Penman equation can be viewed as combining MOST with surface energy balance (see http://biomet.ucdavis.edu/Evapotranspiration/PMDerivation/PMD.htm) with values at the surface being one of the levels for MOST using the aerodynamic resistances for heat r_h and moisture r_v that are inferred from MOST,

$$H = \rho C_p \cdot \frac{T_o - T_a}{r_h}, \tag{4}$$

$$\lambda E = \frac{\rho C_p}{\gamma^*} \cdot \frac{e_s(T_o) - e}{r_h}, \tag{5}$$

where ρ is the density of air, C_p is the specific heat of air, and $\gamma^* = (r_v/r_h) \cdot \gamma$, where γ is the psychometric constant. T_o is the aerodynamic air temperature at the surface, T_a is the air temperature at the reference level, and r_h is the aerodynamic resistance to heat transfer from surface to air.

[19] If $\Delta = de_s/dT$ is the derivative of the saturated vapor pressure (e_s) with respect to T_a, then a first-order approximation of $e_s(T_o)$ is

$$e_s(T_o) = e_s(T_a) + \Delta \cdot (T_o - T_a). \tag{6}$$

Substituting equations (6), (1), and (4) into equation (5), and rearranging the resulting terms of equation (5), we have

$$\lambda E = \frac{\Delta \cdot (R_n - G) + \rho C_p \cdot [e_s(T_a) - e]/r_h}{\Delta + \gamma^*}. \tag{7}$$

If the surface can be regarded as a "big leaf" [*Deardorff*, 1978], r_v can be separated into the canopy resistance (r_c) and the aerodynamic resistance (r_h),

$$\gamma^* = [(r_c + r_h)/r_h] \cdot \gamma = (1 + r_c/r_h) \cdot \gamma, \tag{8}$$

and then we have

$$\lambda E = \frac{\Delta \cdot (R_n - G) + \rho C_p \cdot [e_s(T_a) - e]/r_h}{\Delta + (1 + r_c/r_h) \cdot \gamma}. \tag{9}$$

Equation (9), the Penman-Monteith equation [*Monteith*, 1965], is widely regarded as an accurate expression [*Allen et al.*, 1998]. If $r_v = r_h$, then $\gamma^* = \gamma$, and equation (7) reverts back to the Penman equation. The factor $[e_s(T_a) - e]$ in equation (7) or (9) is called the water vapor pressure deficit (VPD):

$$\begin{aligned} e_s(T_a) - e = e_s(T_a) - e_s(T_a) * RH/100 = e_s(T_a)(1 - RH/100) \\ = VPD. \end{aligned} \tag{10}$$

The factors Δ and γ in equations (7) and (9) depend solely on T_a at a given location [*K. Wang et al.*, 2006]. The Penman-Monteith equation requires a vegetation specific parameter, i.e., r_c [*Beven*, 1979], which is difficult to measure directly. Therefore, it has commonly been used as a diagnostic equation to estimate this term [*Alves and Pereira*, 2000].

[20] The term λE is most sensitive to r_c for forests [*Rana and Katerji*, 1998]. In well watered conditions, r_c is sensitive to R_n variations in the case of low crops or grasslands and is sensitive to VPD for both medium and tall crops, while in water-stressed conditions it is sensitive to soil moisture (θ).

[21] Canopy resistance r_c can be modeled by scaling up from the leaf stomatal resistance r_s. Two widely accepted empirical models of r_s have been developed to capture the response of plant stomata to the environmental variables. The first is the Jarvis-Stewart equation, which describes the response of r_s to environmental and biological controls including VPD, T_a, the solar radiation incident on the canopy (R_s), and the soil moisture (θ) in the upper soil where the plant roots are found [*Jarvis*, 1976; *Stewart*, 1988],

$$g_s = \frac{1}{r_s} = g_0 \cdot f_D(VPD) \cdot f_T(T_a) \cdot f_s(R_s) \cdot f_w(\theta), \qquad (11)$$

where g_0 is a plant functional type dependent maximum value of stomatal conductance, and f_D, f_T, f_s, f_w (all in the range of 0–1) are the stress factors associated with VPD, T_a, R_s, and θ, respectively. Equation (11) may underestimate g_s when RH is high because it correlates g_s linearly to RH [*Wang et al.*, 2009], and a nonlinear function of RH or VPD may reduce the bias [*Leuning*, 1995; *Wang et al.*, 2009].

[22] The second model of r_s is the "Ball-Berry" equation [*Ball et al.*, 1987],

$$g_s = \frac{1}{r_s} = m\frac{A}{C_s}\frac{e}{e_s}P_{atm} + b, \qquad (12)$$

where m is a plant functional type and θ dependent parameter, A is carbon flux into the leaf, C_s is the CO_2 partial pressure at the leaf surface, e is the water vapor pressure at the leaf surface, e_s is the saturation vapor pressure inside the leaf, P_{atm} is the atmospheric pressure, and b is the minimum stomatal conductance when $A = 0$. Net carbon assimilation A can be estimated from

$$A = \min(W_c, W_j, W_e), \qquad (13)$$

where W_c, W_j, and W_e are functions expressing the assimilation rates limited by Rubisco enzyme, light, and export capacity, respectively, for C3 and C4 plants [*Collatz et al.*, 1991; *Sellers et al.*, 1996a, 1996b]. These W functions all depend on plant functional type, leaf temperature, θ, leaf nitrogen, and internal carbon dioxide concentrations, while W_j also depends on leaf level light intensity [*Dickinson et al.*, 2002].

[23] Although the above two models of r_s (equations (11) and (12)) use similar environmental variables [*Zhao et al.*, 2010a], they can be substantially different in value [*Lawrence and Chase*, 2009; *Niyogi and Raman*, 1997] because of their parameterization of environmental stress factors, especially soil water deficit and maximum conductance [*Dickinson et al.*, 1991; *Shuttleworth*, 2007]. The θ required by r_s parameterizations is unavailable at the regional or global scale [*Dirmeyer et al.*, 2004, 2006; *Entin et al.*, 1999; *Gao and Dirmeyer*, 2006; *Schaake et al.*, 2004].

[24] Simplifications of the Penman-Monteith equation have therefore been developed, in particular, that of Priestley and Taylor [*Priestley and Taylor*, 1972],

$$\lambda E = \alpha\frac{\Delta}{\Delta + \gamma} \cdot (R_n - G), \qquad (14)$$

where α, the so-called Priestley-Taylor parameter, is typically of the order of 1.2–1.3 under water unstressed conditions [*Bailey and Davies*, 1981; *Culf*, 1994; *McNaughton and Spriggs*, 1986] but can range from 1.0 to 1.5 [*Brutsaert and Chen*, 1995; *Chen and Brutsaert*, 1995; *Singh and Taillefer*, 1986] and vary with θ limitations, i.e., decreasing with θ [*Burba and Verma*, 2005; *Detto et al.*, 2006; *Granier et al.*, 2007; *Guo et al.*, 2006; *Mu et al.*, 2007b; *Phillips et al.*, 2009]. Applications of the Priestley-Taylor equation to water stressed conditions have assumed α to be a linear function of the θ in the rooting zone [*Fisher et al.*, 2005; *Koster and Suarez*, 1999]. It does not consider explicitly the impact of VPD and r_c.

3. OBSERVATIONS OF *E*

[25] Observational and estimation methods used for E in agricultural research under a Mediterranean climate have been reviewed [*Rana and Katerji*, 2000]. Measurement methods available for E have been reviewed [*Shuttleworth*, 2007; *Verstraeten et al.*, 2008], including wetlands [*Drexler et al.*, 2004]. The present paper is not intended to be an exhaustive and complete review of all the existing E methods, but rather to have a focus on the methods that can be used to provide long-term observations (see Table 1).

[26] The Bowen ratio (BR) and the eddy covariance (EC) techniques provide measurements of λE over a diurnal cycle. They are well established and widely used for continuous measurement projects, such as the FLUXNET network [*Baldocchi et al.*, 2001] and the Atmospheric Radiation Measurement (ARM) project (http://www.arm.gov/). Values of E can be estimated by measuring and balancing all the other water budget components of a lysimeter container [*World Meteorological Organization* (*WMO*), 2008]. Such lysimeter measurements can only represent a scale of several square meters, but the footprints of EC and BR measurements of λE are much larger (Table 1). Scintillometers supply H and λE over a scale from hundreds of meters to kilometers [*DeBruin*, 2009; *Moene et al.*, 2009; *Solignac et al.*, 2009].

[27] On an even larger scale, such as that of a river basin, region, or continent, E can also be estimated from the surface water budget or atmospheric water balance. The surface water budget method provides a robust estimate for multiyear averaged E at regional or global scale. However, this estimation highly depends on the quality of precipitation and streamflow observations. Furthermore, its accuracy is less when used for a finer spatial or temporal scale, such as for monthly estimates.

TABLE 1. Summary of λE Observation and Estimate Methods

Method	Temporal Scale	Spatial Scale	Advantages	Disadvantages
Eddy covariance	half hour to yearly	hundreds of meters depending on measurement height above canopy layer and wind speed	direct measurement of turbulence fluxes (λE and H) and independent observation	energy closure problem; gap in bad weather and other conditions
Bowen ratio	half hour to yearly	hundreds of meters depending on measurement height above canopy layer and wind speed	energy is balanced	diffusivity for water and heat is assumed to be equal; energy balance is assumed (energy components and G are point measurements, and fluxes (λE and H) have a large footprint)
Lysimeter	half hour to yearly	point measurement	direct observation of λE	environment is disturbed
Scintillometer	half hour to yearly	tens of meters to tens of kilometers	capture H and λE over large scale with known footprints	depends on MOST[a] universal functions
Surface water balance	monthly to yearly	hundreds to thousands of kilometers	direct estimate; regional and global estimation can be made	accuracy can only be guaranteed at low temporal (multiyear average) and spatial resolution
Atmospheric water balance	monthly to yearly	hundreds to thousands of kilometers	regional and global estimation can be made	low accuracy

[a]Monin-Obukhov similarity theory.

3.1. Eddy Covariance (EC) Method

[28] The EC technique measures H and λE from the covariance of the heat and moisture fluxes, respectively, with vertical velocity using rapid response sensors at frequencies typically equal to or greater than 10 Hz. Scientists from the Commonwealth Scientific and Industrial Research Organisation (CSIRO) in Australia first applied this approach in the 1950s [*Garratt and Hicks*, 1990; *Högström and Bergström*, 1996], and it has been regarded as the best method to directly measure H and λE and been used for many important boundary layer experiments [*Aubinet et al.*, 1999; *Baldocchi et al.*, 1996, 2001; *Wilson et al.*, 2002].

[29] The instruments for EC include a fast-response, three-dimensional wind sensor (sonic anemometer) to obtain the orthogonal wind components and the speed of sound (used to derive T_a) and an infrared gas analyzer to obtain the water vapor density and the CO_2 concentration. The typical error of its λE is about 5–20% or 20–50 W m^{-2} [*Foken*, 2008; *Vickers et al.*, 2010]. The technique is mathematically complex and requires significant care in setting up and processing data. To date, there is no uniform terminology or single methodology for EC measurement, but much effort has been made by the flux measurement networks to unify their various approaches [*Göckede et al.*, 2008; *Mauder et al.*, 2008].

[30] EC systems have been deployed over the global FLUXNET network, which includes more than 500 sites worldwide (Figure 3), with excellent coverage in Europe and North America [*Baldocchi*, 2008]. The FLUXNET data set offers for the first time several valuable observations of land hydrological variables.

3.1.1. Energy Closure Ratio of the EC Method

[31] Although EC measurements are relatively accurate for a variety of common situations, they can have inaccuracies and/or ambiguous interpretation of their values, and improvements are still needed [*Mahrt*, 2010]. Especially problematic is the energy closure ratio $R = (H + \lambda E)/(R_n - G)$ that has values of about 0.8 averaged from more than 50 sites in Europe and North America [*Wilson et al.*, 2002] (see also Figure 4).

[32] Several reasons for this energy closure problem have been reported and corrected [*Foken*, 2008; *Foken et al.*, 2006]. The energy storage due to photosynthesis and release by plant and soil respiration are generally estimated to be less than a few percent of R_n [*Meyers and Hollinger*, 2004] but may be a more substantial part of the energy balance for periods of less than a day, particularly for forests [*Michiles and Gielow*, 2008; *Moderow et al.*, 2009]. Including heat storage may significantly improve energy balance closure at some sites [*Lindroth et al.*, 2010; *Sánchez et al.*, 2010] but does not change the overall λE estimates. Figure 4 shows that the median of energy closure ratio is about 0.8 for 253 FLUXNET sites after correction of heat storage [*Beer et al.*, 2010].

[33] Recently, other corrections, including averaging and coordinate rotation, and coordinate systems were recognized and implemented [*Finnigan*, 2004; *Finnigan et al.*, 2003; *Fuehrer and Friehe*, 2002; *Göckede et al.*, 2008; *Massman and Lee*, 2002; *Mauder et al.*, 2008]. These corrections substantially increased λE and H estimates and improved the energy closure ratio [*Finnigan et al.*, 2003; *Kanda et al.*, 2004; *Oncley et al.*, 2007]. Use of a longer averaging period may also improve the energy balance ratio [*Finnigan et al.*, 2003; *Foken et al.*, 2006; *Sakai et al.*, 2001; *Sun et al.*, 2006]. However, the averaging period should be short enough to meet the requirement of the EC technique for a steady flow. *Foken* [2008] argued that the EC technique can only measure small eddies, while large eddies in the lower boundary layer also contribute to the energy balance, but since they do not touch the surface and are not in steady state, they cannot be measured with the EC method. A recent study based on 26 European FLUXNET sites supports this argument [*Franssen et al.*, 2010].

[34] Given our limited understanding of the nature of the energy imbalance [*Foken*, 2008], it has been suggested that BR be preserved and that the energy balance be closed on a larger time scale [*Twine et al.*, 2000; *Wohlfahrt et al.*, 2009]. However, studies have shown that the underestimation of λE by the EC method is larger than that for H (see also Table 2 and section 3.7) [*Asanuma et al.*, 2005; *Brunsell et al.*, 2008; *Castellvi et al.*, 2006, 2008; *Prueger et al.*, 2005; *Yang et al.*, 2004; *Zveryaev and Allan*, 2010]. Another difference

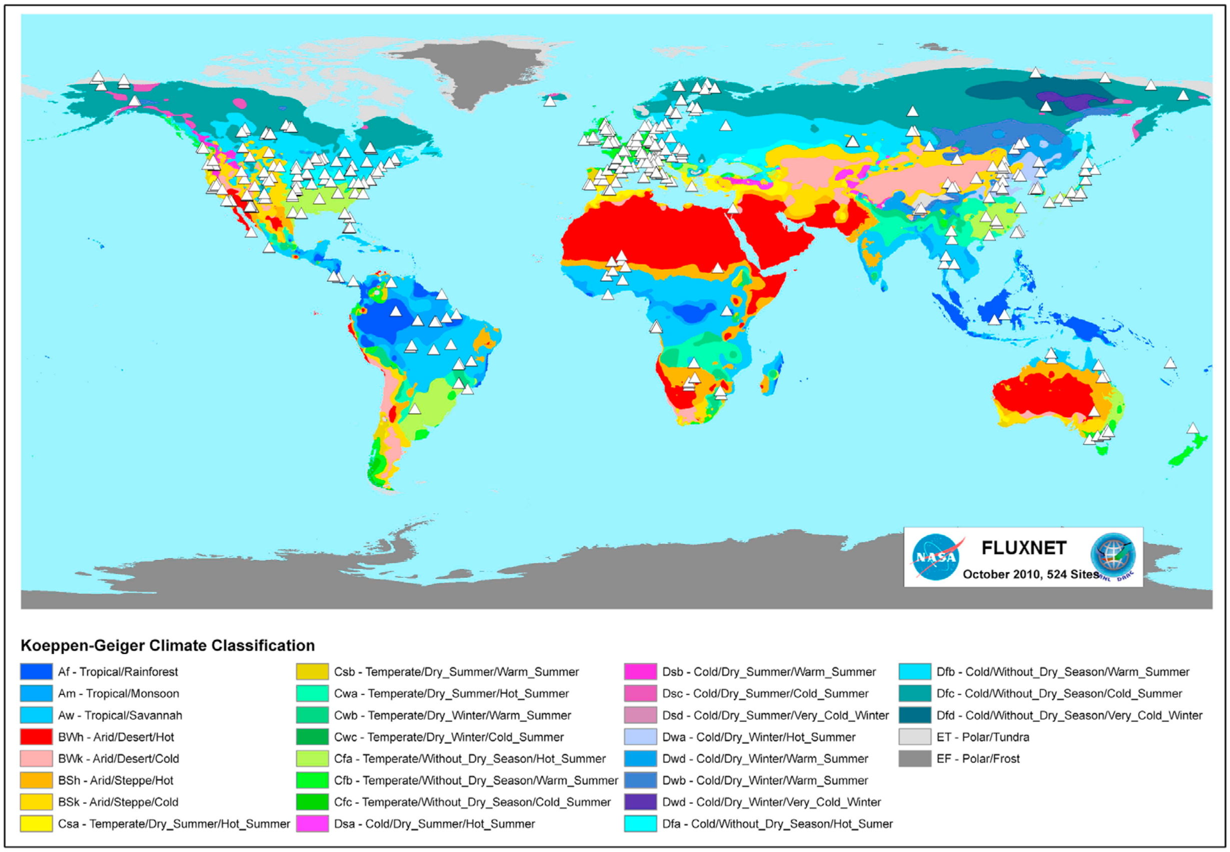

Figure 3. A map of FLUXNET sites and climate (Koppen-Geiger classification) (figure downloaded from http://www.fluxnet.ornl.gov/fluxnet/graphics.cfm).

between λE and H is that λE typically has higher spatial heterogeneity than H [*Hall et al.*, 1992; *Kustas et al.*, 2006; *Vickers et al.*, 2010; *Wolf et al.*, 2008].

3.1.2. Gap-Filling of EC Data

[35] Data streams generated with the EC technique generally include missing data during bad weather conditions (e.g., rainfall) and sensor failures. The average data coverage for the EUROFLUX and AmeriFlux sites was 69% and 75% for λE and H, respectively [*Falge et al.*, 2001b]. These gaps must be filled before the data can be used to infer regional and global long-term hydrological and meteorological time series, and methods have been proposed to do such [*Alavi et al.*, 2006; *Falge et al.*, 2001a, 2001b; *Moffat et al.*, 2007; *Reichstein et al.*, 2005]. Artificial neural network–based techniques may be more accurate than other methods [*Alavi et al.*, 2006; *Moffat et al.*, 2007].

[36] The filling of long gaps (days to weeks) will introduce ~5% uncertainty into the annual values of λE [*Alavi et al.*, 2006; *Hui et al.*, 2004]. In the most extreme cases, the choice of a gap-filling methodology had a significant impact on the estimates of annual λE, possibly altering its annual estimate by more than 15% [*Novick et al.*, 2009].

3.2. Energy Balance Bowen Ratio (BR) Method

[37] The BR method uses simultaneous measurements of vertical gradients of T_a and humidity (q) to partition the surface available energy to H and λE [*Bowen*, 1926]. It is suitable for short vegetation [*Denmead and McIlroy*, 1970; *Tanner*, 1960]. The Bowen ratio β is defined as the ratio of H to λE, which can be related to vertical gradients assuming the aerodynamic resistances to heat and water vapor to be equal in the constant flux layer:

$$\beta = \frac{H}{\lambda E} = \frac{C_p(T_{a1} - T_{a2})}{\lambda(q_1 - q_2)}. \tag{15}$$

Subscripts 1 and 2 express the level. Once β is obtained, λE and H are estimated under the assumption that surface energy is balanced from equation (1).

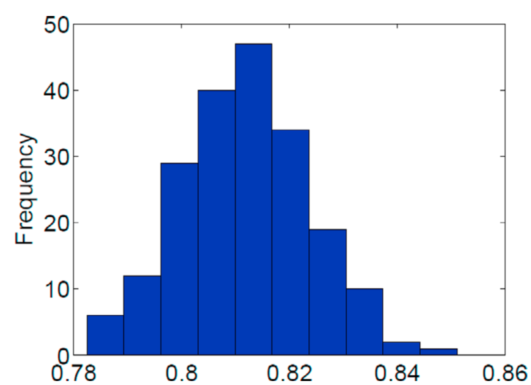

Figure 4. Histogram of the annual mean energy balance closure at FLUXNET sites. Locations and climate of the FLUXNET sites are shown in Figure 3. From *Beer et al.* [2010]. Reprinted with permission.

TABLE 2. Summary of Comparisons of Different Observation Methods for λE and H[a]

Citation	EC and BR	EC and WB	BR and WB	EC and LAS	BR and LAS
Dugas et al. [1991]	$\lambda E_{EC} = 0.72\lambda E_{BR}$; $H_{EC} = 0.76H_{BR}$				
Bausch and Bernard [1992]			$E_{BR} = 1.01E_{WB}$		
Malek and Bingham [1993]	$\lambda E_{EC} = 0.98\lambda E_{BR}$				
Barr et al. [1994]	$\lambda E_{EC} + H_{EC} = 0.89$ $(\lambda E_{BR} + H_{BR})$; $\lambda E_{EC} = \lambda E_{BR} - 74$ W m^{-2}; $H_{EC} = H_{BR} + 59$ W m^{-2}				
den Hartog et al. [1994]	$\lambda E_{EC} = 0.81\lambda E_{BR}$; $H_{EC} = 0.86H_{BR}$				
Rana and Katerji [1996]	$\lambda E_{EC} = 1.06\lambda E_{BR}$ (hourly); $\lambda E_{EC} = 1.02\lambda E_{BR}$ (daily)				
Prueger et al. [1997]			$E_{BR} = E_{WB}$		
Todd et al. [2000]			$E_{BR} = 1.05 - 1.15E_{WB}$		
Wilson et al. [2001]		$E_{EC} \approx 0.98E_{WB}$			
Kohsiek et al. [2002]				$H_{EC} = H_{LAS}$	
Lagouarde et al. [2002]				$H_{EC} = 0.9H_{LAS}$	
Meijninger et al. [2002]				$H_{EC} = H_{LAS}$	
Zhu et al. [2003]	$\lambda E_{EC} = 0.9\lambda E_{BR}$; $H_{EC} = H_{BR}$				
Pauwels and Samson [2006]	$\lambda E_{EC} = 0.91\lambda E_{BR}$				
Gavilán and Berengena [2007]			$E_{BR} = 1.06E_{WB}$		
Li et al. [2008]		$E_{EC} = 0.98E_{WB}$	$E_{BR} = 1.05E_{WB}$		
Pauwels et al. [2008]					$H_{BR} = H_{LAS}$
Zeggaf et al. [2008]			$E_{BR} = 0.94E_{WB}$		
Alfieri et al. [2009]	$\lambda E_{EC} = 0.6\lambda E_{BR}$; $H_{EC} = H_{BR}$				
Chávez et al. [2009]		$E_{EC} \approx 0.7E_{WB}$			
Savage [2009]	$H_{EC} = H_{BR}$			$H_{EC} = H_{LAS}$	
Zeweldi et al. [2010]				$H_{EC} = H_{LAS}$	
X. D. Zhang et al. [2010]				$H_{EC} = H_{LAS}$	

[a]Eddy covariance (EC), energy balance Bowen ratio (BR), water balance weighting lysimeter (WB), and scintillometer (LAS) are reported here. EC and WB direct measure λE or H, while BR is assumed energy balance and LAS depends on MOST functions.

[38] This method requires accurate measurements of T_a and q gradients that may be small as a result of turbulent transfer, especially for irrigated croplands and grasslands. Standard systems need to interchange sensors between different heights to reduce the effect of systematic offset errors in the sensor output [*Cook*, 2007; *Kanemasu et al.*, 1992; *Shuttleworth*, 2007].

[39] The BR system requires less maintenance and is generally cheaper than the EC technique. It is widely used at various agricultural and grass sites. For example, the BR systems of the U.S. Atmosphere Radiation Measurement (ARM; data of its BR systems are available at www.arm.gov) project provide more than 10 years of continuous measurements of λE and H [*Cook*, 2007].

[40] In the BR method, turbulent transfer coefficients for heat and for water vapor are assumed to be identical, as also in the Penman-Monteith equation. This assumption applies for conditions not too far from neutral but may not be valid for strongly stable or strongly unstable conditions [*Angus and Watts*, 1984; *Blad and Rosenber*, 1974]. Furthermore, the two levels at which T_a and q are measured must be within the constant-flux layer, which becomes thin under highly stable conditions. In addition, the BR technique requires that the energy storage and advection be neglected. This requirement can be met for a homogeneous surface or for a long enough time period, e.g., daily or longer. The radiation and ground heat flux components of BR measurements are at points, but the turbulent fluxes are controlled at the landscape scale, i.e., an extensive fetch in the upwind direction provides an airflow over a large surface (i.e., at least 100 times the maximum height of measurement) [*Alfieri et al.*, 2009; *Wiernga*, 1993]. Therefore, the requirement of energy closure is unsuitable for heterogeneous surfaces.

3.3. Lysimeter Method

[41] Lysimeters are standard instruments to measure E without any assumption [*Holmes*, 1984; *Seneviratne et al.*, 2010; *Vaughan et al.*, 2007; *Young et al.*, 1996]. The earliest lysimeters were constructed in 1830 [*Holmes*, 1984]. Traditional lysimeters generally consist of round or square tanks that range from 1 to 5 m^2 in area (large-pan lysimeters have a much larger area, e.g., 92–322 m^2) and from 1 to 4 m in depth [*Scanlon et al.*, 1997]. A detailed review of the role of lysimeter in E measurement and investigation has been made by *Goss and Ehlers* [2009].

[42] Nonweighable lysimeters simply measure the drainage rate or amount of water percolating from the base of the lysimeter. Water storage changes can be estimated in these lysimeters by monitoring water content with a neutron probe or other devices. P can be measured with a rain gauge. Weighable lysimeters measure P, storage changes, and drainage directly, and in this way E may be calculated over time spans as short as 15 min [*Scanlon et al.*, 1997].

[43] Nonweighable lysimeters are used only for long-term measurements but are easily installed and maintained at a low cost and are therefore suitable for network operations. Weighable lysimeters are much more expensive but provide more reliable and precise estimates of short-term values of E. The large weighable and recording lysimeters are recommended for precision measurements in research centers and for standardization and parameterization of other methods of E measurement and for modeling of E [*WMO*, 2008]. The precision of a lysimeter is about 0.05 mm

to 0.1 mm equivalent water for hourly estimates [*Holmes*, 1984].

[44] Lysimeter measurements are considered to provide the most accurate determination of E [*Holmes*, 1984] and are used to compare other techniques [*Scanlon et al.*, 1997]. They are widely used in laboratories and for fieldwork, mainly for agronomic research. In Europe, 117 institutions operate 2930 lysimeters in 18 countries, and among them 269 containers are weighable (see http://www.lysimeter.at/HP_EuLP/reports/Update_lysimetersites_2006_CL.pdf). However, due to their costs, very few weighing lysimeters worldwide have multidecadal measurement records, for instance, the sites of Rietholzbach (http://www.iac.ethz.ch/url/rietholzbach/, in operation since 1976) and Rheindahlen (http://www.niederrheinwasser.de, since 1982).

[45] Disadvantages of lysimeters include the expense of their construction and maintenance, limited areal extent, boundary effects, and disturbance of the natural system [*Rana and Katerji*, 2000; *Scanlon et al.*, 1997; *WMO*, 2008; *Young et al.*, 1996]. Lysimeter measurement of E has a scale much less than that of the EC and BR methods.

3.4. Scintillometer Method

[46] The scintillometry technique for measuring surface fluxes is newer than the EC, BR, and lysimeter methodologies, but it is widely accepted due to its ability to quantify H and λE at the landscape scale, i.e., over several kilometers [*Solignac et al.*, 2009], in particular, by using large-aperture scintillometers (LAS).

[47] A scintillometer consists of a transmitter and a receiver. The receiver measures intensity fluctuations in the radiation emitted by the transmitter caused by scattering by variation in refractive index due to turbulent eddies in the scintillometer path at a height within the atmospheric constant-flux layer. The LAS measures the structure parameter of the refractive index, C_n^2. At optical wavelengths the contribution of temperature fluctuations dominates. That is, the structure parameter of temperature C_t^2 can be deduced from the C_n^2 measurement. On the other hand, for radio wavelengths (>1 mm), water vapor fluctuations contribute most to altering the scintillometer signal, i.e., the structure parameter of moisture C_q^2 can be deduced from the C_n^2 measurement. H and λE can be determined from C_t^2 and C_q^2 with the help of MOST [*DeBruin*, 2009; *Moene et al.*, 2009].

[48] The most important advantage of a scintillometer is that it provides an aggregated flux over different scales [*Lagouarde et al.*, 2002]. Scintillometers are becoming increasingly popular for their validation of H estimates by satellite remote sensing due to their comparable spatial resolutions.

[49] Comparisons of LAS and EC measurements have shown that the LAS works well not only over uniform landscapes [*McAneney et al.*, 1995] but also over heterogeneous surfaces [*Chehbouni et al.*, 2000; *Lagouarde et al.*, 2002; *Meijninger et al.*, 2002] and complex terrain [*Hartogensis et al.*, 2003]. LAS-derived H have also been evaluated against other methods, such as the BR technique, and those using satellite or hydrologic models [*Marx et al.*, 2008; *Pauwels et al.*, 2008].

[50] Scintillometers do not provide the sign of the H, and so prior information as to whether conditions are stable or unstable is necessary to compute it [*Lagouarde et al.*, 2002]. This can be a problem over some irrigated landscapes, where the sign of H can be either positive or negative. Furthermore, existing commercially available scintillometers estimate λE as a residual of surface energy budget. Their use is further complicated by several assumptions that are implicit in processing the data [*Parlange et al.*, 1995]. LAS relies on the validity of MOST for the calculation of surface fluxes [*de Bruin et al.*, 1993]. *X. D. Zhang et al.* [2010] showed that the overestimation of LAS-estimated H [*Chehbouni et al.*, 2000; *Hoedjes et al.*, 2007; *Lagouarde et al.*, 2002; *Von Randow et al.*, 2008] is associated with the higher frictional velocity calculated with MOST. Furthermore, studies reported significant differences of up to 21% between six Kipp & Zonen large-aperture scintillometers [*Kleissl et al.*, 2009, 2008].

3.5. *E* From Surface Water Balance

[51] Estimates of E can be obtained from surface water balance at basin or continental scales with equation (3) using measurements of P, Q, and dw/dt.

3.5.1. Precipitation (*P*)

[52] Precipitation is widely available from either surface rain gauge measurements or by satellite retrievals. Gauge-based data sets have better temporal coverage, extending back to the early twentieth century in most parts of the world and even earlier in some selected regions [*New et al.*, 2001]. Their main limitation has been poor spatial coverage in many parts of the world [*Villarini et al.*, 2008], especially in high latitudes, in arid regions, and in parts of the tropics. In contrast, satellite-based data sets can provide spatially complete coverage but suffer from various discontinuities and do not extend back in time beyond the 1970s at the earliest. Recently, various "merged" satellite and gauge analyses have made attempts to maximize (minimize) the benefits (disadvantages) of satellite and gauge P measurements [*Michaelides et al.*, 2009; *New et al.*, 2001].

[53] The uncertainty of precipitation collected by gauge with careful maintenance should be less than about 10% for liquid precipitation but can be much larger for satellite retrievals. Hence, climatologies from gauges, aside from solid precipitation, can usually be expected to have errors under about 10%. However, it is difficult to even establish any form of climatology from satellite products, in large part because their algorithms often change. Continental P records are available from several data sets [*Trenberth et al.*, 2007b] (see Table 3). Six data sets listed in Table 3 provide a variety of trend estimates for annual P, ranging from -4 to 16 mm per decade over the period from 1980 to 2004.

[54] Two major corrections made to the measurement of P affect the estimated long-term trend of P. The first is accounting for environment-related problems, such as wind, evaporation, environmental noise, and the spatial and temporal variation of the drop size distribution [*Adam and Lettenmaier*, 2003; *Groisman and Legates*, 1994; *Groisman et al.*, 1996; *Karl et al.*, 1993; *Legates and Willmott*, 1990;

TABLE 3. Global Land Precipitation Trends and Characteristics of the Six Global Land Area Precipitation Data Sets Used to Calculate Trends[a]

Series	Period	Gauge Only	Satellite and Gauge	Spatial Infilling	Precipitation Trend (mm per decade) 1951–2005	1979–2005	Citation
GHCN	1900–2005	yes	no	no	−4.56 ± 4.34	4.16 ± 12.44	*Vose et al.* [1992]
PREC/L	1948–2002	yes	no	yes	−5.10 ± 3.25	−6.38 ± 8.78	*Chen et al.* [2002]
GPCP	1979–2002	no	yes	yes		−15.60 ± 19.84	*Adler et al.* [2003]
GPCC VASClimO	1951–2000	yes	no	yes	1.82 ± 5.32	12.82 ± 21.45	*Beck et al.* [2005]
GPCC v.3	1951–2002	yes	no	yes	−6.63 ± 5.18	−14.64 ± 11.67	*Rudolf et al.* [1994]
CRU	1901–2002	yes	no	yes	−3.87 ± 3.89	−0.90 ± 16.24	*Mitchell and Jones* [2005]

[a]From *Trenberth et al.* [2007b]. All trends are based on annual averages.

Michaelides et al., 2009; *Yang et al.*, 2005]. Temperature, snow percentage (percentage of snowfall P), and WS are major factors controlling bias corrections [*Ye et al.*, 2004]. These variables vary between years and result in interannual variations in the appropriate bias correction [*Ye et al.*, 2004].

[55] The second correction is that for the dependence of gauge catch efficiency on WS and snow percentage. Decreases in WS and snow percentage due to the temperature increase will lead to increases in gauge catch over time. Such increases of gauge catch efficiency would indicate a positive trend in the gauge-measured records even without changes of the true P amount [*Førland and Hanssen-Bauer*, 2000]. Trends in P days, affecting changes of wetting and trace corrections, can also affect trends of corrected P. Positive (negative) trends in the number of P days will also transfer to positive (negative) changes in corrected P.

3.5.2. Fresh Water Discharge (Q)

[56] The world's rivers carry, on average, 30–40% of total land P to oceans or inland sinks [*Kundzewicz et al.*, 2007]. According to U.S. Geological Survey (USGS) standards, the uncertainty of discharge measurement from a well-gauged river should be within 5–10% on a daily basis. The accuracy of monthly estimates is expected to be higher. However, relatively few global analyses of river outflow have been made to quantify variations and changes in global Q from land into the oceans, partly because of a lack of reliable, truly global data sets [*Peel and McMahon*, 2006]. Furthermore, flows external to rivers connecting to coastal surface waters such as from submarine groundwater discharge or seawater inflow have not been adequately observed [*Michael et al.*, 2005]. Incomplete records also reduce the accuracy of estimates of Q from the land to oceans [*Di Baldassarre and Montanari*, 2009; *Legates et al.*, 2005; *Peel and McMahon*, 2006]. These errors in river flow data are far from negligible [*Di Baldassarre and Montanari*, 2009], resulting in large uncertainties in global averages of Q and its trend [*Peel and McMahon*, 2006]. Estimates of the trend of Q into oceans have huge discrepancies [*Dai et al.*, 2009; *Gedney et al.*, 2006; *Piao et al.*, 2007].

3.5.3. Terrestrial Water Storage Change (dw/dt)

[57] The least constrained item in equation (3) is dw/dt. Figure 5 shows that it has substantial seasonal variation, as also shown elsewhere [*Güntner*, 2008; *Niu et al.*, 2007; *Ramillien et al.*, 2005; *Rodell et al.*, 2009; *Schmidt et al.*, 2006; *Tiwari et al.*, 2009]. Without accurate estimates of dw/dt, it must be negligible for use of equation (3) so that only yearly estimates of E can be so derived. However, even annual dw/dt is not negligible in all regions. For example, water storage can have large interannual variability due to human water use [*Rodell et al.*, 2009].

[58] The Gravity Recovery and Climate Experiment (GRACE) satellite [*Tapley et al.*, 2004a, 2004b], launched in 2002, allows an estimate of dw/dt on a regional and global scale [*Güntner*, 2008]. Its month-to-month gravity variations can be inverted for global estimates of vertically integrated dw/dt with a spatial resolution of 400 km or greater [*Chen et al.*, 2005], with higher accuracy at larger spatial scales [*Ramillien et al.*, 2005; *Schmidt et al.*, 2006; *Swenson and Wahr*, 2002; *Swenson and Milly*, 2006; *Syed et al.*, 2005; *Tapley et al.*, 2004a; *Wahr et al.*, 2004]. The low-resolution gravimetry products do not provide reliable estimates at the scale of a modest river basin [*Werth and Güntner*, 2010]. GRACE also has problems with near-coastal rivers and watersheds due to coastal "leakage." However, assimilation of GRACE dw/dt into land surface models can improve E estimates at spatial scales smaller than those that GRACE can observe directly [*Güntner*, 2008].

[59] To derive dw/dt at the scale of river basins, appropriate filter techniques have to be applied to the GRACE gravity fields to get a higher spatial resolution [*Swenson and Wahr*, 2002; *Werth et al.*, 2009; *Zhang et al.*, 2009]. Such a spatial filter significantly biases the estimates of the amplitude of annual and monthly mean water storage variations [*Klees et al.*, 2007], but hydrological models can be used to substantially improve the quality of GRACE estimates [*Klees et al.*, 2007; *Werth et al.*, 2009].

3.6. *E* From Atmospheric Water Balance Method

[60] Estimates of E can also be obtained from the atmospheric water budget [*Abdulla et al.*, 1996; *Kustas and Brutsaert*, 1987; *Lenters et al.*, 2000; *Oki et al.*, 1995; *Rasmusson*, 1967, 1968] at the basin or regional scale. It can be written as an equation [*Hirschi et al.*, 2007; *Yeh and Famiglietti*, 2008; *Yeh et al.*, 1998],

$$E = \overline{P} + \overline{\nabla_H \cdot \overline{C}} + \frac{\partial W}{\partial t}, \quad (16)$$

where W represents the column storage of atmospheric water vapor and $\overline{C}$ is the vertically integrated two-dimensional atmospheric water vapor flux. The operator $(\nabla_H \cdot)$ represents

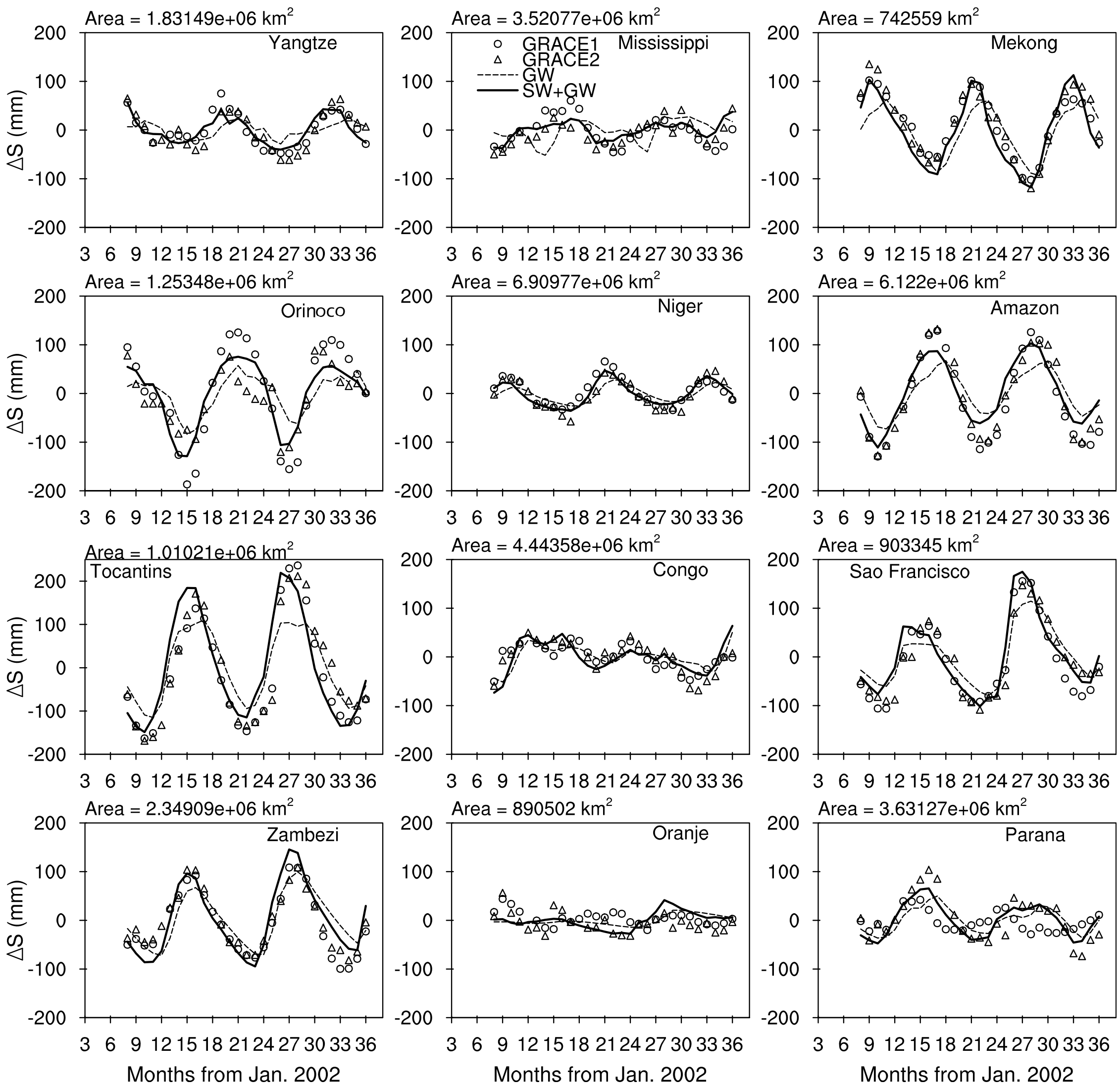

Figure 5. Modeled river basin–averaged anomalies of the terrestrial water storage (unsaturated soil water + groundwater, SW + GW, except for the Mississippi River, where snow water is also included) and groundwater storage (GW) in comparison with Gravity Recovery and Climate Experiment (GRACE) water storage anomaly [*Niu et al.*, 2007]. GRACE1 and GRACE2 represent two versions of GRACE data.

the horizontal divergence, and the overbar signifies temporal average (e.g., monthly means).

[61] This approach requires reanalysis data to estimate $\nabla_H \cdot \overline{\overline{C}}$ and $\partial W/\partial t$ [*Abdulla et al.*, 1996; *Berbery and Rasmusson*, 1999; *Lenters et al.*, 2000; *Maurer et al.*, 2002], but such data have substantial errors [*Roads*, 2003]. For example, the differences between values of derived E over the central United States from different studies have been larger than 100% [*Dominguez and Kumar*, 2008; *Dominguez et al.*, 2008].

[62] This atmospheric budget approach provides a quasi-independent estimate of E but can be applied only to areas large enough that errors in estimates of atmospheric convergence are small [*Lettenmaier and Famiglietti*, 2006]. Studies show that monthly estimates of E from the atmospheric water balance method match favorably with those of the Tropical Rainfall Measuring Mission (TRMM), with correlation coefficients of 0.69. However, the accuracy of annual average E estimates has been significantly less (correlation coefficient dropping to 0.19) [*Roads*, 2003] due to the accumulation of the systematic errors in the reanalysis data.

3.7. Comparisons of the Methods

[63] Methods that observe or estimate λE all have assumptions, and intercomparisons of the methods help to identify their advantages and disadvantages. This section surveys published intercomparisons between the various λE observed or estimated from methods discussed above (Table 2).

[64] The surface water balance method and atmospheric water balance methods can only estimate E at low temporal resolution over a large region. Their scales are substantially

different from those of other methods, which can estimate E at higher temporal resolution, e.g., 30 min, at finer spatial resolution. The flux footprint of BR and EC are similar [*Horst*, 1999], while the flux footprint of a scintillometer depends on the distance between transmitter and receiver. The footprint depends on wind speed and direction, stability, and measurement heights, and it may be more than 100 times the maximum height of measurement for the BR and EC techniques [*Angus and Watts*, 1984; *Kanemasu et al.*, 1992].

[65] The λE estimates from scintillometers depend on the MOST functions as calibrated with EC measurements. Therefore, studies have generally found that scintillometers agree with EC measurements (Table 2). Some studies reported that scintillometer-derived H is higher than that of the EC technique [*Chehbouni et al.*, 2000; *Hoedjes et al.*, 2007; *Lagouarde et al.*, 2002; *Von Randow et al.*, 2008], an overestimation that has been attributed to the selection of the roughness parameterization and universal function of MOST [*X. D. Zhang et al.*, 2010] or to a selection of instrument type [*Kleissl et al.*, 2009, 2008].

[66] Weighable lysimeters supply independent measurements of E. However, they represent a much smaller area than that of the EC and BR measurements. Consequently, comparisons between lysimeter and BR and EC measurements have much scatter. Generally, λE measurements by EC have values that are a little lower than those of weighable lysimeter measurements, while those by BR have values a little higher (Table 2).

[67] Comparisons between EC and BR measurements are the most widely reported, as they have similar footprints. Table 2 shows that EC-measured H can be less or equal to the BR-measured H, while the EC-measured λE is consistently and significantly less than BR-measured λE [*Brotzge and Crawford*, 2003; *Dugas et al.*, 1991].

[68] In addition, estimates of H from the surface renewal analysis method are found to be in good agreement with the values measured by scintillometers [*Anandakumar*, 1999] and EC [*Castellvi and Snyder*, 2009; *Castellvi et al.*, 2006, 2008]. H estimated from the flux variance method has also demonstrated good agreement with surface renewal analysis [*Katul et al.*, 1996] and EC methods [*Kustas et al.*, 1994]. Therefore, the energy closure issue of the EC technique has been regarded by many scientists to be a result of an underestimation of λE [*Castellvi et al.*, 2006, 2008]. In particular, the MOST-based method and the surface renewal method derive similar H at both arid and humid sites, but both methods have higher λE estimates than that of the EC method [*Zhao et al.*, 2010b]. Studies shown in Table 2 tend to support this conclusion. Other evidence also demonstrates that the EC technique tends to accurately estimate H while substantially underestimating λE [*Asanuma et al.*, 2005; *Brunsell et al.*, 2008; *Castellvi et al.*, 2006, 2008; *Yang et al.*, 2004].

3.8. Partitioning of Total *E*

[69] The partitioning of total E in a model between evaporation and transpiration influences its sensitivity to environmental factors. For example, evaporation from soil can tap only near-surface water because deeper soil layers become largely disconnected from the surface during the dry season for bare soil [*Heitman et al.*, 2008]. Transpiration, on the other hand, extracts soil water from the rooting zone, down to a meter or more (Figure 2 and Figure 8). Observations in a semiarid olive orchard site showed that the soil evaporation rate to be positively correlated with VPD but not the transpiration [*Williams et al.*, 2004]. Soil evaporation occurs primarily during and immediately after P, but transpiration more slowly taps deeper soil water and depends on biological controls as well as solar radiation (R_s).

[70] Transpiration is overall the largest contributor to total terrestrial evapotranspiration [*Dirmeyer et al.*, 2006; *Lawrence et al.*, 2007]. When it is incorrectly partitioned into its three components, the E from land surface models may have the wrong sensitivity to environmental factors and so may provide questionable predictions of how E varies climatically. Section 3.8.1 will focus on how the partitioning of total E into its three components is measured.

3.8.1. Transpiration

3.8.1.1. Sap Flow Technique

[71] Transpiration rates for whole plants, individual branches, or tillers can be determined by techniques that measure the rate at which sap ascends through stems [*Rana and Katerji*, 2000; *Shuttleworth*, 2007; *Smith and Allen*, 1996]. Three sap flow techniques have been widely used to measure tree transpiration in forests: heat pulse velocity, tissue heat balance, and radial flowmeters (for reviews, see *Swanson* [1994]). In tissue heat balance methods, the stem is heated electrically and the heat balance is solved for the amount of heat taken up by the moving sap stream, which is then used to calculate the mass flow of sap in the stem. For heat pulse methods, short pulses of heat and the mass flow of sap are determined from the velocity of the heat pulses moving along the stem.

[72] Absolute sap flux rates are estimated by transforming sap velocity to sap flux density via specific wood density and multiplying flux density with conducting sapwood area. Sapwood depth and the number of growth rings within sapwood are important factors affecting flux density [*Dye et al.*, 1991]. Depending on site conditions and tree species, the sapwood cross-sectional area within trees (and within the stand) may vary from rather regular (e.g., plantations, constant growing conditions) to very irregular [*Dye et al.*, 1991; *Phillips et al.*, 1996]. The sap flow method suffers from sampling errors caused by the nonuniformity of flow across the sapwood and the spatial variability of sapwood cross sections throughout the forest [*Fernández et al.*, 2006; *Saugier et al.*, 1997].

[73] To scale up from trees to landscape, measurements have to be made on a representative sample of trees [*Smith and Allen*, 1996]. The variability of sap flux densities among trees is usually low (10–15%) in close stands of temperate coniferous or deciduous forests but is much higher (35–50%) in a tropical rain forest. This variability also increases during a dry spell [*Granier et al.*, 1996]. A set of 10 sap flow sensors usually provides an accurate estimate of

stand transpiration [*Granier et al.*, 1996], but the requirement for the number of sap flow measurements can be more depending on species, conducting type of the xylem, and spatial heterogeneity of the site [*Köstner et al.*, 1998]. Furthermore, it is difficult to use sap flow in estimating the E from the understory. The understory accounted observationally for about 50% of total E at a site in eastern Siberia, Russia [*Kelliher et al.*, 1997].

[74] Intercomparisons have indicated that sap flow measurements give transpiration values similar to those obtained by the water balance method [*Granier*, 1987]. Ecosystem-level transpiration and soil evaporation estimated by the isotope approach were within 4% and 15% of those estimated by scaled sap flow, respectively [*Williams et al.*, 2004].

[75] Sap flow probes can be typically left in place during one vegetation period, without any apparent modification of water transfer properties of the xylem [*Köstner et al.*, 1998]. Tissue heat balance as well as heat pulse velocity methods are appropriate for continuous long-term measurements of tree xylem sap flow [*Köstner et al.*, 1998]. Sap flow can separate tree transpiration from total forest water vapor flux with the help of the EC technique [*Köstner et al.*, 1998; *Sauer et al.*, 2007]. Furthermore, this technique can be used to examine the spatial heterogeneity of fluxes within forest stands.

3.8.1.2. Stable Isotope Technique

[76] Use of stable isotopes of water to determine the possible origins of water used by vegetation relies on the principle that the isotopic composition of water in a plant is the same as that of the source of water used by the plant; this is generally the water in nearby soil, from where it is extracted by the roots [*Brunel et al.*, 1997]. The approach of using stable isotopes of water to determine water sources of vegetation relies upon a number of assumptions [*Brunel et al.*, 1995], as follows: (1) There is no isotopic fractionation of water when it is extracted by the roots; (2) there is no significant change in the isotopic composition of sap water within the plant except in the vicinity of the leaf; (3) no significant errors are associated with the sampling of isotopes or in the extraction and analysis of water from plants and soil; (4) the isotopic composition of the soil water is laterally homogeneous within the rooting area; and (5) the time of sampling was such that time delays associated with transport of isotopes up the plant were not important.

[77] The partitioning of E into transpiration and evaporation can be assessed using continuous measurements of near-surface variations in the stable isotopic composition of water vapor [*Liu et al.*, 2010; *Rothfuss et al.*, 2010; *L. X. Wang et al.*, 2010]. The catchment scale E was derived from the long-term P and Q data. Using stable isotope data for P and Q along with other hydrometeorological information, E can be partitioned into evaporation from soil and water surfaces, evaporation from intercepted rainfall, and transpiration [*Ferguson and Veizer*, 2007; *Lee et al.*, 2010].

3.8.2. Canopy Interception

[78] Interception by the canopy of P (i.e., canopy evaporation) can be measured with two rain gauges, one measuring total rainfall and the other measuring the rainfall under vegetation, so that the interception is calculated as a difference between these two numbers (gross and net rainfall) measured by the rain gauges [*Herbst et al.*, 2008]. However, this term is highly variable [*Bréda et al.*, 2006] due to (1) rain gauge measurements under the canopy being highly dependent on vegetation structure, making them highly variable in space at small scales; (2) climate, especially rain intensity distribution and irradiance, WS and VPD; (3) tree species (higher interception rates are generally recorded in coniferous stands); and (4) leaf area index, upon which the water storage capacity of canopies depends directly. Even the most commonly used methods [*Gash et al.*, 1995] to estimate intercepted P may have substantial errors [*Klaassen et al.*, 1998; *Zhang et al.*, 2006]. Fog may be another important source for canopy water [*Brauman et al.*, 2010; *Katata et al.*, 2010; *Liu et al.*, 2010].

3.8.3. Ratio of Transpiration to Total *E*

[79] The ratio of transpiration to total E depends on vegetation coverage, surface wetness, and the availability of soil water for vegetation root transpiration uptake. In an arid and semiarid olive orchard site, transpiration may account for 100% of the total E prior to irrigation, but only 69–86% of E during peak midday fluxes over the 5 day period following irrigation [*Williams et al.*, 2004]. However, when the surface is wet and vegetation coverage is low, soil evaporation tends to dominate [*Gong et al.*, 2007]. The ratio of plant transpiration to total E increases with vegetation coverage, reaching up to 0.87 during the growing period at an apple orchard [*Gong et al.*, 2007]. Observations show that on average, transpiration accounts for about 70% of E in the Amazonian tropical forest [*Kumagai et al.*, 2005].

4. ENVIRONMENTAL AND BIOLOGICAL CONTROLS OF *E*

[80] Table 4 lists recently published studies as to what controls E under different conditions. Generally, vegetation plays an important role under conditions from arid to humid. Recent modeling studies have confirmed this dependence on vegetation [*Jung et al.*, 2010; *Wang et al.*, 2010b]. Interannual changes in vegetation activity predominantly control interannual changes in E in the growing season [*Lawrence et al.*, 2011; *Suzuki et al.*, 2007]. Satellite-derived vegetation indices can be related to E [*Glenn et al.*, 2010]. Sections 4.1–4.6 will discuss the controls in specific climate regions.

4.1. Tropical Rain Forests

[81] Most humid lands are characterized by shallow water tables that may be reached by deep roots in a forest during dry seasons [*Rodriguez-Iturbe et al.*, 2007]. Turbulent flux measurements have also shown that R_n controls the seasonal variation of E over the rain forest in Amazonia [*Costa et al.*, 2004, 2010; *Fisher et al.*, 2009; *Hutyra et al.*, 2007], a result confirmed by analysis of surface water budget over the Amazon River basin [*Hasler and Avissar*, 2007; *Nepstad et al.*, 1994]. These observations support the hypothesis that most Amazonian trees sustain elevated E rates during the dry

TABLE 4. Controls of λE From Published Experiments

Citation	Site	Latitude, Longitude; Height (m)	Climate: P (mm yr^{-1}), T_a (°C)	Time Period	Results
			Tropical Forests		
Giambelluca et al. [2009a]	tree (8–10 m) shrub	−15.80, −47.90	P = 1440, T_a = 22		water availability constrained dry season λE; Bowen ratio strongly depends on LAI
Giambelluca et al. [2009b]	forest	19.43, −155.26; 1200	P = 2400	2005	λE is strongly controlled by variations in canopy wetness
Bucci et al. [2008]	savanna	−15.95, −47.89	P = 1500, T_a = 22	2002–2003	tree canopy resistance (r_C) increased linearly VPD; LAI was a good predictor of E and g_s
R. A. Fisher et al. [2008]	rain forest	−1.72, −51.45	P = 2270		water availability accounts for contrasting λE in dry season
Tanaka et al. [2008]	forests	Thailand	P = 1400–1800		λE increase with VPD and R_s in two evergreen forest ecosystems
Hasler and Avissar [2007]	rain forest	Tropical Amazonia		1999–2004	λE is in phase with R_n annual cycle
			Semiarid or Arid Regions		
Du et al. [2011]	semiarid forests	36.42, 109.52; 1350	P = 498, T_a = 10.6	2008	transpiration is a function of VPD and R_s
San José et al. [2007]	pineapple field	9.64, −63.62; 195	P = 1018, T_a = 25.9	1997–1999	θ limited E
Gazal et al. [2006]	semiarid riparian forest	31.70, −110.18; 1180	P = 350	2003	LAI, depth to groundwater, and VPD account for daily E
Guo et al. [2006]	desert steppe	47.20, 108.74; 1235	P = 248, T_a = 1.2	2003–2004	LAI and θ linearly related to E/R_n, and E/R_n is a linear function of VPD; LAI and θ account for 79% of E/R_n
Scott et al. [2004]	riparian woodland	31.66, −110.16; 1200	P = 358	2001–2002	trees always had ready access to groundwater
Ivans et al. [2006]	grass, shrub, and juniper	40.25, −112.46; 1600	P = 215	2002–2003	θ and LAI determine λE
Alfieri et al. [2007]	30% C4 grass cover and 70% bare soil	36.88, −100.61;	$P \sim 550$, T_a = 20.4,	2002–2003	θ is the key control on λE
Si et al. [2007]	desert riparian forest	42.00, 101.16	P < =50, T_a = 8.2	2003–2004	transpirations show a significant linear correlation with R_n, T_a, and RH
Chang et al. [2006]	trees	39.35, 100.12	P = 117, T_a = 7.6	2003	VPD accounts for 70% variation in stomatal conductance
Chen et al. [2009]	steppe ecosystems	42.03, 116.26; 1350	P = 399, T_a = 3.3	Dec 2005 to Nov 2006	canopy surface conductance controls, λE_0 is potential λE
Miao et al. [2009]	steppe ecosystems	42.03, 116.26; 1350	P = 399, T_a = 3.3	2005–2007	canopy surface conductance controls λE, grazing reduces $\lambda E/\lambda E_0$
			Boreal Forests		
Jassal et al. [2009]	Douglas fir stands	49.86, −125.34; 300	P = 1400–1600, T_a = 8	1998–2007	λE is positively linearly related to R_n, T_a, and VPD
Migliavacca et al. [2009]	poplar plantation	45.20, 9.05; 60	P = 912, T_a = 12.5	2002–2004	heat wave in 2003 substantially reduced annual NPP but not λE due to the position of the water table remaining close to the roots even during the driest period
Tognetti et al. [2009]	16 year old grafted plants	41.10, 14.72; 250	P = 729; T_a = 13.1	2006–2007	olive trees exhibited a tight stomatal control over transpiration, but insufficient to prevent loss of hydraulic conductance under severe drought stress
Ohta et al. [2008]	forest	62.25, 129.24; 220	P = 260	1998–2006	θ not T_a determines annual variation of $\lambda E/\lambda E_0$
Maximov et al. [2008]	forest	east Siberian	P = 260	1998–2006	LAI determines spatial variation in λE
Zha et al. [2010]	grassland and forest in western Canada	49.70, −112.76	P = 467, T_a = 0.4	1998–2006	LAI determines E among different ecosystems; interannual variation of E was controlled by early spring soil temperature
Bernier et al. [2006]	boreal forest	53.11, −106.03;		2001–2003	θ, R_s, and VPD are the three most important parameters in determining daily λE; θ explains 46% variability of transpiration at the aspen site, 46% and 10% at the jack pine site
McCaughey et al. [2006]	mixed wood forest	48.22, −82.15	P = 831, T_a = 1.3	2003–2004	VPD exerted strong control on the daily λE
Saugier et al. [1997]	boreal forest	53, −104; 579			low rates of transpiration were attributed to the canopy's low leaf area index and the marked reduction in stomatal conductance as vapor pressure deficits increased
Kelliher et al. [1997]	Siberia forest	61.00, 128.00; 300			E was regulated by R_s, VPD, and θ
Betts et al. [1999]	boreal spruce forest	55.89, −98.48		1994–1996	E linearly increased with PAR

TABLE 4. (continued)

Citation	Site	Latitude, Longitude; Height (m)	Climate: P (mm yr^{-1}), T_a (°C)	Time Period	Results
Hogg and Hurdle [1997]	boreal aspen forest	53.64, −106.20; 600	P = 375, T_a = 14.5	1994–1995	transpiration increased linearly with VPD from 0 to about 1 kPa, but then remained remarkably constant at VPD > 1 kPa
Admiral et al. [2006]	Canada peat bog	45.40, −75.5	P = 944, T_a = 6	1997–2000	λE varied with R_n and the magnitude of the fluctuations were affected by VPD and moss water content
Pejam et al. [2006]	moist boreal mixed wood forest	48.22, −82.16;	P = 835	2003–2004	water stress does not play a major role in λE, while energy supply has a strong control on λE
			Wetlands		
Parmentier et al. [2009]	wet land	52.23, 5.07	P = 800, T_a = 10	2005–2006	λE was not affected by water table fluctuations
Sottocornola and Kiely [2010]	northern peatlands	51.92, −9.92; 150	P = 1430	2003–2007	λE was limited not only by the low VPD and cool summer temperatures but also by the low cover of vascular plants and mosses
Sun and Song [2008]	wetland	47.60, 133.52	P = 600, T_a = 1.9	2005	R_n was the main factor affecting λE, while the influence of VPD on λE was relatively small; λE corresponded to LAI in a linear manner when LAI was less than 1
			Temperate Regions		
Suyker and Verma [2010]	irrigated croplands	41.15, −96.50; 360		2001–2006	LAI explains 71% for maize (75% for soybean) $\lambda E/\lambda E_0$, λE_0 is potential λE
Hu et al. [2009]	grassland ecosystems	37.62, 101.33; 3160	P = 580, T_a = −1.7	2003–2005	LAI explains 80% variation of observed transpiration/λE
Aires et al. [2008]	C3/C4 grassland	38.47, −8.02; 190	Mediterranean, P = 570, T_a = 16	2004–2006	λE was strongly controlled by the *VPD* when soil moisture limiting, otherwise evaporative fraction is linearly related to LAI
Suyker and Verma [2008]	irrigated croplands, peak LAI = 4–6	41.15, −96.50, 360	P = 450	2001–2006	daily $\lambda E/\lambda E_0$ linear increase with LAI until LAI reaches 3–4, when $\lambda E/\lambda E_0$ is independent of LAI
Granier et al. [2007]	forests	Europe counties	severe drought	2003	λE were reduced by drought, when the soil relative extractable water dropped below 0.4
Kochendorfer et al. [2011]	riparian cottonwood, LAI = 2.6	38.23, −121.40; 3.5	P = 463, T_a = 15.8.	2004–2005	VPD and groundwater depth determine λE, and the annual λE = 1095 mm > 2 × P
Jongen et al. [2011]	Mediterranean grassland	38.45, −8.02; 190	P = 669, T_a = 15.5	2004–2008	Bowen ratio β was associated with changes in θ, coinciding with plant emergence and senescence
Burba and Verma [2005]	tallgrass prairie and wheat	36.93, −96.69 350	P = 1200, T_a = 15	1997–1999	λE was mostly related to θ and LAI
Leuning et al. [2005]	savanna and forest	−35.65, 148.15, 1200	P = 986 mm	2001–2003	annual $E = P$ at the savanna site; however, annual $E > P$ at forest site during drought of 2002–2003 because trees at both sites were able to extract water deep within the soil profile
David et al. [2004]	sparse evergreen oak woodland	38.54, 8.02, 243	P = 665, T_a = 15	1996–1998	highest transpiration rates occurred during the summer because of the direct access of the root system to a 13 m deep water table
Wilson and Baldocchi [2000]	deciduous forest	35.95, 84.25; 26	P = 1372, T_a = 15.0	1995–1997	annual λE varied with P
Kosugi et al. [2007]	forests	34.97, 136.00	P = 1645, T_a = 13.6	2001–2003	despite large fluctuations in precipitation (1179–1971 mm) during the 3 years, interannual fluctuations in λE were small

season through deep roots, which tap into large reservoirs of soil water that are replenished during the following wet season [*Juárez et al.*, 2007; *Karam and Bras*, 2008]. Studies show that the deeply rooted systems of the Amazon rain forests can resist drought for up to 1–2 years [*Baker et al.*, 2008; *Markewitz et al.*, 2010], although how sensitive the Amazon forests are to severe drought has not been established [*Huete et al.*, 2006; *Lima et al.*, 2010; *Myneni et al.*, 2007; *Phillips et al.*, 2009; *Saleska et al.*, 2007; *Samanta et al.*, 2010]. Differences in drought tolerance of tree species can have a strong impact on the soil water extraction during periods when available soil water is low [*Bittner et al.*, 2010].

[82] In particular, *Saleska et al.* [2007] found from satellite-derived enhanced vegetation index (EVI) that the Amazon forest greened-up more during the 2005 severe drought than during nondrought years. Fewer clouds during drought permit more R_s to reach the surface and the forest to become greener [*Huete et al.*, 2006; *Myneni et al.*, 2007]. However, other studies [*Samanta et al.*, 2011, 2010] indicated that the Amazon forests did not green-up during the 2005 drought after they removed cloud-contaminated EVI data, but a recent study reconfirmed that EVI over the Amazon during the 2005 drought was larger than that for normal years [*Zhao and Running*, 2010]. However, the same paper also confirmed that both gross primary production and net primary production over the Amazon were less in 2005 than in normal years [*Zhao and Running*, 2010]. A special issue on the Amazonian rain forests and drought has been published [*Meir and Woodward*, 2010; *Tollefson*, 2010]. Thirteen papers of this special issue cover studies using model, remote sensing, and ground measurements and show that researchers are still grappling with the impact of the drought on plant growth [*Tollefson*, 2010].

[83] As the carbon uptake and transpiration rates are tightly coupled, this debate has important implications for the climatic variation of E in the Amazon during the 2005 drought. Evidently we lack reliable estimates of these variables. The most reliable data for understanding the response of forests to drought are ground measurements, but these inevitably are limited in their spatial and temporal coverage. Remote sensing offers a partial solution, but any remote sensing–based assessment of ecological responses remains uncertain in the absence of good correlations with ground data [*Meir and Woodward*, 2010], as is also the case for simulations with land models.

[84] Evidence for deep-rooted vegetation has been reported from many regions [*Canadell et al.*, 1996; *Schenk and Jackson*, 2002; *Stone and Kalisz*, 1991]. Such roots have an important impact on E [*Guswa*, 2008]. For example, the highest transpiration rates occur during dry summer in southern Portugal [*David et al.*, 2004], Thailand evergreen forests [*Kume et al.*, 2007], Australian savannas [*O'Grady et al.*, 1999], and secondary woody vegetation in the Brazilian Amazon [*Sommer et al.*, 2002]. However, with shallow roots, the E may be reduced because of water stress during dry periods [*Kume et al.*, 2007; *Vourlitis et al.*, 2002].

4.2. Semiarid and Arid Regions

[85] In semiarid and arid areas, P is the dominant factor in determining E. Annual E is generally equal to a large fraction of the total P [*Ferguson and Veizer*, 2007]. However, where roots of the vegetation reach groundwater, P may not be a good indication of annual E. For example, it was equal to P at a savanna site in tropical Australia but greater than P at a forest site during a drought year because trees were able to extract water from deep within the soil profile [*Leuning et al.*, 2005]. Transpiration shows a significant linear correlation with R_n, T_a, and RH in a desert riparian forest in an extreme arid region [*Si et al.*, 2007]. In another study in an arid region, observations found that variation in VPD accounted for 75% of the variation in tree conductance [*Chang et al.*, 2006].

[86] Vegetation in semiarid regions often depends on underground water. However, only in recent years has the impact of surface water–underground water interaction on vegetation transpiration become a subject of major research interest [*Kalbus et al.*, 2006]. If this dependence were not considered, E would be substantially underestimated during the dry season [*Jiang et al.*, 2009]. Furthermore, the recharge of soil moisture in semiarid regions depends on the P intensity. Only frequently intense storms resulted in infiltration to the root zone, increasing water availability for uptake by deeper roots in a semiarid forest site [*G. Wang et al.*, 2010; *Yaseef et al.*, 2010]. Rainfall with pulses of less than 20 mm did not significant increase transpiration in a water-limited Australian woodland [*Zeppel et al.*, 2008]. However, observations have shown that areas in Africa with similar seasonal rainfall totals have higher fractional woody cover if the local rainfall climatology consists of frequent, less intense P events [*Good and Caylor*, 2011].

[87] Another factor that buffers effects of water stress from P deficits on E is irrigation. Approximately 16% of the world's cropland uses irrigation to supplement its situ rainfall [*Food and Agriculture Organization of the United Nations* (*FAOUN*), 1991], and between 1961 and 2002, the area of irrigation in Asia more than doubled [*Mukherji et al.*, 2009]. Irrigation affects both E and Q. In particular, the long-term average river Q has decreased by more than 10% on one sixth of the global land area due to irrigation [*Döll et al.*, 2009]. Globally, the supply of irrigation water from reservoirs increased from around 18 $km^3\ yr^{-1}$ (adding 5% to the surface water supply) at the beginning of the twentieth century to 460 $km^3\ yr^{-1}$ (adding almost 40% to surface water supply) at the end of the twentieth century [*Biemans et al.*, 2011].

4.3. Boreal Forests

[88] High-latitude ecosystems have generally less E than do freely evaporating surfaces [*Eugster et al.*, 2000; *Kelliher et al.*, 1997; *Saugier et al.*, 1997; *Sellers et al.*, 1995], and evergreen conifer forests have a canopy conductance that is half that of deciduous forests [*Eugster et al.*, 2000]. Most boreal forests are not water stressed because of their slow transpiration. Available energy is the most important

parameter in determining E in these ecosystems [*Admiral et al.*, 2006; *Nemani et al.*, 2003; *Saugier et al.*, 1997]. E in boreal forests is also related to VPD [*Admiral et al.*, 2006; *Hogg and Hurdle*, 1997; *Kelliher et al.*, 1997]. In particular, observations at a southern boreal forest and aspen parkland of Saskatchewan, Canada, showed transpiration to increase linearly with VPD from 0 to about 1 kPa but then to remain remarkably constant at VPD > 1 kPa [*Hogg and Hurdle*, 1997]. During drought, θ [*Kelliher et al.*, 1997] or moss water content [*Admiral et al.*, 2006] may affect E over boreal forests, but the response to θ was found to be very small even in peak drought at a boreal aspen forest because even though near-surface soil water was depleted, the water table remained in the root zone [*Krishnan et al.*, 2006].

4.4. Wetland or Peatland

[89] A wetland is not water stressed, and observations show that potential evaporation may supply a good proxy estimate of E over it [*Mao et al.*, 2002]. Its observed value is closely related to its potential value as calculated from the Penman equation (equation (7)) [*Jacobs et al.*, 2002; *Lafleur et al.*, 2005].

[90] However, over a wetland, the additional effect of vegetation complicates estimation of E as compared to open water. A wetland E may be predominantly controlled by vegetation composition [*Brown et al.*, 2010; *Juan and Shih*, 1997], and values larger than that of open water were observed over a natural wetland and attributed to surface heterogeneity and related roughness effects [*Lott and Hunt*, 2001; *Pauliukonis and Schneider*, 2001]. Northern peatlands have lower latent and higher ground heat fluxes than those over other peatlands [*Sottocornola and Kiely*, 2010].

[91] Observations also indicate that the controlling factors over a wetland are different for different time scales analyzed. Based on the analysis of seasonal variation, during summer months, E from the wetland was driven primarily by R_s, whereas it was driven by VPD in an upland forest. During the leaf expansion period in the upland forest, the dominant driver was R_s. Interannually, however, the E from the upland forest exhibited near-linear responses to VPD [*Mackay et al.*, 2007].

4.5. Temperate Regions

[92] The E in temperate regions is complicated, with no one driving variable being dominant. A comprehensive analysis of the direct and indirect impact of θ, VPD, and R_n on surface energy partitioning was conducted at a U.S. temperate deciduous forest site [*Gu et al.*, 2006]. The direct effect of θ is a rapid decrease in the Bowen ratio β with increasing θ for dry soil but an insensitivity of the β to variations in θ when the soil was wet. The rate of decrease in the β when the soil was dry and the level of θ above which the β became insensitive to changes in θ depend on atmospheric conditions. The direct effect of increased R_n is to increase the β. The direct effect of VPD is very nonlinear: Increasing VPD decreases the β at a low VPD but increases the β at a high VPD. The indirect effects are much more complicated [*Gu et al.*, 2006].

[93] Annual E was found to vary with P, while R_n (or photosynthetically active radiation, or PAR) was only a minor source of variability in E over a broadleaved deciduous forest [*Wilson and Baldocchi*, 2000]. However, PAR and VPD together explained 82% of the daytime hourly variation transpiration in a mixed hardwood forest in northern Michigan [*Bovard et al.*, 2005].

[94] In temperate regions, tolerance to drought depends on root depth and groundwater table level. E at EUROFLUX sites in 2003 was reduced by drought, due to stomatal closure, when the relative extractable water in soil dropped below 0.4 in 2003 during a severe drought [*Granier et al.*, 2007]. A higher sensitivity to drought was found in beech and in broadleaved Mediterranean forests. The coniferous stands appeared to be less drought-sensitive [*Granier et al.*, 2007].Woody vegetation has a stronger tolerance to long droughts than grass [*Detto et al.*, 2006; *Granier et al.*, 2007].

4.6. Nighttime *E*

[95] At the leaf scale, it is a long-held assumption that stomata close at night in the absence of light, causing transpiration to decrease to zero. E models generally rely on R_n as an upper bound, and some models reduce E to zero at night when there is no R_s [*Dawson et al.*, 2007; *Fisher et al.*, 2007]. Advances in sap flow methods [*Burgess et al.*, 2001; *Granier et al.*, 1996; *Köstner et al.*, 1998] have facilitated precise and continuous measurement of plant water use over day-night cycles. Nighttime transpiration and nighttime nonzero stomatal conductance to water vapor have been found to be widespread among a range of tree and shrub species, both C3 and C4 plants, inhabiting a broad range of environments [*Dawson et al.*, 2007; *Snyder et al.*, 2003].

[96] Observations indicate that nighttime transpiration may constitute a significant fraction of the total transpiration [*Novick et al.*, 2009], with higher rates in plants for wetter soil and in plants from ecosystems that are less prone to atmospheric or soil water deficits [*Dawson et al.*, 2007]. VPD and T_a were both well correlated with nighttime transpiration at two AmeriFlux sites in California [*Fisher et al.*, 2007; *Tolk et al.*, 2006]. Another study showed nighttime total E to be driven primarily by WS and VPD [*Novick et al.*, 2009]. The ratio of nighttime to daily total E may increase with surface wetness, varying from 3% to 12% at an irrigated cropland in a semiarid environment [*Tolk et al.*, 2006].

4.7. Impact of CO_2 on *E*

[97] At the leaf level, stomatal apertures tend to close in response to increased CO_2 concentrations [*Ball et al.*, 1987], as reported in numerous experiments (Table 5). Most of these studies have used open-top chambers in which plants are exposed to higher CO_2 concentrations while T_a, RH, and R_s are kept at ambient levels. Large deviations of the sensitivity of stomatal conductance to increased CO_2 occur in Table 5 [*Hetherington and Woodward*, 2003; *Kruijt et al.*, 2008].

[98] However, the response of transpiration and λE to elevated CO_2 is complicated. The reduction in stomatal conductance effectively reduces water loss associated with CO_2 uptake through the same stomata. In this way, water use

TABLE 5. Observed Effects of CO_2 Increases on Stomatal Conductance g_s, Modified From *Kruijt et al.* [2008]

Vegetation/Species	$[CO_2]$ (ppm)	$\Delta g_s/g_s$ (δ, %)	References	Crop Height (cm)	Photosynthesis Type
Potato	680	−59 (6)	*Cure and Acock* [1986]	30	C3
Potato	700	−32 (30)	*Bunce* [2004]	40	C3
Alfalfa	700	−15	*Bunce* [2004]	50	C3
Birch	700	−10 (10)	*Beerling et al.* [1996]	1000	C3
Birch	800	−25[a] (10)	*Wayne et al.* [1998]	50	C3
Beech	700	−12 (10)	*Beerling et al.* [1996]	1000	C3
Beans	700	−38 (10)	*Bunce* [2004]	50	C3
Trees	550	−15.9 (2.4)	*Ainsworth and Long* [2005]	1000	C3
Brassica campestris	600	−41	*Mishra et al.* [1999]	20	C3
Brassica carinata	600	−8.3	*Mishra et al.* [1999]	20	C3
Brassica juncea	600	−20	*Mishra et al.* [1999]	20	C3
Brassica nigra	600	−28	*Mishra et al.* [1999]	20	C3
Douglas fir	550	−40 (43)	*Apple et al.* [2000]	150	C3
Oak	700	−30 (10)	*Beerling et al.* [1996]	1000	C3
Alder	600	−29	*Liang et al.* [1995]	150	C3
Alder	900	−43	*Liang et al.* [1996]	150	C3
Forb	550	−18.7 (5.1)	*Ainsworth and Long* [2005]	50	C3
Barley	680	−52 (30)	*Cure and Acock* [1986]	100	C3
Barley	700	−33 (8)	*Bunce* [2004]	50	C3
Grass	550	−22.2 (5)	*Ainsworth and Long* [2005]	20	C3
Grass	550	−24.9 (7.2)	*Ainsworth and Long* [2005]	50	C4
Grass	700	−33	*Bunce* [2004]	20	C3
Peat bog	560	−25[a]	*Heijmans et al.* [2001]	20	C3
Young tree	700	−25 (3)	*Medlyn et al.* [1999]	150	C3
Legume	550	−22.9 (4.1)	*Ainsworth and Long* [2005]	50	C3
Lolium perenne	700	−20[a]	*Schapendonk et al.* [1997]	20	C3
Maize	680	−37 (3.5)	*Cure and Acock* [1986]	200	C4
Aspen poplar	560	−30	*Noormets et al.* [2001]	200	C3
Soybean	680	−23 (1.5)	*Cure and Acock* [1986]	50	C3
Soybean	700	−25[a]	*Serraj et al.* [1999]	50	C3
Shrub	550	−11.6 (3.9)	*Ainsworth and Long* [2005]	200	C3
Wheat	680	−22 (15)	*Cure and Acock* [1986]	50	C3
Adult tree	700	−9 (5)	*Medlyn et al.* [1999]	2000	C3
Winter wheat	700	−21[a]	*Dijkstra et al.* [1999]	50	C3
Summer wheat	550	−30	*Hunsaker et al.* [2000]	50	C3
Summer wheat	600	−17	*Agrawal and Deepak* [2003]	50	C3

[a]Derived from evapotranspiration measurements [*Witte et al.*, 2006]. Where possible, an estimate of standard error (δ) is given.

efficiency is increased. Elevated CO_2 usually leads to enhanced biomass production. If this enhancement is combined with increased water use efficiency, it may lead to a near-zero net direct CO_2 effect on E [*Kruijt et al.*, 2008]. Furthermore, a reduced E leads to less depletion of soil water, hence less water stress, hence more growth, and thus less reduction of E [*Kruijt et al.*, 2008], a feedback that may be important, especially in drier climates and with natural vegetation.

5. SATELLITE RETRIEVAL OF *E*

[99] This section concentrates on satellite retrieval algorithms for E, their limitations and assumptions associated with these algorithms, and their capability for estimating climatic variability of E. Satellite remote sensing provides reasonable estimates of land surface variables, but these estimates do not measure E. Therefore, most satellite E algorithms relate satellite-derived land surface variables to E using either MOST or the Penman-Monteith equation.

[100] During the past decade a large number of techniques have been proposed to estimate E from satellite observations [*Kalma et al.*, 2008; *Mercado et al.*, 2009]. Methods that use the surface air temperature gradient require unbiased $T_a - T_s$ retrievals and T_a interpolated from ground-based point measurements [*Timmermans et al.*, 2007]. Two different approaches have been proposed to reduce the sensitivity of the flux estimates to uncertainties of T_s and T_a: (1) methods using the temporal variation of T_s [*Anderson et al.*, 1997; *Caparrini et al.*, 2003, 2004b; *Norman et al.*, 2000] and (2) methods using the spatial variation of T_s [*Carlson*, 2007; *Jiang and Islam*, 2001; *K. Wang et al.*, 2006]. Many empirical or semiempirical models relate E to more easily obtained data for radiation, temperature, satellite-derived vegetation index (VI), and VPD from meteorological observations [*J. B. Fisher et al.*, 2008; *Jung et al.*, 2009; *Sheffield et al.*, 2010; *Wang and Liang*, 2008; *Wang et al.*, 2010b].

[101] The issue of satellite remote sensing of E has been reviewed [*Kustas and Norman*, 1996; *Moran and Jackson*, 1991; *Quattrochi and Luvall*, 1999], and *Overgaard et al.* [2006] addressed it from a hydrological perspective and with particular reference to plant sciences, agronomy, and irrigation applications [*Glenn et al.*, 2007; *Gowda et al.*, 2007]. Progress in the measurement and modeling of crop evaporation has been surveyed including also the use of remote sensing for mapping λE across large areas and to a lesser extent for irrigated areas [*Farahani et al.*, 2007]. Ground-based and remote sensing methods for assessing E and θ content across different scales of observation have

TABLE 6. Summary of Estimation of λE Using Satellite Remote Data

Model	Advantages	Disadvantages	Conditions for Best Performance
One-source model		requires parameterization of excessive resistance; high sensitivity to errors of T_s and T_a; only available for clear-sky conditions	dry and sparse surface with large $T_s - T_a$
Two-source model	does not require local calibration	sensitive to errors of T_s and T_a; only available for clear-sky conditions	partial vegetation cover conditions with significant differences between soil and canopy temperatures
Two-source time differencing model	reduced sensitivity to absolute $T_s - T_a$ differences; no local calibration needed and if coupled to boundary layer growth, no observation of T_a required	requires geostationary T_s observations under clear-sky conditions and early morning sounding for determining inversion lapse rate	partial canopy cover conditions with good regional boundary layer development (convective conditions)
T_s-VI model	low sensitivity to errors of T_s; does not require T_a or wind speed	relationship between λE and T_s complicated with temperature and energy control on λE; only available for clear-sky conditions	middle latitude where soil moisture determines λE
Empirical model	simple, low requirements of accuracy of T_s, T_a	most models need local calibration	depends on calibration data
Pemnan-Montheith equation	simple, low requirements of accuracy of T_s, T_a	most models need local calibration	depends on calibration data
Assimilation method	temporal integrated estimation	high sensitivity to errors of T_s and T_a	dry and sparse surface with large $T_s - T_a$

been reviewed comprehensively [*Verstraeten et al.*, 2008], and methods for estimating E with T_s at local, regional, and continental scales have been reviewed [*Kalma et al.*, 2008; *Z. L. Li et al.*, 2009], with particular emphasis on studies published since the early 1990s. Table 6 gives a brief summary of the algorithms reviewed here from a long-term variability and trends perspective.

5.1. One-Source Models

[102] One-source models were first proposed to estimate λE and H from satellite thermal infrared observations in the 1980s. Many one-source models use satellite-derived T_s at a certain view angle to replace the aerodynamic temperature (T_o) in equation (4) to estimate H. The λE is then estimated as a residual of surface energy budget, i.e., equation (1), given G is known or estimated [*Clothier et al.*, 1986; *Jacobsen*, 1999; *Kustas and Daughtry*, 1990; *Kustas et al.*, 1993] as

$$G = R_n \cdot (a \cdot \mathrm{VI} + b), \tag{17}$$

where VI is vegetation index and a and b are constants.

[103] One widely used one-source model is the Surface Energy Balance Algorithm for Land (SEBAL) algorithm [*Bastiaanssen et al.*, 1998a, 1998b]. This algorithm requires only field information on short wave atmospheric transmittance, T_s, vegetation height, empirical relationships for different geographical regions, and time of image acquisition. Its empirical relationships require local calibration [*Teixeira et al.*, 2009a, 2009b].

[104] Another well-known one-source model is the Surface Energy Balance System (SEBS) [*Su*, 2002]. SEBS estimates H and λE from satellite data and routinely available meteorological data, and it has been widely used with high-resolution (Landsat, and Advanced Spaceborne Thermal Emission and Refection Radiometer, or ASTER) or modest-resolution satellite data (Moderate Resolution Imaging Spectroradiometer, or MODIS) [*French et al.*, 2005; *Su et al.*, 2005].

[105] The aerodynamic temperature (T_o) at the surface used in equation (4) is a temperature near the surface where the surface turbulent exchanges of water and heat in the constant flux layer originate [*Norman and Becker*, 1995]. Satellite-derived T_s is a radiative temperature of the land surface within a roughness layer. It is separated from T_o because within a roughness layer water vapor and heat exchange primarily depend on molecule diffusion, which requires much larger gradients than the turbulent exchange in the constant flux layer, as defined by T_o. The universal stability functions that are used to calculate aerodynamic resistance r_h in equation (4) are not valid in the roughness layer [*Sun et al.*, 1999]. The system is more complicated for sparse vegetation, i.e., where T_s is a mixture, depending on view angle, of canopy and soil radiative temperatures. During daytime T_s can be much higher than T_o, especially for bare soil or sparsely vegetated surfaces [*Chehbouni et al.*, 1996; *Friedl*, 2002]. Therefore, use of T_o for T_s in equation (4) may result in a significant overestimation of H [*Sun et al.*, 1999].

[106] Consequently, the utility of satellite-derived T_s for estimating λE has been questioned [*Hall et al.*, 1992; *Shuttleworth*, 1991]. However, in many models, this overestimation of H has been corrected by including in equation (4) an excess resistance to heat exchange, r_{ex} = kB^{-1} = $\ln(z_m/z_h)$, a function of roughness height for momentum transfer (z_m) and roughness height for heat transfer (z_h) [*Blümel*, 1999; *Kustas and Anderson*, 2009; *Su et al.*, 2001; *Verhoef et al.*, 1997]. Over sparse vegetation, kB^{-1} can be very large and variable. It is a function of the structural characteristics of the vegetation (e.g., leaf area index, or LAI), the level of water stress, the view angle of the radiometer, and the climatic conditions [*Blümel*, 1999; *Kustas*

TABLE 7. Summary of Validation and Application of Two-Source Models

Citation	Validation Data
Norman et al. [1995]	Monsoon '90: Arizona semiarid grassland FIFE: Kansas and Oklahoma grasslands
Zhan et al. [1996]	Monsoon '90 (Arizona); FIFE
Anderson et al. [1997]	FIFE
Kustas and Norman [1999]	Arizona, cropland: cotton
Norman et al. [2000]	Monsoon '90, SGP97: shrubland, rangeland/grassland, pasture, bare soil riparian salt cedar
Kustas et al. [2003]	SGP97
Norman et al. [2003]	SGP97
Anderson et al. [2004]	Oklahoma Atmosphere Surface-layer Instrumentation System (OASIS): pasture, scrub, agricultural
Kustas et al. [2004]	SMACEX/SMEX02: cropland, corn, and soybean
Hogue et al. [2005]	SMACEX/SMEX02
Anderson et al. [2007b]	SMACEX/SMEX02
Kustas et al. [2007]	Monsoon '90
Timmermans et al. [2007]	Monsoon '90
Agam et al. [2008]	SMACEX/SMEX02
Li et al. [2008]	SMACEX/SMEX04: semiarid shrub and grass
Anderson et al. [2008]	SGP97
Gonzalez-Dugo et al. [2009]	SMACEX/SMEX02
Kustas and Anderson [2009]	shrub and riparian tree

and Anderson, 2009; *Lhomme and Chehbouni*, 1999; *Lhomme et al.*, 2000; *Su et al.*, 2001; *Verhoef et al.*, 1997; *Yang et al.*, 2009].

5.2. Two-Source Models

[107] Two-source models have been proposed to improve the accuracy of λE estimates using satellite remote sensing data, especially over sparse surfaces [*Blyth and Harding*, 1995; *Dolman*, 1993; *Huntingford et al.*, 1995; *Kabat et al.*, 1997; *Norman et al.*, 1995; *Shuttleworth and Wallace*, 1985; *Wallace*, 1997]. The model proposed by *Norman et al.* [1995] and subsequent improvements are reviewed here.

[108] A two-source model divides the surface into soil and vegetation components, and both parts transfer H and λE to the atmosphere above the surface. A similar division is made in most current land components of climate models. Satellite-derived T_s, is considered to be a composite of the soil (T_{soil}) and canopy temperatures (T_{veg}), and H and λE are also divided into soil and vegetation contributions. Canopy λE can be estimated with the Priestley-Taylor equation [*Priestley and Taylor*, 1972] (equation (14)). The two-source models use iteration to obtain T_{soil}, and T_{veg} from satellite-derived T_s, using an initial value of 1.3 for the α [*Anderson et al.*, 2008; *Kustas and Anderson*, 2009]. Under moisture-stressed conditions, this nominal value of the α will overestimate λE_{veg} and yield negative soil evaporation (λE_{soil}). This negative λE_{soil} is regarded as a non-physical solution during the daytime. The α is therefore iteratively reduced until λE_{soil} approaches zero to obtain a final α, as well as T_{soil} and T_{veg}. The λE and H are then calculated from these estimates.

[109] This modeling scheme has been demonstrated to provide reasonable estimates of system latent heating over a wide range of climatic and vegetation cover conditions [*Anderson et al.*, 2004; *Li et al.*, 2008; *Norman et al.*, 1995, 2003]. However, observations have shown that soil evaporation is an important component of total E (see section 4). Hence, the above described iteration may result in an overestimation of E_{veg}. In a recent study [*Anderson et al.*, 2008], the canopy transpiration is replaced by

$$E_{veg} = \frac{e_s(T_{veg}) - e}{r_c + r_{hc}} \tag{18}$$

where r_c is computed by using an analytical function involved the nominal canopy light-use efficiency [*Anderson et al.*, 2000].

[110] Both the one- and two-source models are sensitive to their use of the temperature differences to estimate H. For example, *Timmermans et al.* [2007] showed that a ± 3 K error in T_s results in an average error about of 75% of H for a typical one-source model [*Bastiaanssen et al.*, 1998a, 1998b] and an averaged error of about 45% for the two-source method [*Norman et al.*, 1995] over subhumid grassland and semiarid rangeland. The methods require unbiased T_s retrievals and T_a interpolated from ground-based point measurements. Attempts at estimating spatial variability in T_a at regional scales with remote sensing suggest an uncertainty of 3–4 K [*Goward et al.*, 1994; *Prince et al.*, 1998]. The uncertainties associated with the T_s retrievals are on the order of several kelvins [*Wang et al.*, 2007a; *Wang and Liang*, 2009]. Consequently, except in areas of low vegetation cover, this derived $T_s - T_a$ may be comparable in value to its uncertainty [*Caselles et al.*, 1998; *Norman et al.*, 2000].

[111] Several methods have used time series of satellite-derived T_s to reduce the sensitivity of the flux estimation to errors [*Anderson et al.*, 1997, 2007a, 2007b; *Mecikalski et al.*, 1999; *Norman et al.*, 2000]. These two-source models have been evaluated over a broad range of cover and climate conditions in grass and croplands in semiarid, subhumid, and humid climates, sparse shrub and grasslands, and densely vegetated riparian sites in arid climates and for canopies having unique canopy structures (e.g., orchards and vineyards) (see Table 7). More testing and validation of the two-source model will be undertaken with particular attention to taller canopies (forests) (Bill Kustas and Martha Anderson, personal communication, 2011).

5.3. T_s-VI Space Methods

[112] In contrast to the one or two-source models, the T_s-VI space method uses spatial variation of T_s to partition R_n into λE and H. If a sufficiently large number of satellite pixels are sampled, the shape of the pixel envelope resembles a triangle or trapezoidal T_s-VI space (Figure 6). The T_s-VI method was first introduced by *Price* [1990]. Its principle is simple: Absorbed R_s heats the surface during the daytime. However, the T_s changes at wet surfaces are small because wet surfaces use more energy for λE and have higher thermal inertia [*K. Wang et al.*, 2006]. The cooling

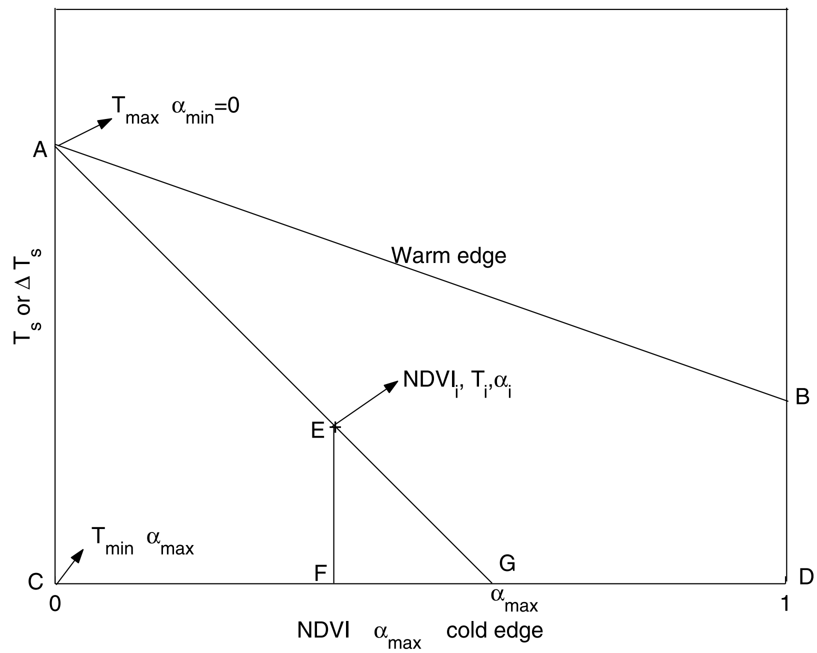

Figure 6. Schematic explaining the Prestley-Taylor parameter, α, from VI-T_s space methods. The trapezoid represents the edges of the VI-T_s space. From *K. Wang et al.* [2006]. Reprinted with permission.

effect of λE and high thermal inertia of wet surfaces together result in low T_s or changes of T_s. Therefore, the warm edge of the T_s-VI space has the lowest evaporative fraction or λE, and the cold edge of the space represents highest evaporative fraction or λE [*Carlson*, 2007; *Murray and Verhoef*, 2007; *Nemani and Running*, 1997; *Verhoef et al.*, 1996].

[113] The T_s-VI method is based on an interpretation of the image (pixel) distribution in T_s-VI space [*Carlson*, 2007]. Linear interpretation of the Priestley-Taylor parameter α is widely used to estimate λE for given surface available energy (Figure 6) [*Jiang and Islam*, 2001; *Nishida et al.*, 2003a, 2003b; *K. Wang et al.*, 2006]:

$$\lambda E = (R_n - G) \cdot \frac{\Delta}{\Delta + \gamma} \cdot \left[\frac{T_{\max} - T_i}{T_{\max} - T_{\min}} (\alpha_{\max} - \alpha_{\min}) + \alpha_{\min} \right]. \tag{19}$$

The $T_{\max}$ and $T_{\min}$ are derived by visual checks from T_s-VI space (Figure 6). The $\alpha_{\max}$ is the maximum α without surface water stress and $\alpha_{\min}$ is often assumed to be zero, corresponding to the fraction of the energy used for λE over the driest bare soil. Because the T_s-VI method makes use of the spatial information of T_s, it does not need accurate values of T_s, i.e., λE (or evaporative fraction) can be accurately derived from satellite brightness temperature without converting to T_s [*Batra et al.*, 2006]. The λE derived from equation (19) primarily depends on T_s and does not depend on VI. Therefore, other methods interpreting spatial variation of T_s, such as albedo-T_s, also work [*Sobrino et al.*, 2007].

[114] Because of its simplicity, the T_s-VI method has been widely accepted. It is reviewed in detail by *Petropoulos et al.* [2009] and *Carlson* [2007]. Some well-known one-source models, such as SEBS and Mapping Evapotranspiration with high Resolution and Internalized Calibration (METRIC) [*Allen et al.*, 2007a, 2007b; *Tittebrand et al.*, 2005], also rely on VI-T_s space (or similarly albedo-T_s space) to estimate λE.

[115] However, model simulations have shown that dependence on the α is not linear as Figure 6 and equation (19) but rather is highly curved [*Carlson*, 2007; *Mallick et al.*, 2009]. The dependence of λE on T_s (or changes in T_s) is complicated because a series of processes are mixed together, i.e., the cooling effect of λE, thermal inertia changing with vegetation, soil moisture and soil texture, and impact of soil moisture, T_a and available energy on λE [*Nemani et al.*, 2003; *Wang and Liang*, 2008].

[116] A key assumption of the T_s-VI method is that λE is negatively correlated with temperature (Figure 6). However, this is not always the case. In high latitudes and cold areas, temperature as a major control of λE is generally positively related to λE [*Iwasaki et al.*, 2010; *Nemani et al.*, 2003]. Therefore, the T_s-VI method is most suitable for a growing season (range of VI is large enough) in middle-latitude areas where soil moisture rather than T_a or available energy is the key control of λE.

[117] Other sources of uncertainty in applying the T_s-VI method to operationally estimate λE include [*Carlson*, 2007; *Mallick et al.*, 2009] the following: (1) The triangle may not be fully determined if the area of interest does not include a full range of land surface types and conditions. (2) The triangle method requires some subjectivity in identifying the warm edge and the dense vegetation and bare soil extremes [*Choi et al.*, 2009; *Timmermans et al.*, 2007]. Identification is more easily obtained from high-resolution imagery. *Tang et al.* [2010] proposed an algorithm for automatically determining the edges of the T_s-VI triangle. (3) The triangle method does not fully consider the dependence of T_s-VI on

surface type. Different land surface types have different aerodynamic resistance.

5.4. Penman-Monteith Models

[118] T_s-VI space methods provide an example of the application of the Priestley-Taylor equation (equation (14)). As already pointed out in section 2.3, this equation does not adequately include a dependence on VPD and r_c. The Penman-Monteith equation has also been widely modified and applied to satellite remotely sensed data. Major difficulties in application of the Penman-Monteith equation include how to parameterize canopy conductance and soil water stress.

[119] *Cleugh et al.* [2007] directly related canopy conductance (inverse of canopy resistance) to satellite-derived leaf area index (LAI) in the Penman-Monteith equation (equation (11)) to estimate λE. *Mu et al.* [2007a] further improved the model by (1) adjusting the canopy conductance based on environmental controls,

$$g_s = g_{s,\min} \cdot \mathrm{LAI} \cdot f(T_{\min}) \cdot f(\mathrm{VPD}), \tag{20}$$

(2) adding the soil evaporation, and (3) separating the land surface into wet surface and dry surface and adding the evaporation from P intercepted by the canopy [*Mu et al.*, 2011]. The model has been applied globally for λE [*Mu et al.*, 2011, 2007a]. Similarly, *Wang et al.* [2010b] used the VI and RH deficit (RHD = 1 − RH/100) to parameterize canopy conductance:

$$g_s \approx (1 - \mathrm{RH}/100) \cdot (a_0 + a_1 \cdot \mathrm{VI}). \tag{21}$$

Equation (20) linearly relates g_s to LAI and will overestimate g_s when LAI is higher than 3 or 4 [*Bucci et al.*, 2008; *Glenn et al.*, 2007; *Lu et al.*, 2003; *Suyker and Verma*, 2008]. Using VI as in equation (21) can effectively correct this issue. *Leuning et al.* [2008] replaced equation (20) with a biophysical two-parameter model, which needs local calibration, limiting its application.

5.5. Empirical Models

[120] Given that satellites can provide only limited information pertaining to λE, a major task in the remote sensing of λE is to identify key factors influencing the processes involved. Long-term continuous measurements collected by global-distributed sites (as reviewed by *Shuttleworth* [2007]) provide an opportunity to do this, especially for data from the FLUXNET and ARM projects.

[121] By analyzing long-term surface λE measurements collected by the ARM project, *Wang et al.* [2007b] found that the dominant parameters controlling λE are R_n, T_a or T_s, and VI, so a simple empirical expression was proposed [*Wang et al.*, 2007b]:

$$\lambda E = R_n(a_0 + a_1 \cdot T + a_2 \cdot \mathrm{VI}). \tag{22}$$

Equation (22) expresses in the simplest form of the dependence of variations of λE on the vegetation that is consistent with the Priestley-Taylor equation while incorporating the influence on vegetation control on λE. A similar equation was proposed to relate vegetation fraction (VF) to λE [*Anderson and Goulden*, 2009; *Choudhury*, 1994; *Kim and Kim*, 2008; *Schüttemeyer et al.*, 2007]:

$$\lambda E = \mathrm{VF} \cdot \alpha \frac{\Delta}{\Delta + \gamma} \cdot (R_n - G), \tag{23}$$

where VF is a linear function of VI. Equations (22) and (23) do not include the effects of soil water stress. The latter was parameterized by adding a dependence on the diurnal temperature range (DTR) and applied globally [*Wang and Liang*, 2008]:

$$\lambda E = R_n(b_0 + b_1 \cdot T + b_2 \cdot \mathrm{VI} + b_3 \cdot \mathrm{DTR}). \tag{24}$$

Water stress has also been accounted for in the Priestley-Taylor formulation by using RH to derive its parameter α [*Yan and Shugart*, 2010]. The above empirical methods (equations (22) and (24)) have a comparable accuracy with more complicated models as shown in an intercomparison of global λE models [*Jiménez et al.*, 2011; *Kalma et al.*, 2008; *Mueller et al.*, 2011b]. The simplicity of the model also allows its global application.

[122] The above empirical methods seek to relate λE to vegetation parameters and key environmental control factors. Similar formulas have been suggested based on a large number of measurements [*Glenn et al.*, 2010]. Methods that empirically link λE to vegetation conditions and potential λE are so-called crop coefficient methods [*Gordon et al.*, 2005; *Rana and Katerji*, 2000]. A detailed discussion about the usage of VI to estimate λE has been given by *Glenn et al.* [2010]. The microwave emissivity difference vegetation index, defined as the difference of microwave land surface emissivity at 19 and 37 GHz, has also been used to estimate λE [*Becker and Choudhury*, 1988; *R. Li et al.*, 2009; *Min and Lin*, 2006].

[123] Other methods have used an artificial neural network or a support vector machine technique to relate satellite retrievals, such as for R_s, T_s, T_a, VI, and land cover, with λE measurements. *Jung et al.* [2010] provided an estimate of global terrestrial λE from 1982 to 2008 using a machine learning method using T_a, P, and VI as explanatory variables to predict λE. These methods are naturally empirical, but their application in other areas is limited because these methods do not provide an explicit formula to follow [*Lu and Zhuang*, 2010; *F. Yang et al.*, 2006].

[124] Most λE algorithms need local calibration. To lessen this requirement, some methods have proposed a universal empirical method that is suitable for different land cover [*Wang and Liang*, 2008; *Wang et al.*, 2010b]. However, experiments do show that the composition of tree species strongly influence λE (see also section 4.3). For example, deciduous species have a much higher λE than coniferous species [*Margolis and Ryan*, 1997; *Yuan et al.*, 2010], and physiological limitations to transpiration in boreal conifers, even when soil water is abundant, reduced λE and increased H over large regions [*Margolis and Ryan*, 1997]. Boreal agriculture has a higher $\lambda E/R_n$ than boreal forests [*A. K. Betts et al.*, 2007], and temperate wheat may have a higher $\lambda E/R_n$ than maize [*Lei and Yang*, 2010]. Therefore, land cover

dependent coefficients as used in LSMs [*Sellers et al.*, 1997] may be a better choice than a universal formulation.

5.6. Assimilation Methods and Temporal Upscaling

[125] Remotely sensed data are acquired instantaneously and so can provide only spatial variation of land surface variables that relate to λE. Furthermore, some of the variables, i.e., albedo, VI, and T_s, can only be accurately estimated from satellite optical and thermal observations under clear-sky conditions. Under cloudy conditions, retrieval is not possible [*Baroncini et al.*, 2008]. Temporally and spatially continuous values require interpolation of the satellite retrievals temporally and spatially, in particular, for cloudy conditions [*Zhao et al.*, 2005]. Land data assimilation provides a physical-based method to do this by merging satellite measurements with estimates from land process models [*Mercado et al.*, 2009; *Reichle*, 2008]. Such an approach has been proposed that uses variational assimilation of satellite T_s with a force-restore equation [*Caparrini et al.*, 2003]. This variational assimilation algorithm uses a bulk transfer model (one-source model) and $T_s - T_a$ to parameterize H (equation (4)) and connects T_s, radiation components, and ground heat flux G [*Boni et al.*, 2001b; *Castelli et al.*, 1999; *Crow and Kustas*, 2005].

[126] These data assimilation approaches have a number of advantages over purely diagnostic approaches. Most important, they provide flux estimates that are continuous in time and are temporally interpolated, using a physically realistic (for bare soil) force-restore prognostic equation [*Boni et al.*, 2001a]. This variational approach demonstrates promise for λE and H retrievals at dry and lightly vegetated sites. However, it is difficult to use for wet and/or heavily vegetated land surfaces [*Crow and Kustas*, 2005]. The single-source nature of the variational approach reduces its performance [*Crow and Kustas*, 2005]. To address this criticism, an algorithm has been developed that incorporates the two-source concept by dividing evaporative fraction into soil and canopy parts [*Caparrini et al.*, 2004b]. More recently, the impact of P on E was explicitly incorporated using an antecedent P index [*Caparrini et al.*, 2004a]. These improvements involve more parameters to be solved from satellite T_s observations that will increase the uncertainty of λE and H estimates [*Crow and Kustas*, 2005]. The variational assimilation method highly depends on the error of $T_s - T_a$, which explains why the algorithm has a higher accuracy for dry and lightly vegetated sites where $T_s - T_a$ is relatively large and the sensitivity of the algorithm to errors of T_s or T_a is relatively small. This algorithm's requirements of accurate estimates of both T_a and T_s at the model pixel scale hamper its wide application.

[127] Recently, satellite remotely sensed T_s was assimilated into a coupled atmosphere-land global data assimilation system [*Jang et al.*, 2010] that explicitly accounted for biases in the model state. However, some studies have reported that their T_s assimilation did not improve the simulation of λE [*Bosilovich et al.*, 2007]. One of the reasons for such lack of improvement is that satellite-derived T_s only represents a skin temperature [*Crow and Wood*, 2003; *Reichle*, 2008], while the land surface model uses a separate canopy temperature and that of the topsoil layer thickness assumed by a model [*Oleson et al.*, 2010; *Tsuang et al.*, 2009]. Assimilation of thermal-based two-source model output instead of T_s appears to provide significant improvement in prognostic predictions of E and root zone soil moisture [*Crow et al.*, 2008].

[128] Assimilating MODIS T_s into a Common Land Model improved the estimation of λE [*Meng et al.*, 2009], but with a large number of difficulties. For example, in the common land model, LAI is specified for the vegetated part only. In contrast, satellite LAI is defined for the total area including both vegetated and nonvegetated fractions. Use of satellite LAI without considering this inconsistency in definition caused much smaller LAI values in the model. As a result, partitioning of surface energy into H and λE, as well as the model-simulated P, was affected substantially [*Jaeger et al.*, 2009].

[129] Satellite remote sensing can provide reasonable estimates of land surface variables that are directly or indirectly related to λE. As section 4 shows, different environmental and biological parameters have different impacts on E under different conditions including climate regimes and land cover types. Auxiliary meteorological observations such as T_a, RH, and WS are essential for some satellite λE algorithms. To obtain values of these parameters at satellite pixel level, it is necessary to do some spatial interpolation from point measurements. Such interpolations introduce substantial errors to the parameters, in particular, T_a. One important goal of the current satellite E algorithm is to reduce the sensitivity to errors of input data. Most algorithms that have produced global E have successfully reduced the sensitivity. Compared to ground-based observations, satellite E retrievals have advantages in their global coverage and higher spatial resolution and provide reasonable spatial variation of E. Most such retrievals were evaluated for diurnal and seasonal cycles. However, the evaluation of climatic variability of satellite-derived λE, at annual and longer time scales, requires observations on these scales [*Wang et al.*, 2010a, 2010b]. In this aspect, both development and application of satellite E retrieval algorithms are highly dependent on ground-based measurements.

6. LAND SURFACE MODELS OF *E*

[130] Land surface models (LSMs) were first designed to provide H and λE for global climate models (GCMs) [*Overgaard et al.*, 2006; *Sellers et al.*, 1997]. Prominent LSMs providing E include models in the Global Land Data Assimilation System (GLDAS) [*Rodell et al.*, 2004] and the second Global Soil Wetness Project (GSWP-2) [*Dirmeyer et al.*, 2006]. LSM development and parameterizations are described in previous reviews [*Dickinson*, 2011; *McGuffie and Henderson-Sellers*, 2001; *Overgaard et al.*, 2006; *Pitman*, 2003; *Sellers et al.*, 1997; *Yang*, 2004].

[131] The MOST provides the basic equations to calculate E for LSMs, modeled as the sum of soil evaporation, vegetation transpiration, and vegetation evaporation. Generally,

the coefficients of parameterization in a specific LSM have been calibrated and evaluated using observations from ground measurements sites that have a scale of hundreds of meters [*Chen and Zhang*, 2009] and therefore need to be upscaled to the scale of LSMs, i.e., 10 km or more [*Brutsaert*, 1999; *Maurer et al.*, 2002]. How this upscaling is done affects the regionally averaged effective coefficients and their calibrations for the LSMs. For example, parallel aggregation of soil and plant resistances have led to E estimates closer to measured values than did a series aggregation [*Were et al.*, 2007]. However, a parallel resistance formulation was found to be more sensitive to errors in vegetation clumping and coverage [*Hogue et al.*, 2005].

[132] In the early 1990s, the Intercomparison of Land Surface Parameterization Schemes (PILPS) was set up to evaluate the performance of LSMs. For lack of real forcing data, the project at its first stage used synthetic atmospheric forcing data. This synthetic atmospheric forcing data seriously affected the evaluation results of LSMs [*Pitman and Henderson-Sellers*, 1998]. More reliable forcing data may partly solve this problem. However, uncoupled systems as in PILPS may lead to an inaccurate estimate of water and energy cycle processes by neglecting processes involving coupling between land and atmosphere [*Santanello et al.*, 2009].

[133] A larger number of short-term extensive experiments and continuous measurements projects have been set up to provide reference data for LSM evaluation [*Shuttleworth*, 2007]. However, these measurements are of short duration. Therefore, most model evaluations have had to focus on the diurnal and seasonal variation of E rather than its interannual variability. For example, the diurnal and seasonal variation of E from land models of reanalysis (e.g., European Centre for Medium Range Weather Forecasts (ECMWF) and National Centers for Environmental Prediction/National Center for Atmospheric Research (NCEP/NCAR)) was evaluated and calibrated with extensive experiments such as First International Satellite Land Surface Climatology Project (FIFE), Boreal Ecosystem-Atmosphere Study (BOREAS), and FLUXNET tower network [*Betts and Jakob*, 2002; *Betts et al.*, 2003, 1996, 1998; *Blyth et al.*, 2010].

[134] To address the requirement of consistent long-term and reliable estimates for λE, the Global Energy and Water Cycle Experiment (GEWEX) Radiation Panel designed a LandFlux initiative. Within this overall effort, the LandFlux project (http://www.iac.ethz.ch/url/research/LandFlux-EVAL) aims to evaluate and intercompare recently developed data sets to provide a benchmark for the upcoming product and other applications. Its first results have been highlighted [*Jiménez et al.*, 2011; *Mueller et al.*, 2011b].

[135] Long-term data sets of observed Q allow evaluation of LSMs from a terrestrial water balance perspective [*Balsamo et al.*, 2009; *Murray et al.*, 2011; *Shmakin et al.*, 2002]. Such observations allow an LSM to be evaluated in the following aspects [*Vano et al.*, 2006]: (1) Does the model simulate the energy balance of the landscape? (2) Is the annual average water balance and interannual variability reasonably simulated? (3) Is the partitioning between surface runoff and soil infiltration to groundwater realistic? (4) Does the model capture the seasonal timing of water flows? However, such an evaluation cannot assess the spatiotemporal distribution of E [*Stöckli et al.*, 2007]. As the measurements of Q spatially integrate all upstream hydrological processes, they can be used to evaluate distributed LSMs, but only if the simulated runoff is properly routed through the river basins [*Zaitchik et al.*, 2010]. Furthermore, dw/dt also needs to be accurately quantified to evaluate an LSM [*Werth and Güntner*, 2010] (see section 3.5).

[136] While only total λE is measured by the EC or BR techniques, it is modeled in LSMs as a sum of soil evaporation, canopy evaporation from P interception, and canopy transpiration. Figure 7 shows that the simulated ratio of global averaged vegetation transpiration to total E varies widely between the 10 LSMs, ranging from 0.25 to 0.64, with a mean of 0.42. Erroneous partitioning of E between transpiration and soil or canopy evaporation substantially affects the accuracy of the climate modeling of hydroclimatology and the influence of land cover change [*Lawrence and Chase*, 2009]. The partitioning of total E into vegetation transpiration and evaporation also affects the simulated gross primary productivity (GPP) [*Bonan et al.*, 2011] because dry leaves both transpire and assimilate carbon but wet leaves mostly evaporate [*Lawrence et al.*, 2007]. Modeling of GPP also impacts the partition of total E. The value of CLM4.0 shown in Figure 7 is from a run with a dynamic-nitrogen cycle and prognostic vegetation. This value of 0.56 reduces to 0.48 when CLM4 is run with prescribed vegetation [*Lawrence et al.*, 2011].

[137] Modeling the soil water availability for transpiration has many difficulties [*Dirmeyer et al.*, 2004, 2006; *Entin et al.*, 1999; *Gao and Dirmeyer*, 2006; *Schaake et al.*, 2004], such as the parameterization of root depth [*Tanaka et al.*, 2008]. Evidence for deep-rooted vegetation has been reported from many regions (see Figure 8) [*Canadell et al.*, 1996; *Schenk and Jackson*, 2002; *Stone and Kalisz*, 1991]. However, most LSMs use values of no more than 2–4 m for rooting depth [*Sellers et al.*, 1996a, 1996b; *Zeng*, 2001], reducing the capability of the vegetation to resist drought. LSMs with unrealistically small rooting depths calculate a spuriously strong impact of water stress on their E [*Beer et al.*, 2010; *Schlosser and Gao*, 2010] (see also Figure 9). In particular, observations show that λE over the Amazon is limited primarily by energy availability [*Costa et al.*, 2004, 2010; *Hasler and Avissar*, 2007; *Juárez et al.*, 2007; *Nepstad et al.*, 1994], but most LSMs have simulated water-limited E [*Karam and Bras*, 2008; *Sen et al.*, 2000; *Werth and Avissar*, 2004].

[138] Besides the availability of soil water for transpiration, additional issues for LSMs include (1) a different dependence of vegetation transpiration on direct than diffuse R_s (or PAR), (2) the response of vegetation transpiration (or total E) to elevated atmospheric CO_2 concentration, (3) impacts of soil nutrients, such as nitrogen, on E, (4) interannual variations of vegetation states, and (5) canopy interception and soil

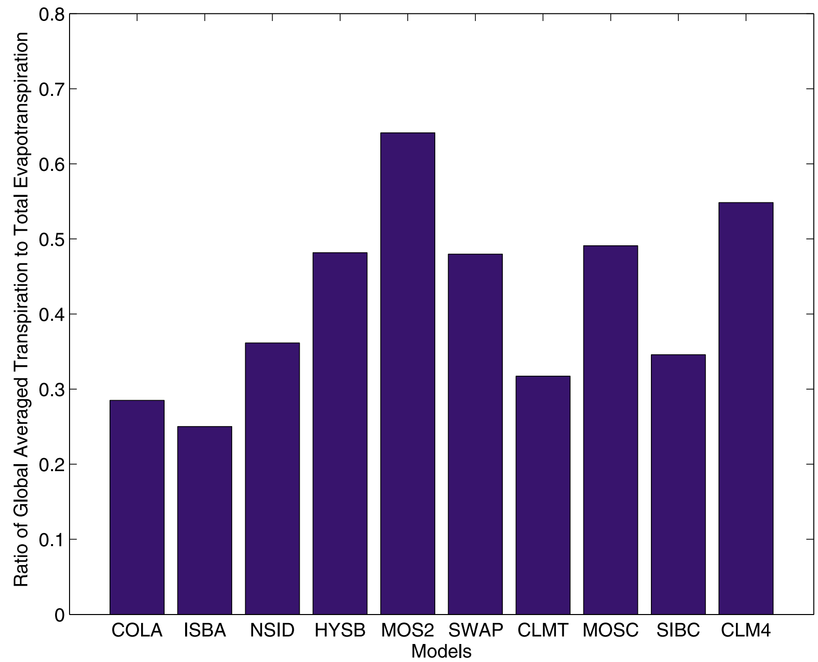

Figure 7. The ratio of global averaged vegetation transpiration to total evapotranspiration as simulated from nine land surface models of the Second Global Soil Wetness Project (GSWP2) [*Dirmeyer et al.*, 1999]. The data are averaged from 10 year data from 1986 to 1995. See http://www.iges.org/gswp/ for the details of the models. The results of Community Land Model version 4.0 (CLM4CN [*Lawrence et al.*, 2011], including carbon-nitrogen cycle with prognostic vegetation) are also included. The ratios vary from 0.25 to 0.64 for the 10 land surface models, with a mean of 0.42.

evaporation parameterization. These effects may be small for diurnal or seasonal variation in E but could become key factors for decadal or longer time periods.

[139] Recent theoretical and observational studies have demonstrated that photosynthesis is also more efficient under diffuse light conditions [*Gu et al.*, 2002]. A global

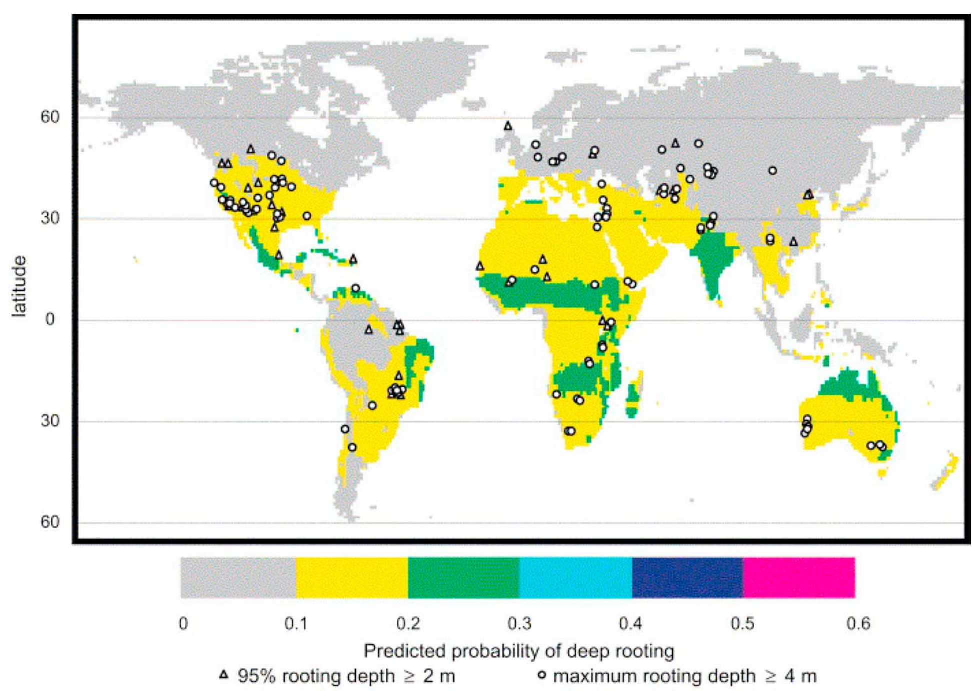

Figure 8. Dots show the observed root depth collected from literature. The contour map shows the predicted probability of deep rooting calculated for 1° × 1° grid cells by the climate-based model. Rooting depths were considered to be deep if 5% or more of all roots in a profile were located below 2 m depth. From *Schenk and Jackson* [2005]. Reprinted with permission.

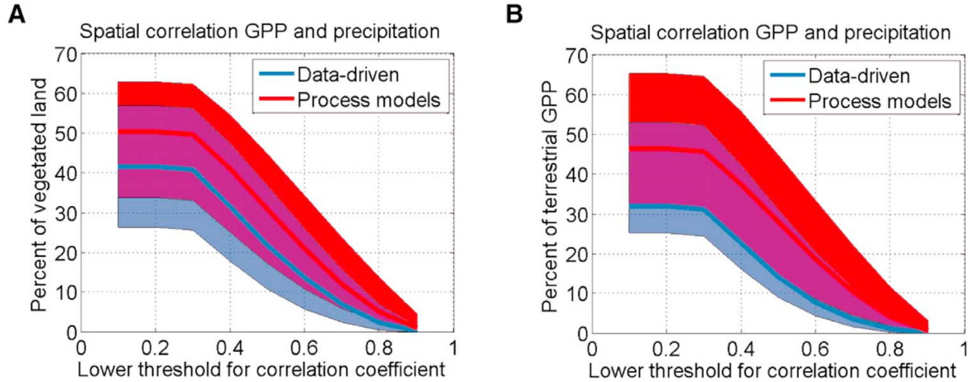

Figure 9. Percentage of (a) vegetated land surface and (b) corresponding gross primary productivity (GPP) that is controlled by precipitation, depending on the chosen threshold for the partial correlation coefficients that signal a control of GPP by a climate factor. The blue areas represent the range of data-driven estimates using different climate sources. This is compared to the range of process-oriented model results in red. Purple shows the overlapping area. The thick lines represent the medians of both ranges. From *Beer et al.* [2010]. Reprinted with permission.

model modified to account for the effects of variations in both direct and diffuse radiation on canopy photosynthesis found that the variations in diffuse fraction, associated largely with the "global dimming" period, enhanced the land carbon uptake by approximately one quarter between 1960 and 1999 [*Mercado et al.*, 2009]. However, very few studies have considered how diffuse radiation affects *E*, although observations indicate that the diffuse fraction may substantially increase the evaporative fraction [*Wang et al.*, 2008].

[140] The response of stomatal conductance and vegetation transpiration to elevated atmospheric CO_2 has been parameterized in LSMs based on observations. Table 5 indicates that plant species differ significantly in these CO_2 responses, i.e., some species are more responsive than others [*Hetherington and Woodward*, 2003; *Kruijt et al.*, 2008]. Furthermore, most of these studies are based on short-term observations of vegetation exposed to elevated CO_2 concentration [*Kruijt et al.*, 2008], and vegetation structure and leaves may not have had enough time to acclimate to the new environmental conditions. Such acclimation may be important for long-term variations [*Calvet et al.*, 2007]. These uncertainties can result in major divergences in climate change projections between state-of-the-art carbon cycle climate models [*R. A. Betts et al.*, 2007; *Bonan*, 2008; *Cramer et al.*, 2001; *Friedlingstein et al.*, 2006; *Gedney et al.*, 2006; *Piao et al.*, 2007]. As a consequence, these physiological aspects have not been included in many modeling applications and are also not part of the standard climate change projections of the Intergovernmental Panel on Climate Change (IPCC) Fourth Assessment Report (AR4) report [*Seneviratne et al.*, 2010].

[141] Most global models without nutrient limitations significantly overestimate land carbon uptake, thus underestimating both the pace and magnitude of the predicted global warming [*Bonan and Levis*, 2010; *Langley and Megonigal*, 2010; *Wang and Houlton*, 2009; *Zaehle et al.*, 2010]. In particular, the control of carbon uptake by nitrogen affects *E* [*Dickinson et al.*, 2002], but this effect remains to be quantified [*Dickinson*, 2012]. A major impediment to including nitrogen limitation in model predictions has been the lack of constraints for rates of nitrogen fixation worldwide. Studies show that increases in nitrogen uptake rather than nitrogen-use efficiency support higher rates of temperate forest productivity under elevated CO_2 [*Finzi et al.*, 2007].

7. CLIMATOLOGY OF GLOBAL *E*

[142] Surface water balance considerations provide estimates of the multiyear averaged climatology of global *E*, *Q*, and *P*. Terrestrial *E* has been estimated to account for about 59% [*Oki and Kanae*, 2006], 61% [*Church*, 1996; *Dai and Trenberth*, 2002; *Dai et al.*, 2009], and 67% [*Trenberth et al.*, 2007b] of total *P* over the land. Estimates of global average *P* over land also vary from 2.05 to 2.21 [*Chen et al.*, 2002; *Dai et al.*, 1997; *New et al.*, 2000; *Xie and Arkin*, 1996]. We therefore infer that the global average *E* estimated from surface water budget is between 1.2 mm/d and 1.5 mm/d and has an average of 1.3 ± 0.1 mm/d.

[143] Table 8 shows climatological estimates of global *E* produced by simple satellite algorithms, LSM simulations driven with observation-based forcing, reanalysis data, and IPCC AR4 simulations from 11 GCMs from 1986 to 1995 [*Mueller et al.*, 2011b]. The estimates of globally averaged *E* vary from 24.1 W m^{-2} (0.83 mm/d) to 42.0 W m^{-2} (1.45 mm/d).

[144] The first two models in Table 8 used the same input data but produced substantially different global averaged *E*. The second model combined the *E* collected by an international suite of EC and BR systems [*Wang and Liang*, 2008]. The underestimation of *E* by the EC technique was corrected in the second model by assuming that the measured Bowen ratio was accurate [*Twine et al.*, 2000], while the first model [*J. B. Fisher et al.*, 2008] did not apply such a correction.

TABLE 8. Global Averaged Terrestrial E From Different Data Sources[a]

Name	Provider Reference	Further Information or Forcing Data	E (mm d^{-1}) (W m^{-2})
UCB[b]	*J. B. Fisher et al.* [2008]	Priestley-Taylor equation, ISLSCP II	0.83 (24.1)
[MAUNI]	*Wang and Liang* [2008]	Empirical model, ISLSCP II	1.24 (35.8)
[PRUNI]	*Sheffield et al.* [2010]	Penman-Monteith equation, ISLSCP II	1.29 (37.5)
[MPI-BGC]	*Jung et al.* [2009]	Empirical model, CRU, GPCC, AVHRR	1.12 (32.6)
[CSIRO]	*Y. Zhang et al.* [2010]	Penman-Monteith equation	1.18 (34.2)
[MODIS]	*Mu et al.* [2011]	Penman-Monteith equation, GMAO, MODIS	1.22 (35.3)
AWB-ETH	*Mueller et al.* [2011a]	Atmospheric water balance (GPCP, ERA-Int)	1.39 (40.2)
[GSWP]	COLA	13 LSMs	1.18 (34.2)
[GLDAS]	NASA GES DISC	4 LSMs	1.27 (36.7)
[I-ORCH]	LSCE	ORCHIDEE LSM with ERA-Int forcing	1.06 (30.8)
[CRU-ORCH]	LSCE	ORCHIDEE LSM with CRU-NCEP forcing	0.95 (27.6)
ERA-INT	ECMWF	reanalysis	1.30 (37.3)
MERRA	NASA/GSFC	reanalysis	1.42 (41.0)
M-LAND	NASA/GSFC	reanalysis	1.31 (37.9)
NCEP	NOAA/OAR/ESRL PSD	reanalysis	1.45 (42.0)
JRA-25	JMA	reanalysis	1.28 (37.1)
IPCC AR4	PCMDI	AR4 11 GCMs	1.28 (36.9)

[a]The global average E derived from surface water budget varies from 1.2 mm d^{-1} to 1.5 mm d^{-1}, with an average of 1.3 $\pm$ 0.1 mm d^{-1}. Model names in brackets do not have real global coverage, i.e., excluding Greenland and Antarctica. Their global averages were calculated according to the models that have areal global coverage. Data were prodivded by Brigitte Muller.

[b]Pixels with monthly λE larger than 300 Wm^{-2} were excluded.

The global averaged E from the second model is consistent with an estimate of the surface water balance estimate [*Wang and Liang*, 2008], indicating that it is necessary to correct the energy balance problem of EC measurements. The resistance in the work of *J. B. Fisher et al.* [2008] was replaced by the formulation in variable infiltration capacity (VIC) model in a revised model [*Sheffield et al.*, 2010] and globally averaged E became higher than in the original version. Another improvement by *Mu et al.* [2007a] that was developed directly using EC measurements at FLUXNET sites also produced a higher E estimation [*Mu et al.*, 2011]. Similarly, *Jung et al.* [2010] corrected the energy balance problem and obtained global averaged E consistent with previous estimations [*Oki and Kanae*, 2006].

[145] The differences between models at a regional scale are much larger than those of the global averaged values. For example, modeled mean annual runoff shows regional differences as large as a factor of 4 between four different models [*Jiménez et al.*, 2011]. The corresponding difference in mean annual E is about a factor of 2 [*Lohmann et al.*, 2004; *Mitchell et al.*, 2004; *Robock et al.*, 2003]. Figure 10 provides an example of the difference of regional E simulated by LSMs over the Southern Great Plains of the United States. Although all the models were evaluated against gauged Q, the four LSMs included in the Global Land Data Assimilation System (GLDAS) yielded very different estimates of E, and there are distinct geographic patterns in the accuracy of each model [*Zaitchik et al.*, 2010].

[146] Differences in E have resulted from both forcing data and model dynamics. Studies show that ERA-40 has a high bias in E because of its high bias in R_s [*Betts et al.*, 2006]. Major problems of ERA-40 are evident throughout the tropics and subtropics, with E so strong over land in the subtropics that it exceeds the actual moisture supply [*Roads and Betts*, 2000; *Trenberth et al.*, 2007a]. Model parameterizations also have an impact on their simulation. Even when models of the North American Land Data Assimilation System receive the same amount of R_s, they can partition the energy flux in a very different manner [*Robock et al.*, 2003].

8. CLIMATIC VARIABILITY OF GLOBAL E

8.1. Pan Evaporation

[147] Pan evaporation, i.e., the evaporation rate of water from a dish located at the ground surface and refilled daily, has been routinely observed at meteorological stations since the 1950s. Evaporation from pans has been assumed to be proportional to the E of a moist surface, such as a lake or irrigated field (see section 4.4). Because pans of various design have produced data for many regions throughout the world over the years, attempts have been made to use these data to estimate E even in nonmoist environments [*Kahler and Brutsaert*, 2006]. A recent study related potential evaporation to ecological diversity [*Fisher et al.*, 2011].

[148] Starting with *Peterson et al.* [1995], numerous studies have reported observations of decreasing pan evaporation over large areas in different regions throughout the world over the past 50 years [*Fu et al.*, 2009; *Roderick et al.*, 2009a, 2009b]. Declines in pan evaporation have been reported across the United States, the former Soviet Union, India, China, Australia, New Zealand, and Canada. These regional trends have typically been in the range of -1 to -4 mm yr^{-2}. In energetic terms, a trend of -2 mm yr^{-2} is equivalent to -0.16 W m^{-2} yr^{-1} or a change of -8.0 W m^{-2} over 50 years.

[149] Initially, it was thought that this declining pan evaporation also meant declining E [*Peterson et al.*, 1995], but for various reasons it does not [*Brutsaert and Parlange*, 1998] but, rather, could be interpreted as evidence for increasing E using the Bouchet's complementary hypothesis. Its general form is

$$(1 + b) \cdot E_{po} = E_{pa} + b \cdot E, \tag{25}$$

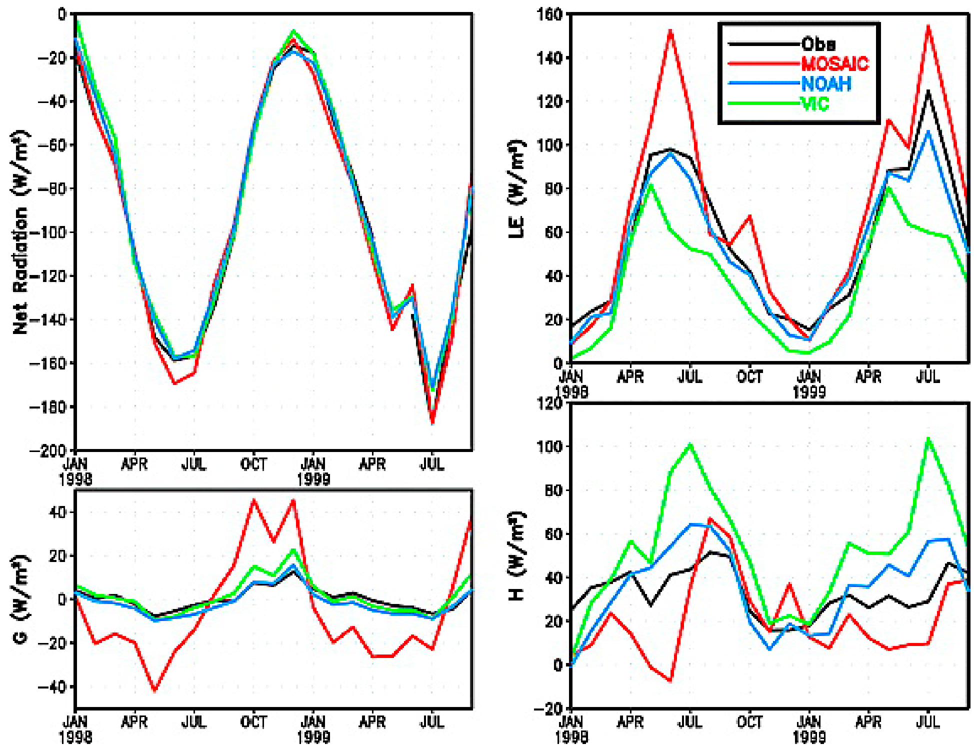

Figure 10. Surface energy budget at a monthly time scale over the U.S. Southern Great Plains region based on available observations from Atmospheric Radiation Measurement sites. Black lines are observations, averaged over all available stations. Red lines are for the Mosaic model, blue for Noah, and green for variable infiltration capacity (VIC). Values for each model are calculated based on a subset of model results that has exactly the same sample size as the observations and are clean comparisons to the observations. All fluxes are positive upward [*Robock et al.*, 2003].

where E_{po} is potential evaporation, E_{pa} is pan evaporation, and b is a constant. E_{po} is often calculated using the Priestley-Taylor eqation (equation (14)). In most studies, b is assumed to be unity.

[150] Bouchet's hypothesis has generated a large number of publications [*Brutsaert*, 2006; *Brutsaert and Stricker*, 1979; *Crago and Crowley*, 2005; *Hobbins et al.*, 2004, 2001; *Kim and Entekhabi*, 1997; *Parlange and Katul*, 1992; *Ramírez et al.*, 2005; *Szilagyi*, 2001; *Xu and Singh*, 2005; *Xu et al.*, 2006; *D. W. Yang et al.*, 2006]. In particular, long-term (1961–1990) E has been modeled with the help of 210 stations of the Solar and Meteorological Surface Observation Network within the conterminous United States. An average over all stations, using pan evaporation measurements, showed an overall increase of about 2–3% in the period from 1961 to 1990 [*Szilagyi*, 2001]. The trends are generally consistent with the surface water balance method over six big river basins in the United States from 1950 to 2000 [*Walter et al.*, 2004].

[151] As a measure of the effectiveness with which heat transfer takes place between the pan and its surroundings, b in equation (25) depends on the environment and therefore can be much larger than unity [*Kahler and Brutsaert*, 2006; *Xu and Singh*, 2005]. The relationship between E and E_{pa} varies substantially depending on b, as shown in Figure 11. Therefore, it is necessary to consider the variation of b when interpreting E_{pa} [*Kahler and Brutsaert*, 2006; *Pettijohn and Salvucci*, 2009].

[152] The agreement between different methods to interpret E_{pa} also depends on their function of the wind speed (WS) [*Szilagyi and Jozsa*, 2008]. *Ramírez et al.* [2005] reported direct observations to support a complementary relationship, but with widely scattered data. Furthermore, many experimental, as well as theoretical results, suggest that no real complementarity exists between areal evaporation and local potential evaporation [*Lhomme and Guilioni*, 2006]. The complementary relationship also ignores VPD and surface temperature changes with the drying-out process [*Lhomme and Guilioni*, 2006].

[153] Models for E based on the complementary relationship also ignore the influence of vegetation. The maximum available soil water is partly determined by vegetation (see section 4) [*Donohue et al.*, 2007; *Guswa*, 2008]. A large increase in rooting depth, such as when deep-rooted perennials are planted on a former crop land, leads to a drawdown of the soil water as the plants grow and the rooting depth increases, and during this root growth period, E can exceed P [*Calder*, 1976]. Satellite observations have shown growing seasons to be increasing in recent decades and consequently an increase in transpiration [*Fung*, 1997; *Lucht et al.*, 2002; *Myneni et al.*, 1997; *Nemani et al.*, 2003; *Peñuelas et al.*, 2009; *Zhou et al.*, 2001; *Piao et al.*, 2007].

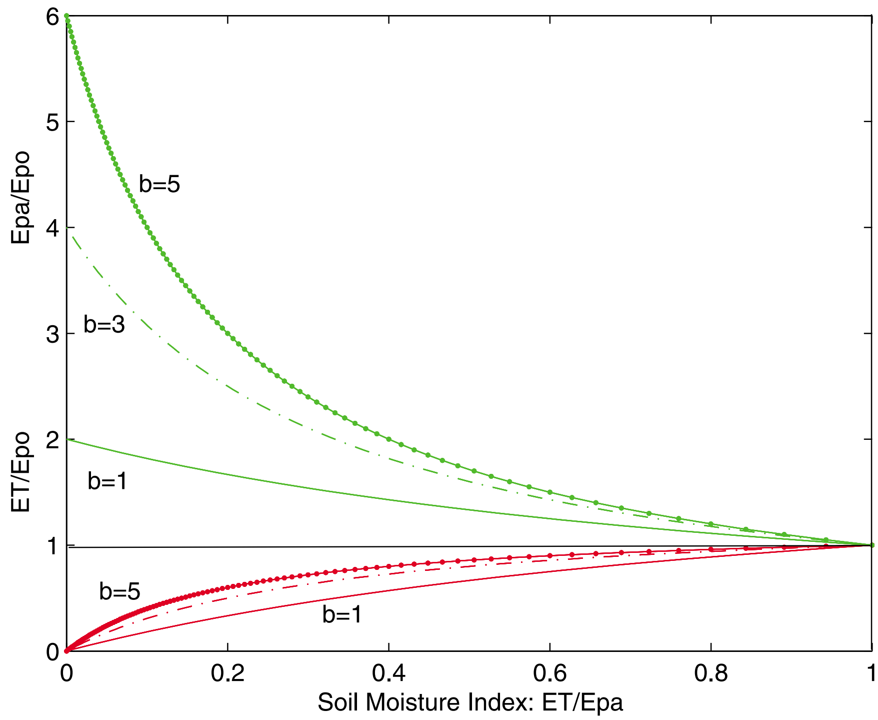

Figure 11. Scaled actual evaporation E+ = E/Epo and scaled pan evaporation Epa+ = Epa/Epo, as functions of the evaporative moisture index EMI = E/(Epa), on the basis of the extended complementary relationship (equation (28)) with b = 1, 3, and 5. Figure modified from *Kahler and Brutsaert* [2006].

[154] Pan evaporation is a measure of the evaporative demand, but E also depends on the supply of water [*Roderick et al.*, 2009a]. Decline in E_{pa} can be attributed to a decline in R_s [*Fu et al.*, 2009; *Roderick and Farquhar*, 2002]. In humid areas, R_s is a determining factor of E, which increases with R_s. However, in an arid area, available water is the determining factor of E and an increase of R_s indicates reduced cloud cover and P. Therefore, in arid areas E generally decreases with R_s [*Wang et al.*, 2010a]. WS is a key parameter of the aerodynamic conductance that determines E_{pa} and has been reported as the major factor controlling reported reduction of E_{pa} [*Fu et al.*, 2009; *Rayner*, 2007; *Roderick et al.*, 2007]. However, the impact of WS on λE is less important than on E_{pa}, as also can be seen from section 4 and Table 4, because stomatal conductance, which can be much larger than aerodynamic conductance [*Sellers et al.*, 1997], controls λE.

8.2. Water Balance Methods

[155] Estimates of atmospheric precipitable water are consistent between theoretical prediction, observations, and model simulations (Table 9). Observations over past decades have also shown that near-surface relative humidity has remained nearly constant [*Dai*, 2006; *Trenberth and Smith*, 2005; *Wentz and Schabel*, 2000; *Willett et al.*, 2007, 2008]. With constant relative humidity, the Clausius-Clapeyron equation predicts that the column total precipitable water increases at a rate of ~7% K^{-1}. GCM simulations also show similar increases [*Held and Soden*, 2006; *Stephens and Ellis*, 2008; *Willett et al.*, 2007]. Thus, all primary data sets

TABLE 9. Reported Trends in Total Column Water Vapor or Precipitable Water and Ocean Surface Hydrological Fluxes[a]

Author	Instrument	Region	Period	Change per Decade
Trenberth et al. [2005]	SSMI	global PW	1987–2004	0.40 ± 0.09 mm (1.3% ± 0.3%)
Vonder Haar et al. [2005]	NVAP reanalysis	global PW	1988–1999	−0.29 mm
Durre et al. [2009]	radiosondes	Northern Hemisphere PW	1973–2006	0.37 mm
Brown et al. [2007]	TMR	global PW	1992–2005	0.9 ± 0.06 mm
Mieruch et al. [2008]	GOME and SCIAMACHY	global PW	1996–2002	0.39 ± 0.15 mm (1.9% ± 0.7%)
Wentz et al. [2007]	SSMI	tropical oceanic PW	1987–2006	0.35 ± 0.11 mm (1.2% ± 0.4%)
		tropical oceanic P		1.4% ± 0.5%
		tropical oceanic E		1.2% ± 0.4%
Liepert and Previdi [2009]	OAFlux[b]	global oceanic E	1987–2004	1.7% ± 0.9%
	HOAPS3[c]			4.7% ± 3.6%

[a]PW, precipitable water; P, precipitation; E, evaporation; SSMI, Special Sensor Microwave Imager; NVAP, NASA Water Vapor Project; TMR, TOPEX Microwave Radiometer; GOME, Global Ozone Monitoring Experiment; SCIAMACHY, Scanning Imaging Absorption Spectrometer for Atmospheric Chartography. Table is cited from *Sherwood et al.* [2010], with permission.
[b]Objectively Analyzed Air-Sea Heat Fluxes.
[c]Hamburg Ocean Atmosphere Parameters and Fluxes From Satellite Data version 3.

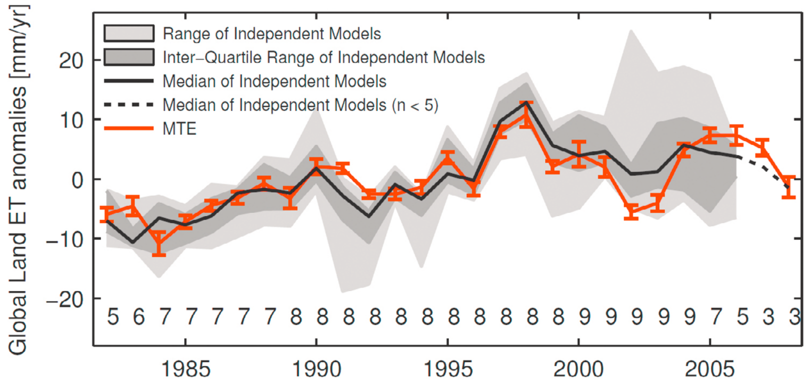

Figure 12. Global land-ET (or *E*) variability according to multiple tree ensemble (MTE) and nine independent models. Error bars indicate one standard deviation within the MTE. Numbers at the bottom show the number of models available each year. From *Jung et al.* [2010]. Reprinted with permission.

support the conclusion that water vapor mixing ratios in the troposphere are increasing at roughly the rate expected from the Clausius-Clapeyron equation. The few analyses that have found otherwise have relied on secondary data sets that are less suitable for quantifying trends [*Sherwood et al.*, 2010].

[156] Theoretical analysis and model simulations show that global mean P and E will increase more slowly with temperature than does precipitable water because of energy constraints on the processes, i.e., a change of latent heating of the atmosphere must be balanced by changes of the radiative heating [*Boer*, 1993; *Held and Soden*, 2006; *Richter and Xie*, 2008; *Schneider et al.*, 2010; *Wild and Liepert*, 2010]. Simulations of climate change find that global mean P and evaporation increase with global mean surface temperature at a rate of only 2–3% K^{-1} [*Allen and Ingram*, 2002; *Held and Soden*, 2006; *Knutson and Manabe*, 1995; *Stephens and Ellis*, 2008]. However, a significant trend of global P over land is not easily obtained from available data because of large interannual variability and inconsistencies between data sources (Table 3; see also section 3.5.1).

[157] There have also been attempts to quantify long-term changes in continental Q [*Dai et al.*, 2009; *Milliman et al.*, 2008]. For example, *Labat et al.* [2004] analyzed records (of lengths varying from 4 to 182 years) from 221 rivers, accounting for ~51% of global runoff, but only a small fraction of these rivers had data for the early decades of the twentieth century. They found large decadal to multidecadal variations in continental runoff and suggested a 4% increase in global runoff per 1°C global surface warming. This result was questioned [*Legates et al.*, 2005; *Peel and McMahon*, 2006] on the basis of use of insufficient streamflow data. Substantial differences in the global Q data used, e.g., *Gedney et al.* [2006] versus *Piao et al.* [2007], resulted in different conclusions as to what causes long-term variation in E and Q. Major obstacles in estimating continental Q included incomplete gauging records or, even more daunting, unmonitored streamflows [*Gerten et al.*, 2008]. Furthermore, its estimation does not account for changes of reservoir storage. Over the second half of the twentieth century, about 7000 km^3 of reservoir storage was filled, equivalent to roughly 20% of the discharge of global rivers to the oceans [*Vörösmarty et al.*, 1997; *Vörösmarty and Sahagian*, 2000]. Recently the GRACE data have been available to constrain terrestrial soil water change, showing substantial interannual variation [*Rodell et al.*, 2009; *Tiwari et al.*, 2009].

[158] Table 9 shows that global atmospheric water vapor increases at a rate of ~7% K^{-1}. However, P and E are expected to increase at a much lower rate of 2–3% K^{-1} [*Sherwood et al.*, 2010]. A recent study shows that relative humidity decreased over land since 2000 [*Simmons et al.*, 2010], and, if so, water vapor over land for this period would also have increased at a rate lower than ~7% K^{-1}. It is difficult to derive a significant trend of terrestrial E from water balance because (1) there is large interannual variability of P and inconsistencies between difference data sources, and (2) the discharge Q directly into oceans is difficult to estimate.

8.3. Satellite Remote Sensing

[159] Satellite retrievals are good at characterizing the spatial variability of E. However, their application to describe climatic variability is still not established. With accumulation of satellite observations, some algorithms have produced global or regional data sets of E for more than 10 years (see Table 8). In particular, *Jung et al.* [2010] provided an estimate of global terrestrial E from 1982 to 2008 using a machine learning method, with T_a, P, and VI as explanatory variables to predict E. The authors concluded that global E increased from 1982 to 1997 but decreased since 1998 (Figure 12). Their algorithm depends on the use of VI to predict E because vegetation is one of its most important controlling factors shown in Table 4. However, their conclusions are questionable because their method excludes R_s, which is another key parameter in determining E, especially in moist regions (section 4 and Table 4). Analysis of E measurements at 21 pantropical sites has demonstrated that R_n was the strongest determinant of E and explained 87% of the variance in monthly E across the sites [*Fisher et al.*, 2009].

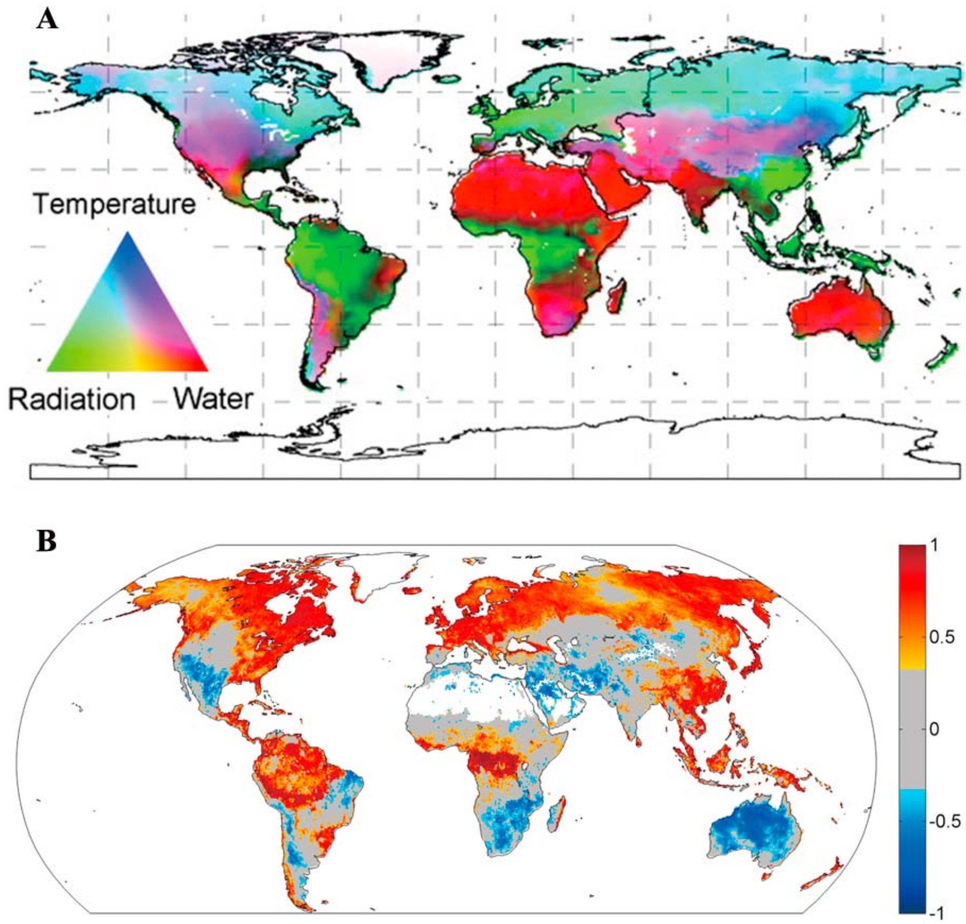

Figure 13. (a) Geographic distribution of potential climatic constraints to plant growth derived from long-term climate statistics. From *Nemani et al.* [2003]. Reprinted with permission. (b) Pearson's correlation coefficient of E and temperature. Correlations that are not significant ($p > 0.1$) are displayed in gray. From *Jung et al.* [2010]. Reprinted with permission.

[160] The method of *Jung et al.* [2010] was trained with data collected by the global FLUXNET sites. As the length of observations for each site is on average 2 years [*Friend et al.*, 2007], their method depends primarily on seasonal and spatial variations of T_a to do its regressions, but E over tropical forests is strongly R_s limited (see Figure 13 and Table 4) [*Myneni et al.*, 2007; *Nemani et al.*, 2003]. Because R_s and T_a have similar seasonal cycles, T_a provides a surrogate for R_s on this time scale and so implies the E of tropical forests [*Jung et al.*, 2010]. Because of this correlation, the method of Jung et al. should be accurate for seasonal variations of E. However, its performance for interannual or decadal variation in E has not been evaluated and is suspect. On these time scales, variations of R_s are substantially different from those of T_a.

[161] Figure 14 demonstrates this point by showing calculated monthly anomalies of R_s and T_a from 1982 to 2008 at about 100 stations in tropical regions (23.5°S–23.5°N) where both R_s and T_a are available at least 120 months. It shows that E would be overestimated in 1998 and substantially underestimated from 2002 to 2003 if it were obtained from T_a rather than R_s. As tropical forests have the largest E over land, inaccuracies in their estimation would contribute substantially to errors in estimating the variation of global E. Indeed, Figure 12 also shows that the machine learning method estimated that E is substantially less than that of the process-based models from 2002 to 2003 [*Jung et al.*, 2010]. The Pinatubo volcano eruption in 1991 (Figure 14) and consequent reduction of R_s from 1991 to 1992 leads to a T_a-derived E that overestimates global E compared to process-based models for this period.

[162] Vegetation extracts soil water with its roots [*Nepstad et al.*, 1994] so that transpiration can increase with R_s even under water-stressed conditions [*Teuling et al.*, 2009] (see section 4.1). As it does not include this buffering effect of R_s, the machine learning method produces too strong a response of E to P changes and so predicts a stronger variability of global E than process-based models after 2000 (Figure 12), although the process-based models have already been regarded as having a spuriously strong impact of water stress on their E [*Beer et al.*, 2010; *Schlosser and Gao*, 2010].

8.4. Land Surface Model Simulation

[163] Studies have shown that the continued increase in atmospheric CO_2 concentrations will decrease stomatal conductance [*Kruijt et al.*, 2008] so that plants will become

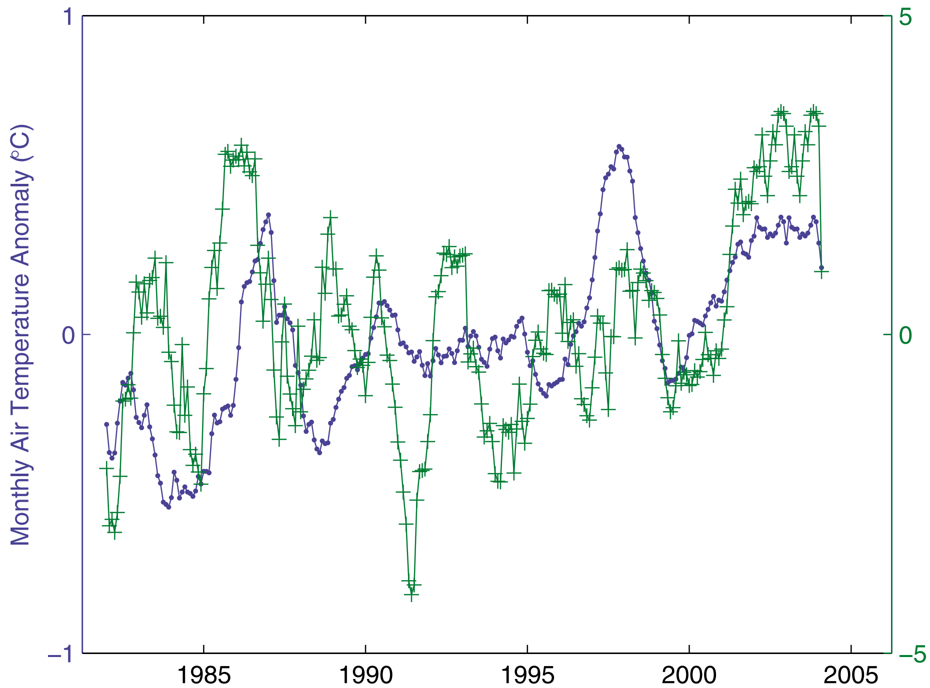

Figure 14. Time series of surface incident solar radiation (R_s) and air temperature (T_a) averaged from about 100 stations in the tropics (23.5°S–23.5°N). R_s was either directly observed or derived from sunshine duration observation. Sunshine duration records the time during a day that direct solar beam irradiance exceeds 120 W m^{-2}, from which daily R_s can be derived [*Yang and Koike*, 2005]. Locations of the stations are given by *Wang et al.* [2010a]. The stations have a higher density in Central America and Southeast Asia. A 12 month smooth is applied to R_s and T_a anomalies.

more efficient at water use and may use less water. This effect of CO_2 physiology may be important for the hydrological cycle on a century time scale [*R. A. Betts et al.*, 2007; *Gedney et al.*, 2006]. *Gedney et al.* [2006] attributed the variations in their constructed continental runoff in the twentieth century to the increase of stomatal resistance with increased CO_2 (the CO_2 physiology effect) because their model could not reproduce the variation in runoff with forcing only by known climate variations. They found that simulated trends in continental runoff were consistent with a CO_2 physiology effect [*Gedney et al.*, 2006]. The physiological effect of doubled CO_2 concentrations on plant transpiration could increase simulated global mean runoff by 6% relative to preindustrial levels [*R. A. Betts et al.*, 2007], as also was found in a simulation of the Community Land Model 3.5 (8.4%) [*Cao et al.*, 2010]. Several climate models have also indicated that in a 2 × CO_2 environment, T_a and P would increase but that Q would increase faster than P [*Bonan and Levis*, 2010; *Langley and Megonigal*, 2010; *Wang and Houlton*, 2009; *Zaehle et al.*, 2010].

[164] However, these results may be questionable in the following aspects: First, most models have not allowed their vegetation to increase leaf density as a response to the physiological effects of increased CO_2 and consequent changes in climate [*Way et al.*, 2011]. Some models did include these interactions but did not account for the nitrogen down regulation that reduces the plant's photosynthetic activity and as such resulted in a weak negative response for vegetation. If all the possible interactions were combined in climate simulations with 2 × CO_2, the associated increase in P could contribute more to an increase of E than of Q [*Bounoua et al.*, 2010].

[165] The current rate of increase in ambient CO_2 concentration is about 1.9 ppm yr^{-1}, which scaled from their estimate of the physiological impact of doubling by *R. A. Betts et al.* [2007] and *Cao et al.* [2010], implying a trend in global terrestrial E of about 0.09 kg m^{-2} yr^{-2} (or −0.0074 W m^{-2} yr^{-1}), a value much less than that resulting from R_s and P [*Jung et al.*, 2010; *Wang et al.*, 2010a]. In particular, the substantial increase of summer θ from 1958 to the mid 1990s in Ukraine and Russia can only be explained as a result of a downward trend in R_s, not as an effect of CO_2 physiology [*Robock and Li*, 2006]. Similarly, it is the decadal variability of P, not a CO_2 physiological effect, that explains most of the interannual and longer-term variability in streamflow from 1950 to 2000 [*Krakauer and Fung*, 2008]. The effect on P of CO_2 physiology is estimated to be much less than that of R_s [*Allen and Ingram*, 2002; *Andrews et al.*, 2009; *Bala et al.*, 2008].

[166] *Gedney et al.* [2006] inferred that their model could not reproduce the variation in runoff without the effect of CO_2 physiology. As shown in section 8.2, their observed runoff was based on insufficient streamflow data [*Peel and McMahon*, 2006] and its long-term trend is different from other recent estimates [*Dai et al.*, 2009]. Furthermore, a recent study shows that another model (Interactions Between Soil, Biosphere, and Atmosphere–Total Runoff Integrating Pathways, or ISBA-TRIP) can capture the observed trend in

river runoff during the 1960–1994 period over most continents without including land use changes and/or biophysical CO_2 effects, at least when the comparison is made over 154 large rivers and with a minimum amount of missing data [*Alkama et al.*, 2011].

9. CONCLUSIONS AND DISCUSSION

[167] Terrestrial evapotranspiration, E, is the transfer of water from land surfaces to the atmosphere through turbulence. The MOST theory relates these turbulence fluxes to the differences between mean temperature and humidity at two levels in a horizontally homogeneous and stationary constant flux layer. This theory was established several decades ago [*Foken*, 2006; *Garratt et al.*, 1996]; its universal functions and von Kármán constant were calibrated and evaluated by EC measurements during the 1970s to early 1980s when the EC method energy closure problem was not identified and corrected [*Hess et al.*, 1981; *Kader and Yaglom*, 1990; *Kaimal et al.*, 1976]. Hence, the MOST universal functions still need to be recalibrated with available λE and H fluxes. Its functions are appropriate for use in low-resolution models and assume flat, horizontally homogeneous surfaces and steady state conditions with neutral or weakly stable or unstable stratification. However, their capability over complex terrain and with increased-resolution models is not established [*Baklanov et al.*, 2011].

[168] Currently, there are six major methods that can provide continuous E estimations, i.e., EC, BR, weighable lysimeters, scintillometer, surface water balance, and atmosphere water balance methods. Estimates from a scintillometer depend on the MOST functions and the use of EC measurements to evaluate or calibrate these estimates. Weighable lysimeters supply independent measurements of E but represent a much smaller area than that of EC and BR measurements.

[169] Only the EC method provides a direct measure of the turbulent λE. However, it has suffered from an energy balance problem, very likely due to its not accounting for the contribution from the large eddies that contribute to E but do not touch down to the surface. Data coverage of the EC technique is only about 70% with losses from bad weather conditions and sensor failures. These gaps must be filled before the data can be used to infer monthly or annual values of E; however, the choice of gap-filling methodology may introduce a $\sim$5% uncertainty in annual values of E.

[170] The EC and BR methods are widely accepted and deployed to provide high-quality and high-temporal-resolution E data, such as the global FLUXNET and the U.S. ARM project. These observations provide E estimates at half-hour temporal resolution and reliable diurnal and seasonal variations of E at local scale. They have been widely used to investigate the controlling factors of E under different conditions and also provide key data sets for evaluation of satellite λE algorithms and land surface modeling simulations. However, since their measurements are of short duration and sparse spatial coverage, they cannot provide long-term regional or global estimates of E.

[171] The impact of environmental factors on E depends on climate conditions and land surface cover types, while vegetation has a consistent and positive impact on E. Available energy is the key determining factor for λE in hot tropical rain forests and boreal forests, as they are generally water unstressed. Furthermore, their root systems can extract water from deep soil and they have a relatively strong drought tolerance. In semiarid and arid regions, precipitation provides a good constraint on annual E. However, deep-rooted vegetation can result in values higher than those of annual precipitation. The heterogeneity and roughness of vegetation may make E over a wetland higher than that over open water. Temperate regions are more complicated, as no single factor is dominant.

[172] The MOST and the Penman-Monteith equations depend on turbulence, and so are partly empirical with assumptions needed. Further parameterizations and assumptions are needed to relate E to satellite-derived land surface variables. Although Penman-Monteith is in principle desirable from MOST and surface energy balance, in practice it is a very different approach. The MOST-like methods use $T_s - T_a$ and therefore require accurate estimates of both T_s and T_a. This sensitivity is substantially reduced by the Penman-Montheith-like methods that use available energy and canopy conductance, the latter of which is usually parameterized as a function of the vegetation index or leaf area index. These empirical parameterizations may require local calibration. Evaluation studies show that satellite-derived λE has an accuracy of about 15–30% [*Kalma et al.*, 2008] while the accuracy of EC measurements is 5–20% [*Foken*, 2008].

[173] Terrestrial surface water budget, P minus Q, provides an estimate of global mean E from 1.2 mm d^{-1} to 1.5 mm d^{-1}, with an average of 1.3 ± 0.1 mm d^{-1}. However, this estimate is only robust for multiyear averaged values because the terrestrial water storage change, one important component of water budget, is not available for this method. The GRACE observations show that terrestrial water storage change has substantial monthly and interannual variability.

[174] The availability of ground observations continues to be critical and should therefore strongly be fostered at the international level [*Seneviratne et al.*, 2010]. Any remote sensing–based assessment and model simulation is questionable without a solid evaluation with ground-based measurements [*Meir and Woodward*, 2010]. Most process-based land models were calibrated or evaluated with tower flux measurements of total λE and H fluxes [*Betts et al.*, 1996, 1998] or P-Q observations. Existing evaluation of LSM and satellite retrievals experiments focus on diurnal or seasonal variation of E. Because it occurs on many time scales [*Scott et al.*, 1997; *A. Wang et al.*, 2006], the capability of LSM and satellite remote sensing algorithms that have been evaluated on short time scales in predicting climatic variability of λE is still unclear because its variation at different time scales may be controlled by different variables. For example, at a spruce forest site at the Ore Mountains in Germany [*Clausnitzer et al.*, 2011], interannual variation of transpiration was strongly related to VPD and photosynthetically

active radiation (PAR; solar radiation in the visible band) while on a monthly or seasonal basis, the impact of precipitation was more important.

[175] Partitioning of E can be observed at a local scale. However, it is highly dependent on climate, vegetation structure, and precipitation intensity. Therefore, information as to how total λE is partitioned into soil evaporation, canopy evaporation, and canopy transpiration is lacking, and the LSM simulated ratios of global averaged vegetation transpiration to total evapotranspiration range from 0.25 to 0.64 for 10 widely accepted models, with an average of 0.42. Published evidence shows that existing LSMs have a spuriously strong sensitivity to soil moisture and drought, probably because they have difficulty in modeling water availability for transpiration.

[176] The following aspects could provide data to help to improve the LSM representations of E: Multiscale approaches combining multiple measuring methods may better constrain estimates of E fluxes [*McCabe and Wood*, 2006]; and multisensor approaches, in combination with available atmospheric observations, can be used to obtain a comprehensive and hydrometeorologically consistent characterization of the land surface water cycle [*McCabe et al.*, 2008]. Such new measurements are required [*Loescher et al.*, 2007] to (1) improve the integration between measurements and modeling methodologies, (2) improve the spatial resolution of measurements, (3) enhance our ability to take more and better measurements through distributed sensor networks, and (4) improve our ability to measure and quantify the subsurface hydrology.

[177] Carbon uptake and E are coupled together through photosynthesis [*Beer et al.*, 2007, 2010]. Consequently, the gross primary production and E are closely related [*Law et al.*, 2002; *Niyogi et al.*, 2009; *Schwalm et al.*, 2010]. Many studies have considered climate change and carbon uptake, including the impacts of diffuse radiation and nitrogen on carbon uptake. However, few studies address their influence on E. Further efforts should be paid to the coupled carbon and water cycle parameterizations in model development.

[178] The dependence of E on soil moisture has received much attention and has been parameterized in LSMs [*Koster et al.*, 2004; *Manabe*, 1969; *Sellers et al.*, 1997; *Seneviratne et al.*, 2010]. However, the climate dependence of E on soil moisture of most land surface models have not been validated for lack of reference data, in particular, accurate soil moisture data at a model grid scale [*Seneviratne et al.*, 2010]. A finer-resolution LSM, especially one with better resolved orography, would improve the prediction of the spatial patterns of E [*Gent et al.*, 2010]. Improving the representation of fundamental processes in LSMs rather than just optimizing parameters is key to improve land surface models [*Abramowitz et al.*, 2007; *Hogue et al.*, 2005].

NOTATION

α	Priestley-Taylor parameter.
β	Bowen ratio.
C_n^2	Structure parameter of the refractive index.
C_p	Specific heat of air.
C_q^2	Structure parameter of moisture.
C_t^2	Structure parameter of temperature.
Δ	Derivative of e_s with respect to T_a.
dw/dt	Terrestrial water storage change.
E	Terrestrial evapotranspiration.
E_{pa}	Pan evaporation.
E_{po}	Potential evaporation.
E_{soil}	Soil evaporation.
E_{veg}	Vegetation transpiration.
e_s	Saturated water vapor pressure.
G	Ground heat flux.
γ	Psychometric constant.
H	Sensible heat flux.
P	Precipitation
Q	River discharge.
θ	Soil moisture.
q	Specific humidity.
ρ	Air density.
r_c	Canopy resistance.
r_h	Aerodynamic resistance to heat transfer from surface to air.
R_n	Surface net radiation.
R_s	Surface incident solar radiation.
r_s	Stomatal resistance.
r_v	Aerodynamic resistance to water vapor transfer from surface to atmosphere.
T_a	Near-surface air temperature.
T_o	Aerodynamic air temperature at the surface.
T_s	Surface skin temperature.
T_{soil}	Soil temperature.
T_{veg}	Vegetation temperature.
λE	Latent heat flux.

[179] **ACKNOWLEDGMENTS.** K.W. is funded by the National Basic Research Program of China (2012CB955302 and 2010CB950504), National Natural Science Foundation of China (41175126), and the State Key Laboratory of Earth Surface Processes and Resource Ecology. R.E.D. is funded by DOE grant DE-SC0002246 and NSF grant ATM-0720619. We thank Martha Anderson, Jimenez Carlos, Joshua B. Fisher, William P. Kustas, Matthew McCabe, Qiaozhen Mu, and Brigitte Muller for their critical comments and suggestions. Xin Guo drew Figure 2. We acknowledge valuable suggestions from Steve Running and two anonymous reviewers.

[180] The Editor on this paper was Greg Okin. He thanks Steven Running and two anonymous reviewers.

REFERENCES

Abdulla, F. A., D. P. Lettenmaier, E. F. Wood, and J. A. Smith (1996), Application of a macroscale hydrologic model to estimate the water balance of the Arkansas Red River basin, *J. Geophys. Res.*, *101*(D3), 7449–7459, doi:10.1029/95JD02416.

Abramowitz, G., A. Pitman, H. Gupta, E. Kowalczyk, and Y. Wang (2007), Systematic bias in land surface models, *J. Hydrometeorol.*, *8*(5), 989–1001, doi:10.1175/JHM628.1.

Adam, J. C., and D. P. Lettenmaier (2003), Adjustment of global gridded precipitation for systematic bias, *J. Geophys. Res.*, *108*(D9), 4257, doi:10.1029/2002JD002499.

Adler, R. F., et al. (2003), The Version-2 Global Precipitation Climatology Project (GPCP) monthly precipitation analysis (1979–present), *J. Hydrometeorol.*, *4*(6), 1147–1167, doi:10.1175/1525-7541(2003)004<1147:TVGPCP>2.0.CO;2.

Admiral, S. W., P. M. Lafleur, and N. T. Roulet (2006), Controls on latent heat flux and energy partitioning at a peat bog in eastern Canada, *Agric. For. Meteorol.*, *140*(1–4), 308–321, doi:10.1016/j.agrformet.2006.03.017.

Agam, N., W. P. Kustas, M. C. Anderson, F. Q. Li, and P. D. Colaizzi (2008), Utility of thermal image sharpening for monitoring field-scale evapotranspiration over rainfed and irrigated agricultural regions, *Geophys. Res. Lett.*, *35*, L02402, doi:10.1029/2007GL032195.

Agrawal, M., and S. S. Deepak (2003), Physiological and biochemical responses of two cultivars of wheat to elevated levels of CO_2 and SO_2, singly and in combination, *Environ. Pollut.*, *121*(2), 189–197, doi:10.1016/S0269-7491(02)00222-1.

Ainsworth, E. A., and S. P. Long (2005), What have we learned from 15 years of free-air CO_2 enrichment (FACE)? A meta-analytic review of the responses of photosynthesis, canopy properties and plant production to rising CO_2, *New Phytol.*, *165*(2), 351–372, doi:10.1111/j.1469-8137.2004.01224.x.

Aires, L. M., C. A. Pio, and J. S. Pereira (2008), The effect of drought on energy and water vapour exchange above a Mediterranean C3/C4 grassland in southern Portugal, *Agric. For. Meteorol.*, *148*(4), 565–579, doi:10.1016/j.agrformet.2007.11.001.

Alavi, N., J. S. Warland, and A. A. Berg (2006), Filling gaps in evapotranspiration measurements for water budget studies: Evaluation of a Kalman filtering approach, *Agric. For. Meteorol.*, *141*(1), 57–66, doi:10.1016/j.agrformet.2006.09.011.

Alfieri, J. G., P. D. Blanken, D. N. Yates, and K. Steffen (2007), Variability in the environmental factors driving evapotranspiration from a grazed rangeland during severe drought conditions, *J. Hydrometeorol.*, *8*(2), 207–220, doi:10.1175/JHM569.1.

Alfieri, J. G., P. D. Blanken, D. Smith, and J. Morgan (2009), Concerning the measurement and magnitude of heat, water vapor, and carbon dioxide exchange from a semiarid grassland, *J. Appl. Meteorol. Climatol.*, *48*(5), 982–996, doi:10.1175/2008JAMC1873.1.

Alkama, R., B. Decharme, H. Douville, and A. Ribes (2011), Trends in global and basin-scale runoff over the late twentieth century: Methodological issues and sources of uncertainty, *J. Clim.*, *24*(12), 3000–3014, doi:10.1175/2010JCLI3921.1.

Allen, M. R., and W. J. Ingram (2002), Constraints on future changes in climate and the hydrologic cycle, *Nature*, *419*(6903), 224–232, doi:10.1038/nature01092.

Allen, R. G., L. S. Pereira, D. Raes, and M. Smith (1998), Crop evapotranspiration: Guidelines for computing crop water requirements, *FAO Irrig. Drain. Pap. 56*, Food and Agric. Organ. of the United Nations, Rome.

Allen, R. G., M. Tasumi, and R. Trezza (2007a), Satellite-based energy balance for mapping evapotranspiration with internalized calibration (METRIC)—Model, *J. Irrig. Drain. Eng.*, *133*(4), 380–394, doi:10.1061/(ASCE)0733-9437(2007)133:4(380).

Allen, R. G., M. Tasumi, A. Morse, R. Trezza, J. L. Wright, W. Bastiaanssen, W. Kramber, I. Lorite, and C. W. Robison (2007b), Satellite-based energy balance for mapping evapotranspiration with internalized calibration (METRIC)—Applications, *J. Irrig. Drain. Eng.*, *133*(4), 395–406, doi:10.1061/(ASCE)0733-9437(2007)133:4(395).

Alsdorf, D. E., E. Rodríguez, and D. P. Lettenmaier (2007), Measuring surface water from space, *Rev. Geophys.*, *45*, RG2002, doi:10.1029/2006RG000197.

Alves, I., and L. S. Pereira (2000), Modelling surface resistance from climatic variables?, *Agric. Water Manage.*, *42*(3), 371–385, doi:10.1016/S0378-3774(99)00041-4.

Anandakumar, K. (1999), Sensible heat flux over a wheat canopy: Optical scintillometer measurements and surface renewal analysis estimations, *Agric. For. Meteorol.*, *96*(1–3), 145–156, doi:10.1016/S0168-1923(99)00026-X.

Anderson, M. C., J. M. Norman, G. R. Diak, W. P. Kustas, and J. R. Mecikalski (1997), A two-source time-integrated model for estimating surface fluxes using thermal infrared remote sensing, *Remote Sens. Environ.*, *60*(2), 195–216, doi:10.1016/S0034-4257(96)00215-5.

Anderson, M. C., J. M. Norman, T. P. Meyers, and G. R. Diak (2000), An analytical model for estimating canopy transpiration and carbon assimilation fluxes based on canopy light-use efficiency, *Agric. For. Meteorol.*, *101*, 265–289, doi:10.1016/S0168-1923(99)00170-7.

Anderson, M. C., J. M. Norman, J. R. Mecikalski, R. D. Torn, W. P. Kustas, and J. B. Basara (2004), A multiscale remote sensing model for disaggregating regional fluxes to micrometeorological scales, *J. Hydrometeorol.*, *5*(2), 343–363, doi:10.1175/1525-7541(2004)005<0343:AMRSMF>2.0.CO;2.

Anderson, M. C., J. M. Norman, J. R. Mecikalski, J. A. Otkin, and W. P. Kustas (2007a), A climatological study of evapotranspiration and moisture stress across the continental United States based on thermal remote sensing: 2. Surface moisture climatology, *J. Geophys. Res.*, *112*, D11112, doi:10.1029/2006JD007507.

Anderson, M. C., J. M. Norman, J. R. Mecikalski, J. A. Otkin, and W. P. Kustas (2007b), A climatological study of evapotranspiration and moisture stress across the continental United States based on thermal remote sensing: 1. Model formulation, *J. Geophys. Res.*, *112*, D10117, doi:10.1029/2006JD007506.

Anderson, M. C., J. M. Norman, W. P. Kustas, R. Houborg, P. J. Starks, and N. Agam (2008), A thermal-based remote sensing technique for routine mapping of land-surface carbon, water and energy fluxes from field to regional scales, *Remote Sens. Environ.*, *112*(12), 4227–4241, doi:10.1016/j.rse.2008.07.009.

Anderson, R. G., and M. L. Goulden (2009), A mobile platform to constrain regional estimates of evapotranspiration, *Agric. For. Meteorol.*, *149*(5), 771–782, doi:10.1016/j.agrformet.2008.10.022.

Andrews, T., P. M. Forster, and J. M. Gregory (2009), A surface energy perspective on climate change, *J. Clim.*, *22*(10), 2557–2570, doi:10.1175/2008JCLI2759.1.

Angus, D. E., and P. J. Watts (1984), Evapotranspiration—How good is the Bowen ratio method?, *Agric. Water Manage.*, *8*(1–3), 133–150, doi:10.1016/0378-3774(84)90050-7.

Apple, M. E., D. M. Olszyk, D. P. Ormrod, A. Lewis, D. Southworth, and D. T. Tingey (2000), Morphology and stomatal function of Douglas fir needles exposed to climate chance: Elevated CO_2 and temperature, *Int. J. Plant Sci.*, *161*(1), 127–132, doi:10.1086/314237.

Arora, V. (2002), Modeling vegetation as a dynamic component in soil-vegetation-atmosphere transfer schemes and hydrological models, *Rev. Geophys.*, *40*(2), 1006, doi:10.1029/2001RG000103.

Asanuma, J., H. Ishikawa, I. Tamagawa, Y. M. Ma, T. Hayashi, Y. Q. Qi, and J. M. Wang (2005), Application of the band-pass covariance technique to portable flux measurements over the Tibetan Plateau, *Water Resour. Res.*, *41*, W09407, doi:10.1029/2005WR003954.

Aubinet, M., et al. (1999), Estimates of the annual net carbon and water exchange of forests: The EUROFLUX methodology, in *Advances in Ecological Research*, vol. 30, edited by A. Fitter and D. Rafaelli, pp. 113–175, Academic, San Diego, Calif., doi:10.1016/S0065-2504(08)60018-5.

Bailey, W. G., and J. A. Davies (1981), Evaporation from soybeans, *Boundary Layer Meteorol.*, *20*(4), 417–428, doi:10.1007/BF00122292.

Baker, I. T., L. Prihodko, A. S. Denning, M. Goulden, S. Miller, and H. R. da Rocha (2008), Seasonal drought stress in the Amazon: Reconciling models and observations, *J. Geophys. Res.*, *113*, G00B01, doi:10.1029/2007JG000644.

Baklanov, A. A., B. Grisogono, R. Bornstein, L. Mahrt, S. S. Zilitinkevich, P. Taylor, S. E. Larsen, M. W. Rotach, and H. J. S. Fernando (2011), The nature, theory, and modeling of atmospheric planetary boundary layers, *Bull. Am. Meteorol. Soc.*, *92*(2), 123–128, doi:10.1175/2010BAMS2797.1.

Bala, G., P. B. Duffy, and K. E. Taylor (2008), Impact of geoengineering schemes on the global hydrological cycle, *Proc. Natl. Acad. Sci. U. S. A.*, *105*(22), 7664–7669, doi:10.1073/pnas.0711648105.

Baldocchi, D. (2008), Breathing of the terrestrial biosphere: Lessons learned from a global network of carbon dioxide flux measurement systems, *Aust. J. Bot.*, *56*(1), 1–26, doi:10.1071/BT07151.

Baldocchi, D., R. Valentini, S. Running, W. Oechel, and R. Dahlman (1996), Strategies for measuring and modelling carbon dioxide and water vapour fluxes over terrestrial ecosystems, *Global Change Biol.*, *2*(3), 159–168, doi:10.1111/j.1365-2486.1996.tb00069.x.

Baldocchi, D., et al. (2001), FLUXNET: A new tool to study the temporal and spatial variability of ecosystem scale carbon dioxide, water vapor, and energy flux densities, *Bull. Am. Meteorol. Soc.*, *82*(11), 2415–2434, doi:10.1175/1520-0477(2001)082<2415:FANTTS>2.3.CO;2.

Ball, J. T., I. E. Woodrow, and J. A. Berry (1987), A model predicting stomatal conductance and its contribution to control of photosynthesis under different environmental conditions, in *Progress in Photosynthesis Research*, edited by J. Biggins, pp. 221–234, Martinus Nijhof, Zoetermeer, Netherlands.

Balsamo, G., A. Beljaars, K. Scipal, P. Viterbo, B. van den Hurk, M. Hirschi, and A. K. Betts (2009), A revised hydrology for the ECMWF model: Verification from field site to terrestrial water storage and impact in the Integrated Forecast System, *J. Hydrometeorol.*, *10*(3), 623–643, doi:10.1175/2008JHM1068.1.

Baroncini, F., F. Castelli, F. Caparrini, and S. Ruffo (2008), A dynamic cloud masking and filtering algorithm for MSG retrieval of land surface temperature, *Int. J. Remote Sens.*, *29*(12), 3365–3382, doi:10.1080/01431160701469032.

Barr, A. G., K. M. King, T. J. Gillespie, G. Hartog, and H. H. Neumann (1994), A comparison of Bowen ratio and eddy correlation sensible and latent heat flux measurements above deciduous forest, *Boundary Layer Meteorol.*, *71*(1–2), 21–41, doi:10.1007/BF00709218.

Bastiaanssen, W. G. M., M. Menenti, R. A. Feddes, and A. A. M. Holtslag (1998a), A remote sensing surface energy balance algorithm for land (SEBAL): 1. Formulation, *J. Hydrol.*, *212-213*(1–4), 198–212, doi:10.1016/S0022-1694(98)00253-4.

Bastiaanssen, W. G. M., H. Pelgrum, J. Wang, Y. Ma, J. F. Moreno, G. J. Roerink, and T. van der Wal (1998b), A remote sensing surface energy balance algorithm for land (SEBAL): 2. Validation, *J. Hydrol.*, *212-213*(1–4), 213–229, doi:10.1016/S0022-1694(98)00254-6.

Batra, N., S. Islam, V. Venturini, G. Bisht, and J. Jiang (2006), Estimation and comparison of evapotranspiration from MODIS and AVHRR sensors for clear sky days over the Southern Great Plains, *Remote Sens. Environ.*, *103*(1), 1–15, doi:10.1016/j.rse.2006.02.019.

Bausch, W. C., and T. M. Bernard (1992), Spatial averaging Bowen-ratio system: Description and lysimeter comparison, *Trans. ASAE*, *35*(1), 121–128.

Beck, C., J. Grieser, and B. Rudolf (2005), A new monthly precipitation climatology for the global land areas for the period 1951 to 2000, in *Climate Status Report 2004*, pp. 181–190, German Meteorol. Serv., Offenbach am Main, Germany. [Available at http://www.dwd.de/de/FundE/Klima/KLIS/prod/KSB/ksb04/28_precipitation.pdf]

Becker, F., and B. J. Choudhury (1988), Relative sensitivity of normalized difference vegetation index (NDVI) and microwave polarization difference index (MPDI) for vegetation and desertification monitoring, *Remote Sens. Environ.*, *24*(2), 297–311, doi:10.1016/0034-4257(88)90031-4.

Beer, C., M. Reichstein, P. Ciais, G. D. Farquhar, and D. Papale (2007), Mean annual GPP of Europe derived from its water balance, *Geophys. Res. Lett.*, *34*, L05401, doi:10.1029/2006GL029006.

Beer, C., et al. (2010), Terrestrial gross carbon dioxide uptake: Global distribution and covariation with climate, *Science*, *329*(5993), 834–838, doi:10.1126/science.1184984.

Beerling, D. J., J. Heath, F. I. Woodward, and T. A. Mansfield (1996), Drought-CO_2 interactions in trees observations and mechanisms, *New Phytol.*, *134*(2), 235–242, doi:10.1111/j.1469-8137.1996.tb04628.x.

Berbery, E. H., and E. M. Rasmusson (1999), Mississippi moisture budgets on regional scales, *Mon. Weather Rev.*, *127*(11), 2654–2673, doi:10.1175/1520-0493(1999)127<2654:MMBORS>2.0.CO;2.

Bernier, P. Y., P. Bartlett, T. A. Black, A. Barr, N. Kljun, and J. H. McCaughey (2006), Drought constraints on transpiration and canopy conductance in mature aspen and jack pine stands, *Agric. For. Meteorol.*, *140*(1–4), 64–78, doi:10.1016/j.agrformet.2006.03.019.

Betts, A. K., and C. Jakob (2002), Evaluation of the diurnal cycle of precipitation, surface thermodynamics, and surface fluxes in the ECMWF model using LBA data, *J. Geophys. Res.*, *107*(D20), 8045, doi:10.1029/2001JD000427.

Betts, A. K., J. H. Ball, A. C. M. Beljaars, M. J. Miller, and P. A. Viterbo (1996), The land surface-atmosphere interaction: A review based on observational and global modeling perspectives, *J. Geophys. Res.*, *101*(D3), 7209–7225, doi:10.1029/95JD02135.

Betts, A. K., P. Viterbo, A. Beljaars, H.-L. Pan, S.-Y. Hong, M. Goulden, and S. Wofsy (1998), Evaluation of land-surface interaction in ECMWF and NCEP/NCAR reanalysis models over grassland (FIFE) and boreal forest (BOREAS), *J. Geophys. Res.*, *103*(D18), 23,079–23,085, doi:10.1029/98JD02023.

Betts, A. K., M. Goulden, and S. Wofsy (1999), Controls on evaporation in a boreal spruce forest, *J. Clim.*, *12*(6), 1601–1618, doi:10.1175/1520-0442(1999)012<1601:COEIAB>2.0.CO;2.

Betts, A. K., J. H. Ball, and P. Viterbo (2003), Evaluation of the ERA-40 surface water budget and surface temperature for the Mackenzie River Basin, *J. Hydrometeorol.*, *4*(6), 1194–1211, doi:10.1175/1525-7541(2003)004<1194:EOTESW>2.0.CO;2.

Betts, A. K., J. H. Ball, A. G. Barr, T. A. Black, J. H. McCaughey, and P. Viterbo (2006), Assessing land-surface-atmosphere coupling in the ERA-40 reanalysis with boreal forest data, *Agric. For. Meteorol.*, *140*(1–4), 365–382, doi:10.1016/j.agrformet.2006.08.009.

Betts, A. K., R. L. Desjardins, and D. Worth (2007), Impact of agriculture, forest and cloud feedback on the surface energy budget in BOREAS, *Agric. For. Meteorol.*, *142*(2–4), 156–169, doi:10.1016/j.agrformet.2006.08.020.

Betts, R. A., et al. (2007), Projected increase in continental runoff due to plant responses to increasing carbon dioxide, *Nature*, *448*(7157), 1037–1041, doi:10.1038/nature06045.

Beven, K. (1979), Sensitivity analysis of the Penman-Monteith actual evapotranspiration estimates, *J. Hydrol.*, *44*(3–4), 169–190, doi:10.1016/0022-1694(79)90130-6.

Biemans, H., I. Haddeland, P. Kabat, F. Ludwig, R. W. A. Hutjes, J. Heinke, W. von Bloh, and D. Gerten (2011), Impact of reservoirs on river discharge and irrigation water supply during the 20th century, *Water Resour. Res.*, *47*, W03509, doi:10.1029/2009WR008929.

Bittner, S., U. Talkner, I. Krämer, F. Beese, D. Hölscher, and E. Priesack (2010), Modeling stand water budgets of mixed temperate broad-leaved forest stands by considering variations in species specific drought response, *Agric. For. Meteorol.*, *150*(10), 1347–1357, doi:10.1016/j.agrformet.2010.06.006.

Blad, B. L., and N. J. Rosenber (1974), Lysimetric calibration of the Bowen ratio–energy balance method for evapotranspiration estimation in the central Great Plains, *J. Appl. Meteorol.*, *13*(2), 227–236, doi:10.1175/1520-0450(1974)013<0227:LCOTBR>2.0.CO;2.

Blümel, K. (1999), A simple formula for estimation of the roughness length for heat transfer over partly vegetated surfaces, *J. Appl. Meteorol.*, *38*(6), 814–829, doi:10.1175/1520-0450(1999)038<0814:ASFFEO>2.0.CO;2.

Blyth, E. M., and R. J. Harding (1995), Application of aggregation models to surface heat flux from the Sahelian tiger bush, *Agric. For. Meteorol.*, *72*(3–4), 213–235, doi:10.1016/0168-1923(94)02164-F.

Blyth, E., J. Gash, A. Lloyd, M. Pryor, G. P. Weedon, and J. Shuttleworth (2010), Evaluating the JULES land surface model energy fluxes using FLUXNET data, *J. Hydrometeorol.*, *11*(2), 509–519, doi:10.1175/2009JHM1183.1.

Boer, G. J. (1993), Climate change and the regulation of the surface moisture and energy budgets, *Clim. Dyn.*, *8*(5), 225–239, doi:10.1007/BF00198617.

Bonan, G. B. (2008), Forests and climate change: Forcings, feedbacks, and the climate benefits of forests, *Science*, *320*(5882), 1444–1449, doi:10.1126/science.1155121.

Bonan, G. B., and S. Levis (2010), Quantifying carbon-nitrogen feedbacks in the Community Land Model (CLM4), *Geophys. Res. Lett.*, *37*, L07401, doi:10.1029/2010GL042430.

Bonan, G. B., P. J. Lawrence, K. W. Oleson, S. Levis, M. Jung, M. Reichstein, D. M. Lawrence, and S. C. Swenson (2011), Improving canopy processes in the Community Land Model version 4(CLM4) using global flux fields empirically inferred from FLUXNET data, *J. Geophys. Res.*, *116*, G02014, doi:10.1029/2010JG001593.

Boni, G., D. Entekhabi, and F. Castelli (2001a), Land data assimilation with satellite measurements for the estimation of surface energy balance components and surface control on evaporation, *Water Resour. Res.*, *37*(6), 1713–1722, doi:10.1029/2001WR900020.

Boni, G., F. Castelli, and D. Entekhabi (2001b), Sampling strategies and assimilation of ground temperature for the estimation of surface energy balance components, *IEEE Trans. Geosci. Remote Sens.*, *39*(1), 165–172, doi:10.1109/36.898678.

Bosilovich, M. G., J. D. Radakovich, A. da Silva, R. Todling, and F. Verter (2007), Skin temperature analysis and bias correction in a coupled land-atmosphere data assimilation system, *J. Meteorol. Soc. Jpn.*, *85A*, 205–228, doi:10.2151/jmsj.85A.205.

Bounoua, L., F. G. Hall, P. J. Sellers, A. Kumar, G. J. Collatz, C. J. Tucker, and M. L. Imhoff (2010), Quantifying the negative feedback of vegetation to greenhouse warming: A modeling approach, *Geophys. Res. Lett.*, *37*, L23701, doi:10.1029/2010GL045338.

Bovard, B. D., P. S. Curtis, C. S. Vogel, H. B. Su, and H. P. Schmid (2005), Environmental controls on sap flow in a northern hardwood forest, *Tree Physiol.*, *25*(1), 31–38, doi:10.1093/treephys/25.1.31.

Bowen, I. S. (1926), The ratio of heat losses by conduction and by evaporation from any water surface, *Phys. Rev.*, *27*(6), 779, doi:10.1103/PhysRev.27.779.

Brauman, K. A., D. L. Freyberg, and G. C. Daily (2010), Forest structure influences on rainfall partitioning and cloud interception: A comparison of native forest sites in Kona, Hawai'i, *Agric. For. Meteorol.*, *150*(2), 265–275, doi:10.1016/j.agrformet.2009.11.011.

Bréda, N., R. Huc, A. Granier, and E. Dreyer (2006), Temperate forest trees and stands under severe drought: A review of ecophysiological responses, adaptation processes and long-term consequences, *Ann. For. Sci.*, *63*(6), 625–644, doi:10.1051/forest:2006042.

Brotzge, J. A., and K. C. Crawford (2003), Examination of the surface energy budget: A comparison of eddy correlation and Bowen ratio measurement systems, *J. Hydrometeorol.*, *4*(2), 160–178, doi:10.1175/1525-7541(2003)4<160:EOTSEB>2.0.CO;2.

Brown, S., S. Desai, S. Keihm, W. W. Lu, and C. Ruf (2007), Ocean water vapor and cloud burden trends derived from the TOPEX Microwave Radiometer, in *IGARSS: 2007 IEEE International Geoscience and Remote Sensing Symposium*, vol. 1-12, *Sensing and Understanding Our Planet*, pp. 886–889, Inst. of Electr. and Electron. Eng., New York.

Brown, S. M., R. M. Petrone, C. Mendoza, and K. J. Devito (2010), Surface vegetation controls on evapotranspiration from a subhumid western boreal plain wetland, *Hydrol. Processes*, *24*(8), 1072–1085, doi:10.1002/hyp.7569.

Brunel, J.-P., G. R. Walker, and A. K. Kennett-Smith (1995), Field validation of isotopic procedures for determining sources of water used by plants in a semi-arid environment, *J. Hydrol.*, *167*(1–4), 351–368, doi:10.1016/0022-1694(94)02575-V.

Brunel, J. P., G. R. Walker, J. C. Dighton, and B. Monteny (1997), Use of stable isotopes of water to determine the origin of water used by the vegetation and to partition evapotranspiration: A case study from HAPEX-Sahel, *J. Hydrol.*, *188–189*, 466–481, doi:10.1016/S0022-1694(96)03188-5.

Brunsell, N. A., J. M. Ham, and C. E. Owensby (2008), Assessing the multi-resolution information content of remotely sensed variables and elevation for evapotranspiration in a tall-grass prairie environment, *Remote Sens. Environ.*, *112*(6), 2977–2987, doi:10.1016/j.rse.2008.02.002.

Brutsaert, W. (1999), Aspects of bulk atmospheric boundary layer similarity under free-convective conditions, *Rev. Geophys.*, *37*(4), 439–451, doi:10.1029/1999RG900013.

Brutsaert, W. (2006), Indications of increasing land surface evaporation during the second half of the 20th century, *Geophys. Res. Lett.*, *33*(20), L20403, doi:10.1029/2006GL027532.

Brutsaert, W., and D. Chen (1995), Desorption and the two stages of drying of natural tallgrass prairie, *Water Resour. Res.*, *31*(5), 1305–1313, doi:10.1029/95WR00323.

Brutsaert, W., and M. B. Parlange (1998), Hydrologic cycle explains the evaporation paradox, *Nature*, *396*(6706), 30, doi:10.1038/23845.

Brutsaert, W., and H. Stricker (1979), Advection-aridity approach to estimate actual regional evapotranspiration, *Water Resour. Res.*, *15*(2), 443–450, doi:10.1029/WR015i002p00443.

Bucci, S. J., F. G. Scholz, G. Goldstein, W. A. Hoffmann, F. C. Meinzer, A. C. Franco, T. Giambelluca, and F. Miralles-Wilhelm (2008), Controls on stand transpiration and soil water utilization along a tree density gradient in a neotropical savanna, *Agric. For. Meteorol.*, *148*(6–7), 839–849, doi:10.1016/j.agrformet.2007.11.013.

Bunce, J. A. (2004), Carbon dioxide effects on stomatal responses to the environment and water use by crops under field conditions, *Oecologia*, *140*(1), 1–10, doi:10.1007/s00442-003-1401-6.

Burba, G. G., and S. B. Verma (2005), Seasonal and interannual variability in evapotranspiration of native tallgrass prairie and cultivated wheat ecosystems, *Agric. For. Meteorol.*, *135*(1–4), 190–201, doi:10.1016/j.agrformet.2005.11.017.

Burgess, S. S. O., M. A. Adams, N. C. Turner, C. R. Beverly, C. K. Ong, A. A. H. Khan, and T. M. Bleby (2001), An improved heat pulse method to measure low and reverse rates of sap flow in woody plants, *Tree Physiol.*, *21*(9), 589–598, doi:10.1093/treephys/21.9.589.

Businger, J. A., J. C. Wyngaard, Y. Izumi, and E. F. Bradley (1971), Flux-profile relationships in atmospheric surface layer, *J. Atmos. Sci.*, *28*(2), 181–189, doi:10.1175/1520-0469(1971)028<0181:FPRITA>2.0.CO;2.

Calder, I. R. (1976), Measurement of water losses from a forested area using a natural lysimeter, *J. Hydrol.*, *30*(4), 311–325, doi:10.1016/0022-1694(76)90115-3.

Calvet, J. C., A. L. Gibelin, J. L. Roujean, E. Martin, P. Le Moigne, H. Douville, and J. Noilhan (2007), Past and future scenarios of the effect of carbon dioxide on plant growth and transpiration for three vegetation types of southwestern France, *Atmos. Chem. Phys. Discuss.*, *7*(2), 4761–4779, doi:10.5194/acpd-7-4761-2007.

Canadell, J., R. B. Jackson, J. B. Ehleringer, H. A. Mooney, O. E. Sala, and E. D. Schulze (1996), Maximum rooting depth of vegetation types at the global scale, *Oecologia*, *108*(4), 583–595, doi:10.1007/BF00329030.

Cao, L., G. Bala, K. Caldeira, R. Nemani, and G. Ban-Weiss (2010), Importance of carbon dioxide physiological forcing to future climate change, *Proc. Natl. Acad. Sci. U. S. A.*, *107*(21), 9513–9518, doi:10.1073/pnas.0913000107.

Caparrini, F., F. Castelli, and D. Entekhabi (2003), Mapping of land-atmosphere heat fluxes and surface parameters with remote sensing data, *Boundary Layer Meteorol.*, *107*(3), 605–633, doi:10.1023/A:1022821718791.

Caparrini, F., F. Castelli, and D. Entekhabi (2004a), Estimation of surface turbulent fluxes through assimilation of radiometric surface temperature sequences, *J. Hydrometeorol.*, *5*(1), 145–159, doi:10.1175/1525-7541(2004)005<0145:EOSTFT>2.0.CO;2.

Caparrini, F., F. Castelli, and D. Entekhabi (2004b), Variational estimation of soil and vegetation turbulent transfer and heat flux parameters from sequences of multisensor imagery, *Water Resour. Res.*, *40*, W12515, doi:10.1029/2004WR003358.

Carlson, T. (2007), An overview of the "triangle method" for estimating surface evapotranspiration and soil moisture from satellite imagery, *Sensors*, *7*(8), 1612–1629, doi:10.3390/s7081612.

Caselles, V., M. M. Artigao, E. Hurtado, C. Coll, and A. Brasa (1998), Mapping actual evapotranspiration by combining landsat TM and NOAA-AVHRR images: Application to the Barrax area, Albacete, Spain, *Remote Sens. Environ.*, *63*(1), 1–10, doi:10.1016/S0034-4257(97)00108-9.

Castelli, F., D. Entekhabi, and E. Caporali (1999), Estimation of surface heat flux and an index of soil moisture using adjoint-state surface energy balance, *Water Resour. Res.*, *35*(10), 3115–3125, doi:10.1029/1999WR900140.

Castellvi, F., and R. L. Snyder (2009), Sensible heat flux estimates using surface renewal analysis: A study case over a peach orchard, *Agric. For. Meteorol.*, *149*(9), 1397–1402.

Castellvi, F., A. Martinez-Cob, and O. Perez-Coveta (2006), Estimating sensible and latent heat fluxes over rice using surface renewal, *Agric. For. Meteorol.*, *139*(1–2), 164–169, doi:10.1016/j.agrformet.2006.07.005.

Castellvi, F., R. L. Snyder, and D. D. Baldocchi (2008), Surface energy-balance closure over rangeland grass using the eddy covariance method and surface renewal analysis, *Agric. For. Meteorol.*, *148*(6–7), 1147–1160, doi:10.1016/j.agrformet.2008.02.012.

Chahine, M. T. (1992), The hydrological cycle and its influence on climate, *Nature*, *359*(6394), 373–380, doi:10.1038/359373a0.

Chang, X., W. Zhao, Z. Zhang, and Y. Su (2006), Sap flow and tree conductance of shelter-belt in arid region of China, *Agric. For. Meteorol.*, *138*(1–4), 132–141, doi:10.1016/j.agrformet.2006.04.003.

Chávez, J. L., T. A. Howell, and K. S. Copeland (2009), Evaluating eddy covariance cotton ET measurements in an advective environment with large weighing lysimeters, *Irrig. Sci.*, *28*(1), 35–50, doi:10.1007/s00271-009-0179-7.

Chehbouni, A., D. Lo Seen, E. G. Njoku, and B. M. Monteny (1996), Examination of the difference between radiative and aerodynamic surface temperatures over sparsely vegetated surfaces, *Remote Sens. Environ.*, *58*(2), 177–186, doi:10.1016/S0034-4257(96)00037-5.

Chehbouni, A., C. Watts, J. P. Lagouarde, Y. H. Kerr, J. C. Rodriguez, J. M. Bonnefond, F. Santiago, G. Dedieu, D. C. Goodrich, and C. Unkrich (2000), Estimation of heat and momentum fluxes over complex terrain using a large aperture scintillometer, *Agric. For. Meteorol.*, *105*(1–3), 215–226, doi:10.1016/S0168-1923(00)00187-8.

Chen, D. Y., and W. Brutsaert (1995), Diagnostics of land surface spatial variability and water vapor flux, *J. Geophys. Res.*, *100*(D12), 25,595–25,606, doi:10.1029/95JD00973.

Chen, F., and Y. Zhang (2009), On the coupling strength between the land surface and the atmosphere: From viewpoint of surface exchange coefficients, *Geophys. Res. Lett.*, *36*, L10404, doi:10.1029/2009GL037980.

Chen, J. L., C. R. Wilson, J. S. Famiglietti, and M. Rodell (2005), Spatial sensitivity of the Gravity Recovery and Climate Experiment (GRACE) time-variable gravity observations, *J. Geophys. Res.*, *110*, B08408, doi:10.1029/2004JB003536.

Chen, M., P. Xie, J. E. Janowiak, and P. A. Arkin (2002), Global land precipitation: A 50-yr monthly analysis based on gauge observations, *J. Hydrometeorol.*, *3*(3), 249–266, doi:10.1175/1525-7541(2002)003<0249:GLPAYM>2.0.CO;2.

Chen, S., J. Chen, G. Lin, W. Zhang, H. Miao, L. Wei, J. Huang, and X. Han (2009), Energy balance and partition in Inner Mongolia steppe ecosystems with different land use types, *Agric. For. Meteorol.*, *149*(11), 1800–1809, doi:10.1016/j.agrformet.2009.06.009.

Choi, M., W. P. Kustas, M. C. Anderson, R. G. Allen, F. Li, and J. H. Kjaersgaard (2009), An intercomparison of three remote sensing-based surface energy balance algorithms over a corn and soybean production region (Iowa, U.S.) during SMACEX, *Agric. For. Meteorol.*, *149*(12), 2082–2097, doi:10.1016/j.agrformet.2009.07.002.

Choudhury, B. J. (1994), Synergism of multispectral satellite-observations for estimating regional land-surface evaporation, *Remote Sens. Environ.*, *49*(3), 264–274, doi:10.1016/0034-4257(94)90021-3.

Church, T. M. (1996), An underground route for the water cycle, *Nature*, *380*(6575), 579–580, doi:10.1038/380579a0.

Clausnitzer, F., B. Köstner, K. Schwärzel, and C. Bernhofer (2011), Relationships between canopy transpiration, atmospheric conditions and soil water availability—Analyses of long-term sap-flow measurements in an old Norway spruce forest at the Ore Mountains/Germany, *Agric. For. Meteorol.*, *151*(8), 1023–1034, doi:10.1016/j.agrformet.2011.04.007.

Cleugh, H. A., R. Leuning, Q. Mu, and S. W. Running (2007), Regional evaporation estimates from flux tower and MODIS satellite data, *Remote Sens. Environ.*, *106*(3), 285–304, doi:10.1016/j.rse.2006.07.007.

Clothier, B. E., K. L. Clawson, P. J. Pinter, M. S. Moran, R. J. Reginato, and R. D. Jackson (1986), Estimation of soil heat flux from net radiation during the growth of alfalfa, *Agric. For. Meteorol.*, *37*(4), 319–329, doi:10.1016/0168-1923(86)90069-9.

Collatz, G. J., J. T. Ball, C. Grivet, and J. A. Berry (1991), Physiological and environmental regulation of stomatal conductance, photosynthesis and transpiration: A model that includes a laminar boundary layer, *Agric. For. Meteorol.*, *54*(2–4), 107–136, doi:10.1016/0168-1923(91)90002-8.

Cook, D. R. (2007), Energy balance Bowen ratio (EBBR) handbook, Clim. Res. Facil., U.S. Dep. of Energy, Washington, D. C. [Available at http://www.arm.gov/instruments/ebbr.]

Costa, M. H., J. C. Souza-Filho, and A. Ribeiro (2004), Comments on "The regional evapotranspiration of the Amazon," *J. Hydrometeorol.*, *5*(6), 1279–1280, doi:10.1175/JHM-393.1.

Costa, M. H., M. C. Biajoli, L. Sanches, A. C. M. Malhado, L. R. Hutyra, H. R. da Rocha, R. G. Aguiar, and A. C. de Araújo (2010), Atmospheric versus vegetation controls of Amazonian tropical rain forest evapotranspiration: Are the wet and seasonally dry rain forests any different?, *J. Geophys. Res.*, *115*, G04021, doi:10.1029/2009JG001179.

Crago, R., and R. Crowley (2005), Complementary relationships for near-instantaneous evaporation, *J. Hydrol.*, *300*(1–4), 199–211, doi:10.1016/j.jhydrol.2004.06.002.

Cramer, W., et al. (2001), Global response of terrestrial ecosystem structure and function to CO_2 and climate change: Results from six dynamic global vegetation models, *Global Change Biol.*, *7*(4), 357–373, doi:10.1046/j.1365-2486.2001.00383.x.

Crow, W., and W. Kustas (2005), Utility of assimilating surface radiometric temperature observations for evaporative fraction and heat transfer coefficient retrieval, *Boundary Layer Meteorol.*, *115*(1), 105–130, doi:10.1007/s10546-004-2121-0.

Crow, W. T., and E. F. Wood (2003), The assimilation of remotely sensed soil brightness temperature imagery into a land surface model using Ensemble Kalman filtering: A case study based on ESTAR measurements during SGP97, *Adv. Water Resour.*, *26*(2), 137–149, doi:10.1016/S0309-1708(02)00088-X.

Crow, W. T., W. P. Kustas, and J. H. Prueger (2008), Monitoring root-zone soil moisture through the assimilation of a thermal remote sensing-based soil moisture proxy into a water balance model, *Remote Sens. Environ.*, *112*(4), 1268–1281, doi:10.1016/j.rse.2006.11.033.

Culf, A. D. (1994), Equilibrium evaporation beneath a growing convective boundary layer, *Boundary Layer Meteorol.*, *70*(1–2), 37–49, doi:10.1007/BF00712522.

Cure, J. D., and B. Acock (1986), Crop responses to carbon dioxide doubling: A literature survey, *Agric. For. Meteorol.*, *38*(1–3), 127–145, doi:10.1016/0168-1923(86)90054-7.

Dai, A. (2006), Recent climatology, variability, and trends in global surface humidity, *J. Clim.*, *19*(15), 3589–3606, doi:10.1175/JCLI3816.1.

Dai, A., and K. E. Trenberth (2002), Estimates of freshwater discharge from continents: Latitudinal and seasonal variations, *J. Hydrometeorol.*, *3*(6), 660–687, doi:10.1175/1525-7541(2002)003<0660:EOFDFC>2.0.CO;2.

Dai, A., I. Y. Fung, and A. D. Del Genio (1997), Surface observed global land precipitation variations during 1900–88, *J. Clim.*, *10*(11), 2943–2962, doi:10.1175/1520-0442(1997)010<2943:SOGLPV>2.0.CO;2.

Dai, A., T. T. Qian, K. E. Trenberth, and J. D. Milliman (2009), Changes in continental freshwater discharge from 1948 to 2004, *J. Clim.*, *22*(10), 2773–2792, doi:10.1175/2008JCLI2592.1.

David, T. S., M. I. Ferreira, S. Cohen, J. S. Pereira, and J. S. David (2004), Constraints on transpiration from an evergreen oak tree in southern Portugal, *Agric. For. Meteorol.*, *122*(3–4), 193–205, doi:10.1016/j.agrformet.2003.09.014.

Dawson, T. E., S. S. O. Burgess, K. P. Tu, R. S. Oliveira, L. S. Santiago, J. B. Fisher, K. A. Simonin, and A. R. Ambrose (2007), Nighttime transpiration in woody plants from contrasting ecosystems, *Tree Physiol.*, *27*(4), 561–575, doi:10.1093/treephys/27.4.561.

Deardorff, J. W. (1978), Efficient prediction of ground surface temperature and moisture, with inclusion of a layer of vegetation, *J. Geophys. Res.*, *83*(C4), 1889–1903, doi:10.1029/JC083iC04p01889.

DeBruin, H. A. R. (2009), Time to think: Reflections of a pre-pensioned scintillometer researcher, *Bull. Am. Meteorol. Soc.*, *90*(5), ES17–ES26, doi:10.1175/2008BAMS2704.2.

de Bruin, H. A. R., W. Kohsiek, and B. J. J. M. Hurk (1993), A verification of some methods to determine the fluxes of momentum, sensible heat, and water vapour using standard deviation and structure parameter of scalar meteorological quantities, *Boundary Layer Meteorol.*, *63*(3), 231–257, doi:10.1007/BF00710461.

den Hartog, G., H. H. Neumann, K. M. King, and A. C. Chipanshi (1994), Energy budget measurements using eddy correlation and Bowen ratio techniques at the Kinosheo Lake tower site during the Northern Wetlands Study, *J. Geophys. Res.*, *99*(D1), 1539–1549, doi:10.1029/93JD00032.

Denmead, O. T., and I. C. McIlroy (1970), Measurements of non-potential evaporation from wheat, *Agric. Meteorol.*, *7*, 285–302, doi:10.1016/0002-1571(70)90024-5.

Detto, M., N. Montaldo, J. D. Albertson, M. Mancini, and G. Katul (2006), Soil moisture and vegetation controls on evapotranspiration in a heterogeneous Mediterranean ecosystem on Sardinia, Italy, *Water Resour. Res.*, *42*, W08419, doi:10.1029/2005WR004693.

Di Baldassarre, G., and A. Montanari (2009), Uncertainty in river discharge observations: A quantitative analysis, *Hydrol. Earth Syst. Sci.*, *13*(6), 913–921, doi:10.5194/hess-13-913-2009.

Dickinson, R. E. (2011), Coupling atmospheric circulation models to bio-physical, bio-chemical, and biological processes at the land surface, in *The Development of Atmospheric General Circulation Models: Complexity, Synthesis and Computation*, edited by L. Donner, W. Schubert, and R. Somerville, pp. 177–197, Cambridge Univ. Press, Cambridge, U. K.

Dickinson, R. E. (2012), Interaction between future climate and terrestrial carbon and nitrogen, in *The Future of the World's Climate*, edited by A. Henderson-Sellers and K. McGuffie, pp. 289–308, Elsevier, Waltham, Mass.

Dickinson, R. E., A. Henderson-Sellers, C. Rosenzweig, and P. J. Sellers (1991), Evapotranspiration models with canopy resistance for use in climate models: A review, *Agric. For. Meteorol.*, *54*(2–4), 373–388, doi:10.1016/0168-1923(91)90014-H.

Dickinson, R. E., et al. (2002), Nitrogen controls on climate model evapotranspiration, *J. Clim.*, *15*(3), 278–295, doi:10.1175/1520-0442(2002)015<0278:NCOCME>2.0.CO;2.

Dijkstra, P., A. H. M. C. Schapendonk, K. O. Groenwold, M. Jansen, and S. C. Van De Geijn (1999), Seasonal changes in the response of winter wheat to elevated atmospheric CO_2 concentration grown in open-top chambers and field tracking enclosures, *Global Change Biol.*, *5*(5), 563–576, doi:10.1046/j.1365-2486.1999.00249.x.

Dirmeyer, P. A., A. J. Dolman, and N. Sato (1999), The pilot phase of the Global Soil Wetness Project, *Bull. Am. Meteorol. Soc.*, *80*(5), 851–878, doi:10.1175/1520-0477(1999)080<0851:TPPOTG>2.0.CO;2.

Dirmeyer, P. A., Z. Guo, and X. Gao (2004), Comparison, validation, and transferability of eight multiyear global soil wetness products, *J. Hydrometeorol.*, *5*(6), 1011–1033, doi:10.1175/JHM-388.1.

Dirmeyer, P. A., X. Gao, M. Zhao, Z. Guo, T. Oki, and N. Hanasaki (2006), GSWP-2: Multimodel analysis and implications for our perception of the land surface, *Bull. Am. Meteorol. Soc.*, *87*(10), 1381–1397, doi:10.1175/BAMS-87-10-1381.

Döll, P., K. Fiedler, and J. Zhang (2009), Global-scale analysis of river flow alterations due to water withdrawals and reservoirs, *Hydrol. Earth Syst. Sci.*, *13*(12), 2413–2432, doi:10.5194/hess-13-2413-2009.

Dolman, A. J. (1993), A multiple-source land surface energy balance model for use in general circulation models, *Agric. For. Meteorol.*, *65*(1–2), 21–45, doi:10.1016/0168-1923(93)90036-H.

Dominguez, F., and P. Kumar (2008), Precipitation recycling variability and ecoclimatological stability—A study using NARR data: Part I. Central U.S. plains ecoregion, *J. Clim.*, *21*(20), 5165–5186, doi:10.1175/2008JCLI1756.1.

Dominguez, F., P. Kumar, and E. R. Vivoni (2008), Precipitation recycling variability and ecoclimatological stability—A study using NARR data: Part II. North American monsoon region, *J. Clim.*, *21*(20), 5187–5203, doi:10.1175/2008JCLI1760.1.

Donohue, R. J., M. L. Roderick, and T. R. McVicar (2007), On the importance of including vegetation dynamics in Budyko's hydrological model, *Hydrol. Earth Syst. Sci.*, *11*(2), 983–995, doi:10.5194/hess-11-983-2007.

Drexler, J. Z., R. L. Snyder, D. Spano, and K. T. U. Paw (2004), A review of models and micrometeorological methods used to estimate wetland evapotranspiration, *Hydrol. Processes*, *18*(11), 2071–2101, doi:10.1002/hyp.1462.

Du, S., Y.-L. Wang, T. Kume, J.-G. Zhang, K. Otsuki, N. Yamanaka, and G.-B. Liu (2011), Sapflow characteristics and climatic responses in three forest species in the semiarid Loess Plateau region of China, *Agric. For. Meteorol.*, *151*(1), 1–10, doi:10.1016/j.agrformet.2010.08.011.

Dugas, W. A., L. J. Fritschen, L. W. Gay, A. A. Held, A. D. Matthias, D. C. Reicosky, P. Steduto, and J. L. Steiner (1991), Bowen-ratio, eddy-correlation, and portable chamber measurements of sensible and latent-heat flux over irrigated spring wheat, *Agric. For. Meteorol.*, *56*(1–2), 1–20, doi:10.1016/0168-1923(91)90101-U.

Durre, I., C. N. Williams, X. G. Yin, and R. S. Vose (2009), Radiosonde-based trends in precipitable water over the Northern

Hemisphere: An update, *J. Geophys. Res.*, *114*, D05112, doi:10.1029/2008JD010989.
Dye, P. J., B. W. Olbrich, and A. G. Poulter (1991), The influence of growth rings in Pinus patula on heat pulse velocity and sap flow measurement, *J. Exp. Bot.*, *42*(7), 867–870, doi:10.1093/jxb/42.7.867.
Dyer, A. J. (1974), A review of flux-profile relationships, *Boundary Layer Meteorol.*, *7*(3), 363–372, doi:10.1007/BF00240838.
Eltahir, E. A. B., and R. L. R. L. Bras (1996), Precipitation recycling, *Rev. Geophys.*, *34*(3), 367–378, doi:10.1029/96RG01927.
Entin, J. K., A. Robock, K. Y. Vinnikov, V. Zabelin, S. X. Liu, A. Namkhai, and T. Adyasuren (1999), Evaluation of Global Soil Wetness Project soil moisture simulations, *J. Meteorol. Soc. Jpn.*, *77*(1B), 183–198.
Eugster, W., et al. (2000), Land-atmosphere energy exchange in Arctic tundra and boreal forest: Available data and feedbacks to climate, *Global Change Biol.*, *6*, 84–115, doi:10.1046/j.1365-2486.2000.06015.x.
Falge, E., et al. (2001a), Gap filling strategies for defensible annual sums of net ecosystem exchange, *Agric. For. Meteorol.*, *107*(1), 43–69, doi:10.1016/S0168-1923(00)00225-2.
Falge, E., et al. (2001b), Gap filling strategies for long term energy flux data sets, *Agric. For. Meteorol.*, *107*(1), 71–77, doi:10.1016/S0168-1923(00)00235-5.
Farahani, H. J., T. A. Howell, W. J. Shuttleworth, and W. C. Bausch (2007), Evapotranspiration: Progress in measurement and modeling in agriculture, *Trans. ASABE*, *50*(5), 1627–1638.
Ferguson, P. R., and J. Veizer (2007), Coupling of water and carbon fluxes via the terrestrial biosphere and its significance to the Earth's climate system, *J. Geophys. Res.*, *112*, D24S06, doi:10.1029/2007JD008431.
Fernández, J. E., P. J. Durán, M. J. Palomo, A. Diaz-Espejo, V. Chamorro, and I. F. Girón (2006), Calibration of sap flow estimated by the compensation heat pulse method in olive, plum and orange trees: Relationships with xylem anatomy, *Tree Physiol.*, *26*(6), 719–728, doi:10.1093/treephys/26.6.719.
Finnigan, J. J. (2004), A re-evaluation of long-term flux measurement techniques: Part II. Coordinate systems, *Boundary Layer Meteorol.*, *113*(1), 1–41, doi:10.1023/B:BOUN.0000037348.64252.45.
Finnigan, J. J., R. Clement, Y. Malhi, R. Leuning, and H. A. Cleugh (2003), A re-evaluation of long-term flux measurement techniques: Part I. Averaging and coordinate rotation, *Boundary Layer Meteorol.*, *107*(1), 1–48, doi:10.1023/A:1021554900225.
Finzi, A. C., et al. (2007), Increases in nitrogen uptake rather than nitrogen-use efficiency support higher rates of temperate forest productivity under elevated CO_2, *Proc. Natl. Acad. Sci. U. S. A.*, *104*(35), 14,014–14,019, doi:10.1073/pnas.0706518104.
Fisher, J. B., T. A. DeBiase, Y. Qi, M. Xu, and A. H. Goldstein (2005), Evapotranspiration models compared on a Sierra Nevada forest ecosystem, *Environ. Modell. Software*, *20*(6), 783–796, doi:10.1016/j.envsoft.2004.04.009.
Fisher, J. B., D. D. Baldocchi, L. Misson, T. E. Dawson, and A. H. Goldstein (2007), What the towers don't see at night: Nocturnal sap flow in trees and shrubs at two AmeriFlux sites in California, *Tree Physiol.*, *27*(4), 597–610, doi:10.1093/treephys/27.4.597.
Fisher, J. B., K. P. Tu, and D. D. Baldocchi (2008), Global estimates of the land-atmosphere water flux based on monthly AVHRR and ISLSCP-II data, validated at 16 FLUXNET sites, *Remote Sens. Environ.*, *112*(3), 901–919, doi:10.1016/j.rse.2007.06.025.
Fisher, J. B., et al. (2009), The land-atmosphere water flux in the tropics, *Global Change Biol.*, *15*(11), 2694–2714, doi:10.1111/j.1365-2486.2008.01813.x.
Fisher, J. B., R. J. Whittaker, and Y. Malhi (2011), ET come home: Potential evapotranspiration in geographical ecology, *Global Ecol. Biogeogr.*, *20*(1), 1–18, doi:10.1111/j.1466-8238.2010.00578.x.
Fisher, R. A., M. Williams, M. de Lourdes Ruivo, A. L. de Costa, and P. Meir (2008), Evaluating climatic and soil water controls on evapotranspiration at two Amazonian rainforest sites, *Agric. For. Meteorol.*, *148*(6–7), 850–861, doi:10.1016/j.agrformet.2007.12.001.
Foken, T. (2006), 50 years of the Monin-Obukhov similarity theory, *Boundary Layer Meteorol.*, *119*(3), 431–447, doi:10.1007/s10546-006-9048-6.
Foken, T. (2008), The energy balance closure problem: An overview, *Ecol. Appl.*, *18*(6), 1351–1367, doi:10.1890/06-0922.1.
Foken, T., F. Wimmer, M. Mauder, C. Thomas, and C. Liebethal (2006), Some aspects of the energy balance closure problem, *Atmos. Chem. Phys.*, *6*, 4395–4402, doi:10.5194/acp-6-4395-2006.
Food and Agriculture Organization of the United Nations (FAOUN) (1991), *1990 Production Yearbook*, 323 pp., Rome.
Førland, E. J., and I. Hanssen-Bauer (2000), Increased precipitation in the Norwegian Arctic: True or false?, *Clim. Change*, *46*(4), 485–509, doi:10.1023/A:1005613304674.
Franssen, H. J. H., R. Stöckli, I. Lehner, E. Rotenberg, and S. I. Seneviratne (2010), Energy balance closure of eddy-covariance data: A multisite analysis for European FLUXNET stations, *Agric. For. Meteorol.*, *150*(12), 1553–1567, doi:10.1016/j.agrformet.2010.08.005.
French, A. N., et al. (2005), Surface energy fluxes with the Advanced Spaceborne Thermal Emission and Reflection radiometer (ASTER) at the Iowa 2002 SMACEX site (USA), *Remote Sens. Environ.*, *99*(1–2), 55–65, doi:10.1016/j.rse.2005.05.015.
Friedl, M. A. (2002), Forward and inverse modeling of land surface energy balance using surface temperature measurements, *Remote Sens. Environ.*, *79*(2–3), 344–354, doi:10.1016/S0034-4257(01)00284-X.
Friedlingstein, P., et al. (2006), Climate-carbon cycle feedback analysis: Results from the C^4MIP model intercomparison, *J. Clim.*, *19*(14), 3337–3353, doi:10.1175/JCLI3800.1.
Friend, A. D., et al. (2007), FLUXNET and modelling the global carbon cycle, *Global Change Biol.*, *13*(3), 610–633, doi:10.1111/j.1365-2486.2006.01223.x.
Fu, G. B., S. P. Charles, and J. J. Yu (2009), A critical overview of pan evaporation trends over the last 50 years, *Clim. Change*, *97*(1–2), 193–214, doi:10.1007/s10584-009-9579-1.
Fuehrer, P. L., and C. A. Friehe (2002), Flux corrections revisited, *Boundary Layer Meteorol.*, *102*(3), 415–458, doi:10.1023/A:1013826900579.
Fung, I. (1997), Climate change—A greener north, *Nature*, *386*(6626), 659–660, doi:10.1038/386659a0.
Gao, X., and P. A. Dirmeyer (2006), A multimodel analysis, validation, and transferability study of global soil wetness products, *J. Hydrometeorol.*, *7*(6), 1218–1236, doi:10.1175/JHM551.1.
Garratt, J. R., and B. B. Hicks (1990), Micrometeorological and PBL experiments in Australia, *Boundary Layer Meteorol.*, *50*(1–4), 11–29, doi:10.1007/BF00120516.
Garratt, J. R., G. D. Hess, W. L. Physick, and P. Bougeault (1996), The atmospheric boundary layer—Advances in knowledge and application, *Boundary Layer Meteorol.*, *78*(1–2), 9–37, doi:10.1007/BF00122485.
Gash, J. H. C., C. R. Lloyd, and G. Lachaud (1995), Estimating sparse forest rainfall interception with an analytical model, *J. Hydrol.*, *170*(1–4), 79–86, doi:10.1016/0022-1694(95)02697-N.
Gavilán, P., and J. Berengena (2007), Accuracy of the Bowen ratio-energy balance method for measuring latent heat flux in a semiarid advective environment, *Irrig. Sci.*, *25*(2), 127–140, doi:10.1007/s00271-006-0040-1.
Gazal, R. M., R. L. Scott, D. C. Goodrich, and D. G. Williams (2006), Controls on transpiration in a semiarid riparian cottonwood forest, *Agric. For. Meteorol.*, *137*(1–2), 56–67, doi:10.1016/j.agrformet.2006.03.002.
Gedney, N., P. M. Cox, R. A. Betts, O. Boucher, C. Huntingford, and P. A. Stott (2006), Detection of a direct carbon dioxide effect

in continental river runoff records, *Nature*, *439*(7078), 835–838, doi:10.1038/nature04504.

Gent, P., S. Yeager, R. Neale, S. Levis, and D. Bailey (2010), Improvements in a half degree atmosphere/land version of the CCSM, *Clim. Dyn.*, *34*(6), 819–833, doi:10.1007/s00382-009-0614-8.

Gerten, D., S. Rost, W. von Bloh, and W. Lucht (2008), Causes of change in 20th century global river discharge, *Geophys. Res. Lett.*, *35*, L20405, doi:10.1029/2008GL035258.

Giambelluca, T. W., F. G. Scholz, S. J. Bucci, F. C. Meinzer, G. Goldstein, W. A. Hoffmann, A. C. Franco, and M. P. Buchert (2009a), Evapotranspiration and energy balance of Brazilian savannas with contrasting tree density, *Agric. For. Meteorol.*, *149*(8), 1365–1376, doi:10.1016/j.agrformet.2009.03.006.

Giambelluca, T. W., R. E. Martin, G. P. Asner, M. Huang, R. G. Mudd, M. A. Nullet, J. K. DeLay, and D. Foote (2009b), Evapotranspiration and energy balance of native wet montane cloud forest in Hawai'i, *Agric. For. Meteorol.*, *149*(2), 230–243, doi:10.1016/j.agrformet.2008.08.004.

Giorgi, F., and R. Avissar (1997), Representation of heterogeneity effects in Earth system modeling: Experience from land surface modeling, *Rev. Geophys.*, *35*(4), 413–437, doi:10.1029/97RG01754.

Gleick, G. H. (1989), Climate change, hydrology, and water resources, *Rev. Geophys.*, *27*(3), 329–344, doi:10.1029/RG027i003p00329.

Glenn, E. P., A. R. Huete, P. L. Nagler, K. K. Hirschboeck, and P. Brown (2007), Integrating remote sensing and ground methods to estimate evapotranspiration, *Crit. Rev. Plant Sci.*, *26*(3), 139–168, doi:10.1080/07352680701402503.

Glenn, E., P. Nagler, and A. Huete (2010), Vegetation index methods for estimating evapotranspiration by remote sensing, *Surv. Geophys.*, *31*(6), 531–555, doi:10.1007/s10712-010-9102-2.

Göckede, M., et al. (2008), Quality control of CarboEurope flux data: Part 1. Coupling footprint analyses with flux data quality assessment to evaluate sites in forest ecosystems, *Biogeosciences*, *5*(2), 433–450, doi:10.5194/bg-5-433-2008.

Gong, D., S. Kang, L. Yao, and L. Zhang (2007), Estimation of evapotranspiration and its components from an apple orchard in northwest China using sap flow and water balance methods, *Hydrol. Processes*, *21*(7), 931–938, doi:10.1002/hyp.6284.

Gonzalez-Dugo, M. P., C. M. U. Neale, L. Mateos, W. P. Kustas, J. H. Prueger, M. C. Anderson, and F. Li (2009), A comparison of operational remote sensing-based models for estimating crop evapotranspiration, *Agric. For. Meteorol.*, *149*(11), 1843–1853, doi:10.1016/j.agrformet.2009.06.012.

Good, S. P., and K. K. Caylor (2011), Climatological determinants of woody cover in Africa, *Proc. Natl. Acad. Sci. U. S. A.*, *108*(12), 4902–4907, doi:10.1073/pnas.1013100108.

Gordon, L. J., W. Steffen, B. F. Jonsson, C. Folke, M. Falkenmark, and A. Johannessen (2005), Human modification of global water vapor flows from the land surface, *Proc. Natl. Acad. Sci. U. S. A.*, *102*(21), 7612–7617, doi:10.1073/pnas.0500208102.

Goss, M. J., and W. Ehlers (2009), The role of lysimeters in the development of our understanding of soil water and nutrient dynamics in ecosystems, *Soil Use Manage.*, *25*(3), 213–223, doi:10.1111/j.1475-2743.2009.00230.x.

Goward, S. N., R. H. Waring, D. G. Dye, and J. L. Yang (1994), Ecological remote-sensing at OTTER: Satellite macroscale observations, *Ecol. Appl.*, *4*(2), 322–343, doi:10.2307/1941937.

Gowda, P. H., J. L. Chavez, P. D. Colaizzi, S. R. Evett, T. A. Howell, and J. A. Tolk (2007), Remote sensing based energy balance algorithms for mapping ET: Current status and future challenges, *Trans. ASABE*, *50*(5), 1639–1644.

Granier, A. (1987), Evaluation of transpiration in a Douglas-fir stand by means of sap flow measurements, *Tree Physiol.*, *3*(4), 309–320.

Granier, A., P. Biron, N. BréDa, J.-Y. Pontailler, and B. Saugier (1996), Transpiration of trees and forest stands: Short and long-term monitoring using sapflow methods, *Global Change Biol.*, *2*(3), 265–274, doi:10.1111/j.1365-2486.1996.tb00078.x.

Granier, A., et al. (2007), Evidence for soil water control on carbon and water dynamics in European forests during the extremely dry year: 2003, *Agric. For. Meteorol.*, *143*(1–2), 123–145, doi:10.1016/j.agrformet.2006.12.004.

Groisman, P. Y., and D. R. Legates (1994), The accuracy of United States precipitation data, *Bull. Am. Meteorol. Soc.*, *75*(2), 215–227, doi:10.1175/1520-0477(1994)075<0215:TAOUSP>2.0.CO;2.

Groisman, P. Y., D. R. Easterling, R. G. Quayle, V. S. Golubev, A. N. Krenke, and A. Y. Mikhailov (1996), Reducing biases in estimates of precipitation over the United States: Phase 3 adjustments, *J. Geophys. Res.*, *101*(D3), 7185–7195, doi:10.1029/95JD02600.

Gu, L. H., D. Baldocchi, S. B. Verma, T. A. Black, T. Vesala, E. M. Falge, and P. R. Dowty (2002), Advantages of diffuse radiation for terrestrial ecosystem productivity, *J. Geophys. Res.*, *107*(D6), 4050, doi:10.1029/2001JD001242.

Gu, L., T. Meyers, S. G. Pallardy, P. J. Hanson, B. Yang, M. Heuer, K. P. Hosman, J. S. Riggs, D. Sluss, and S. D. Wullschleger (2006), Direct and indirect effects of atmospheric conditions and soil moisture on surface energy partitioning revealed by a prolonged drought at a temperate forest site, *J. Geophys. Res.*, *111*, D16102, doi:10.1029/2006JD007161.

Güntner, A. (2008), Improvement of global hydrological models using GRACE data, *Surv. Geophys.*, *29*(4–5), 375–397, doi:10.1007/s10712-008-9038-y.

Guo, Z. C., et al. (2006), GLACE: The Global Land-Atmosphere Coupling Experiment: Part II. Analysis, *J. Hydrometeorol.*, *7*(4), 611–625, doi:10.1175/JHM511.1.

Guswa, A. J. (2008), The influence of climate on root depth: A carbon cost-benefit analysis, *Water Resour. Res.*, *44*, W02427, doi:10.1029/2007WR006384.

Hall, F. G., K. F. Huemmrich, S. J. Goetz, P. J. Sellers, and J. E. Nickeson (1992), Satellite remote sensing of surface energy balance: Success, failures, and unresolved issues in FIFE, *J. Geophys. Res.*, *97*(D17), 19,061–19,089, doi:10.1029/92JD02189.

Hartogensis, O. K., C. J. Watts, J. C. Rodriguez, and H. A. R. De Bruin (2003), Derivation of an effective height for scintillometers: La Poza experiment in northwest Mexico, *J. Hydrometeorol.*, *4*(5), 915–928, doi:10.1175/1525-7541(2003)004<0915:DOAEHF>2.0.CO;2.

Hasler, N., and R. Avissar (2007), What controls evapotranspiration in the Amazon Basin?, *J. Hydrometeorol.*, *8*(3), 380–395, doi:10.1175/JHM587.1.

Heijmans, M., W. J. Arp, and F. Berendse (2001), Effects of elevated CO_2 and vascular plants on evapotranspiration in bog vegetation, *Global Change Biol.*, *7*(7), 817–827, doi:10.1046/j.1354-1013.2001.00440.x.

Heitman, J. L., R. Horton, T. J. Sauer, and T. M. DeSutter (2008), Sensible heat observations reveal soil-water evaporation dynamics, *J. Hydrometeorol.*, *9*(1), 165–171, doi:10.1175/2007JHM963.1.

Held, I. M., and B. J. Soden (2000), Water vapor feedback and global warming, *Annu. Rev. Energy Environ.*, *25*(1), 441–475, doi:10.1146/annurev.energy.25.1.441.

Held, I. M., and B. J. Soden (2006), Robust responses of the hydrological cycle to global warming, *J. Clim.*, *19*(21), 5686–5699, doi:10.1175/JCLI3990.1.

Herbst, M., P. T. W. Rosier, D. D. McNeil, R. J. Harding, and D. J. Gowing (2008), Seasonal variability of interception evaporation from the canopy of a mixed deciduous forest, *Agric. For. Meteorol.*, *148*(11), 1655–1667, doi:10.1016/j.agrformet.2008.05.011.

Hess, G. D., B. B. Hicks, and T. Yamada (1981), The impact of the Wangara experiment, *Boundary Layer Meteorol.*, *20*(2), 135–174, doi:10.1007/BF00119899.

Hetherington, A. M., and F. I. Woodward (2003), The role of stomata in sensing and driving environmental change, *Nature*, *424*(6951), 901–908, doi:10.1038/nature01843.
Hirschi, M., S. I. Seneviratne, S. Hagemann, and C. Schar (2007), Analysis of seasonal terrestrial water storage variations in regional climate simulations over Europe, *J. Geophys. Res.*, *112*, D22109, doi:10.1029/2006JD008338.
Hobbins, M. T., J. A. Ramirez, T. C. Brown, and L. Claessens (2001), The complementary relationship in estimation of regional evapotranspiration: The complementary relationship areal evapotranspiration and advection-aridity models, *Water Resour. Res.*, *37*(5), 1367–1387, doi:10.1029/2000WR900358.
Hobbins, M. T., J. A. Ramírez, and T. C. Brown (2004), Trends in pan evaporation and actual evapotranspiration across the conterminous U.S.: Paradoxical or complementary?, *Geophys. Res. Lett.*, *31*, L13503, doi:10.1029/2004GL019846.
Hoedjes, J. C. B., A. Chehbouni, J. Ezzahar, R. Escadafal, and H. A. R. De Bruin (2007), Comparison of large aperture scintillometer and eddy covariance measurements: Can thermal infrared data be used to capture footprint-induced differences?, *J. Hydrometeorol.*, *8*(2), 144–159, doi:10.1175/JHM561.1.
Hogg, E. H., and P. A. Hurdle (1997), Sap flow in trembling aspen: Implications for stomatal responses to vapor pressure deficit, *Tree Physiol.*, *17*(8–9), 501–509.
Högström, U. (1988), Non-dimensional wind and temperature profiles in the atmospheric surface layer: A re-evaluation, *Boundary Layer Meteorol.*, *42*(1–2), 55–78, doi:10.1007/BF00119875.
Högström, U., and H. Bergström (1996), Organized turbulence structures in the near-neutral atmospheric surface layer, *J. Atmos. Sci.*, *53*(17), 2452–2464, doi:10.1175/1520-0469(1996)053<2452:OTSITN>2.0.CO;2.
Hogue, T. S., L. Bastidas, H. Gupta, S. Sorooshian, K. Mitchell, and W. Emmerich (2005), Evaluation and transferability of the Noah land surface model in semiarid environments, *J. Hydrometeorol.*, *6*(1), 68–84, doi:10.1175/JHM-402.1.
Holmes, J. W. (1984), Measuring evapotranspiration by hydrological methods, *Agric. Water Manage.*, *8*(1–3), 29–40, doi:10.1016/0378-3774(84)90044-1.
Horst, T. W. (1999), The footprint for estimation of atmosphere-surface exchange fluxes by profile techniques, *Boundary Layer Meteorol.*, *90*(2), 171–188, doi:10.1023/A:1001774726067.
Hu, Z., et al. (2009), Partitioning of evapotranspiration and its controls in four grassland ecosystems: Application of a two-source model, *Agric. For. Meteorol.*, *149*(9), 1410–1420, doi:10.1016/j.agrformet.2009.03.014.
Huete, A. R., K. Didan, Y. E. Shimabukuro, P. Ratana, S. R. Saleska, L. R. Hutyra, W. Z. Yang, R. R. Nemani, and R. Myneni (2006), Amazon rainforests green-up with sunlight in dry season, *Geophys. Res. Lett.*, *33*, L06405, doi:10.1029/2005GL025583.
Hui, D., S. Wan, B. Su, G. Katul, R. Monson, and Y. Luo (2004), Gap-filling missing data in eddy covariance measurements using multiple imputation (MI) for annual estimations, *Agric. For. Meteorol.*, *121*(1–2), 93–111, doi:10.1016/S0168-1923(03)00158-8.
Hunsaker, D. J., B. A. Kimball, P. J. Pinter, G. W. Wall, R. L. LaMorte, F. J. Adamsen, S. W. Leavitt, T. L. Thompson, A. D. Matthias, and T. J. Brooks (2000), CO_2 enrichment and soil nitrogen effects on wheat evapotranspiration and water use efficiency, *Agric. For. Meteorol.*, *104*(2), 85–105, doi:10.1016/S0168-1923(00)00157-X.
Huntingford, C., S. Allen, and R. Harding (1995), An intercomparison of single and dual-source vegetation-atmosphere transfer models applied to transpiration from sahelian savannah, *Boundary Layer Meteorol.*, *74*(4), 397–418, doi:10.1007/BF00712380.
Huntington, T. G. (2006), Evidence for intensification of the global water cycle: Review and synthesis, *J. Hydrol.*, *319*(1–4), 83–95, doi:10.1016/j.jhydrol.2005.07.003.
Hutyra, L. R., J. W. Munger, S. R. Saleska, E. Gottlieb, B. C. Daube, A. L. Dunn, D. F. Amaral, P. B. de Camargo, and S. C. Wofsy (2007), Seasonal controls on the exchange of carbon and water in an Amazonian rain forest, *J. Geophys. Res.*, *112*, G03008, doi:10.1029/2006JG000365.
Ivans, S., L. Hipps, A. J. Leffler, and C. Y. Ivans (2006), Response of water vapor and CO_2 fluxes in semiarid lands to seasonal and intermittent precipitation pulses, *J. Hydrometeorol.*, *7*(5), 995–1010, doi:10.1175/JHM545.1.
Iwasaki, H., H. Saito, K. Kuwao, T. C. Maximov, and S. Hasegawa (2010), Forest decline caused by high soil water conditions in a permafrost region, *Hydrol. Earth Syst. Sci.*, *14*(2), 301–307, doi:10.5194/hess-14-301-2010.
Jackson, R. B., S. R. Carpenter, C. N. Dahm, D. M. McKnight, R. J. Naiman, S. L. Postel, and S. W. Running (2001), Water in a changing world, *Ecol. Appl.*, *11*(4), 1027–1045, doi:10.1890/1051-0761(2001)011[1027:WIACW]2.0.CO;2.
Jacobs, J. M., S. L. Mergelsberg, A. F. Lopera, and D. A. Myers (2002), Evapotranspiration from a wet prairie wetland under drought conditions: Paynes Prairie Preserve, Florida, USA, *Wetlands*, *22*(2), 374–385, doi:10.1672/0277-5212(2002)022[0374:EFAWPW]2.0.CO;2.
Jacobsen, A. (1999), Estimation of the soil heat flux/net radiation ratio based on spectral vegetation indexes in high-latitude Arctic areas, *Int. J. Remote Sens.*, *20*(2), 445–461, doi:10.1080/014311699213532.
Jaeger, E. B., R. Stockli, and S. I. Seneviratne (2009), Analysis of planetary boundary layer fluxes and land-atmosphere coupling in the regional climate model CLM, *J. Geophys. Res.*, *114*, D17106, doi:10.1029/2008JD011658.
Jang, K., S. Kang, J. Kim, C. B. Lee, T. Kim, J. Kim, R. Hirata, and N. Saigusa (2010), Mapping evapotranspiration using MODIS and MM5 four-dimensional data assimilation, *Remote Sens. Environ.*, *114*(3), 657–673, doi:10.1016/j.rse.2009.11.010.
Jarvis, P. G. (1976), Interpretation of variations in leaf water potential and stomatal conductance found in canopies in field, *Philos. Trans. R. Soc. London B*, *273*(927), 593–610, doi:10.1098/rstb.1976.0035.
Jassal, R. S., T. A. Black, D. L. Spittlehouse, C. Brummer, and Z. Nesic (2009), Evapotranspiration and water use efficiency in different-aged Pacific Northwest Douglas-fir stands, *Agric. For. Meteorol.*, *149*(6–7), 1168–1178, doi:10.1016/j.agrformet.2009.02.004.
Jiang, L., and S. Islam (2001), Estimation of surface evaporation map over Southern Great Plains using remote sensing data, *Water Resour. Res.*, *37*(2), 329–340, doi:10.1029/2000WR900255.
Jiang, X., G.-Y. Niu, and Z.-L. Yang (2009), Impacts of vegetation and groundwater dynamics on warm season precipitation over the Central United States, *J. Geophys. Res.*, *114*, D06109, doi:10.1029/2008JD010756.
Jiménez, C., et al. (2011), Global intercomparison of 12 land surface heat flux estimates, *J. Geophys. Res.*, *116*, D02102, doi:10.1029/2010JD014545.
Jongen, M., J. S. Pereira, L. M. I. Aires, and C. A. Pio (2011), The effects of drought and timing of precipitation on the inter-annual variation in ecosystem-atmosphere exchange in a Mediterranean grassland, *Agric. For. Meteorol.*, *151*(5), 595–606, doi:10.1016/j.agrformet.2011.01.008.
Juan, C. H., and S. F. Shih (1997), A lysimeter system for evapotranspiration estimation for wetland vegetation, *Proc. Soil Crop Sci. Soc. Fla.*, *56*, 125–130.
Juárez, R. I. N., M. G. Hodnett, R. Fu, M. L. Goulden, and C. von Randow (2007), Control of dry season evapotranspiration over the Amazonian forest as inferred from observations at a southern Amazon forest site, *J. Clim.*, *20*(12), 2827–2839, doi:10.1175/JCLI4184.1.
Jung, M., M. Reichstein, and A. Bondeau (2009), Towards global empirical upscaling of FLUXNET eddy covariance observations: Validation of a model tree ensemble approach using a biosphere model, *Biogeosciences*, *6*(10), 2001–2013, doi:10.5194/bg-6-2001-2009.

Jung, M., et al. (2010), Recent decline in the global land evapotranspiration trend due to limited moisture supply, *Nature*, *467*(7318), 951–954, doi:10.1038/nature09396.

Kabat, P., A. J. Dolman, and J. A. Elbers (1997), Evaporation, sensible heat and canopy conductance of fallow savannah and patterned woodland in the Sahel, *J. Hydrol.*, *188-189*, 494–515, doi:10.1016/S0022-1694(96)03190-3.

Kader, B. A., and A. M. Yaglom (1990), Mean fields and fluctuation moments in unstably stratified turbulent boundary layers, *J. Fluid Mech.*, *212*, 637–662.

Kahler, D. M., and W. Brutsaert (2006), Complementary relationship between daily evaporation in the environment and pan evaporation, *Water Resour. Res.*, *42*, W05413, doi:10.1029/2005WR004541.

Kaimal, J. C., J. C. Wyngaard, D. A. Haugen, O. R. Cot, Y. Izumi, S. J. Caughey, and C. J. Readings (1976), Turbulence structure in the convective boundary layer, *J. Atmos. Sci.*, *33*(11), 2152–2169, doi:10.1175/1520-0469(1976)033<2152:TSITCB>2.0.CO;2.

Kalbus, E., F. Reinstorf, and M. Schirmer (2006), Measuring methods for groundwater-surface water interactions: A review, *Hydrol. Earth Syst. Sci.*, *10*(6), 873–887, doi:10.5194/hess-10-873-2006.

Kalma, J. D., T. R. McVicar, and M. F. McCabe (2008), Estimating land surface evaporation: A review of methods using remotely sensed surface temperature data, *Surv. Geophys.*, *29*(4–5), 421–469, doi:10.1007/s10712-008-9037-z.

Kanda, M., A. Inagaki, M. O. Letzel, S. Raasch, and T. Watanabe (2004), LES study of the energy imbalance problem with eddy covariance fluxes, *Boundary Layer Meteorol.*, *110*(3), 381–404, doi:10.1023/B:BOUN.0000007225.45548.7a.

Kanemasu, E. T., et al. (1992), Surface flux measurements in FIFE: An overview, *J. Geophys. Res.*, *97*(D17), 18,547–18,555, doi:10.1029/92JD00254.

Karam, H. N., and R. L. Bras (2008), Climatological basin-scale Amazonian evapotranspiration estimated through a water budget analysis, *J. Hydrometeorol.*, *9*(5), 1048–1060, doi:10.1175/2008JHM888.1.

Karl, T. R., R. G. Quayle, and P. Y. Groisman (1993), Detecting climate variations and change: New challenges for observing and data management systems, *J. Clim.*, *6*(8), 1481–1494, doi:10.1175/1520-0442(1993)006<1481:DCVACN>2.0.CO;2.

Katata, G., H. Nagai, M. Kajino, H. Ueda, and Y. Hozumi (2010), Numerical study of fog deposition on vegetation for atmosphere-land interactions in semi-arid and arid regions, *Agric. For. Meteorol.*, *150*(3), 340–353, doi:10.1016/j.agrformet.2009.11.016.

Katul, G., C.-I. Hsieh, R. Oren, D. Ellsworth, and N. Phillips (1996), Latent and sensible heat flux predictions from a uniform pine forest using surface renewal and flux variance methods, *Boundary Layer Meteorol.*, *80*(3), 249–282.

Keenan, T., S. Sabate, and C. Gracia (2010), Soil water stress and coupled photosynthesis-conductance models: Bridging the gap between conflicting reports on the relative roles of stomatal, mesophyll conductance and biochemical limitations to photosynthesis, *Agric. For. Meteorol.*, *150*(3), 443–453, doi:10.1016/j.agrformet.2010.01.008.

Kelliher, F. M., et al. (1997), Evaporation from an eastern Siberian larch forest, *Agric. For. Meteorol.*, *85*(3–4), 135–147, doi:10.1016/S0168-1923(96)02424-0.

Kim, C. P., and D. Entekhabi (1997), Examination of two methods for estimating regional evaporation using a coupled mixed layer and land surface model, *Water Resour. Res.*, *33*(9), 2109–2116, doi:10.1029/97WR01564.

Kim, S., and H. S. Kim (2008), Neural networks and genetic algorithm approach for nonlinear evaporation and evapotranspiration modeling, *J. Hydrol.*, *351*(3–4), 299–317, doi:10.1016/j.jhydrol.2007.12.014.

Klaassen, W., F. Bosveld, and E. de Water (1998), Water storage and evaporation as constituents of rainfall interception, *J. Hydrol.*, *212–213*, 36–50, doi:10.1016/S0022-1694(98)00200-5.

Klees, R., E. A. Zapreeva, H. C. Winsemius, and H. H. G. Savenije (2007), The bias in GRACE estimates of continental water storage variations, *Hydrol. Earth Syst. Sci.*, *11*(4), 1227–1241, doi:10.5194/hess-11-1227-2007.

Kleissl, J., J. Gomez, S. H. Hong, J. M. H. Hendrickx, T. Rahn, and W. L. Defoor (2008), Large aperture scintillometer intercomparison study, *Boundary Layer Meteorol.*, *128*(1), 133–150, doi:10.1007/s10546-008-9274-1.

Kleissl, J., C. J. Watts, J. C. Rodriguez, S. Naif, and E. R. Vivoni (2009), Scintillometer intercomparison study—Continued, *Boundary Layer Meteorol.*, *130*(3), 437–443, doi:10.1007/s10546-009-9352-z.

Knutson, T. R., and S. Manabe (1995), Time-mean response over the tropical pacific to increased CO_2 in a coupled ocean-atmosphere model, *J. Clim.*, *8*(9), 2181–2199, doi:10.1175/1520-0442(1995)008<2181:TMROTT>2.0.CO;2.

Kochendorfer, J., E. G. Castillo, E. Haas, W. C. Oechel, and K. T. Paw U (2011), Net ecosystem exchange, evapotranspiration and canopy conductance in a riparian forest, *Agric. For. Meteorol.*, *151*(5), 544–553, doi:10.1016/j.agrformet.2010.12.012.

Kohsiek, W., W. M. L. Meijninger, A. F. Moene, B. G. Heusinkveld, O. K. Hartogensis, W. Hillen, and H. A. R. De Bruin (2002), An extra large aperture scintillometer for long range applications, *Boundary Layer Meteorol.*, *105*(1), 119–127, doi:10.1023/A:1019600908144.

Koster, R. D., and M. J. Suarez (1999), A simple framework for examining the interannual variability of land surface moisture fluxes, *J. Clim.*, *12*(7), 1911–1917, doi:10.1175/1520-0442(1999)012<1911:ASFFET>2.0.CO;2.

Koster, R. D., et al. (2004), Regions of strong coupling between soil moisture and precipitation, *Science*, *305*(5687), 1138–1140, doi:10.1126/science.1100217.

Köstner, B., A. Granier, and J. Cermák (1998), Sapflow measurements in forest stands: Methods and uncertainties, *Ann. For. Sci.*, *55*(1–2), 13–27, doi:10.1051/forest:19980102.

Kosugi, Y., S. Takanashi, H. Tanaka, S. Ohkubo, M. Tani, M. Yano, and T. Katayama (2007), Evapotranspiration over a Japanese cypress forest: I. Eddy covariance fluxes and surface conductance characteristics for 3 years, *J. Hydrol.*, *337*(3–4), 269–283, doi:10.1016/j.jhydrol.2007.01.039.

Krakauer, N. Y., and I. Fung (2008), Mapping and attribution of change in streamflow in the coterminous United States, *Hydrol. Earth Syst. Sci.*, *12*(4), 1111–1120, doi:10.5194/hess-12-1111-2008.

Krishnan, P., T. A. Black, N. J. Grant, A. G. Barr, E. H. Hogg, R. S. Jassal, and K. Morgenstern (2006), Impact of changing soil moisture distribution on net ecosystem productivity of a boreal aspen forest during and following drought, *Agric. For. Meteorol.*, *139*(3–4), 208–223, doi:10.1016/j.agrformet.2006.07.002.

Kruijt, B., J. P. M. Witte, C. M. J. Jacobs, and T. Kroon (2008), Effects of rising atmospheric CO_2 on evapotranspiration and soil moisture: A practical approach for the Netherlands, *J. Hydrol.*, *349*(3–4), 257–267, doi:10.1016/j.jhydrol.2007.10.052.

Kumagai, T. O., T. M. Saitoh, Y. Sato, H. Takahashi, O. J. Manfroi, T. Morooka, K. Kuraji, M. Suzuki, T. Yasunari, and H. Komatsu (2005), Annual water balance and seasonality of evapotranspiration in a Bornean tropical rainforest, *Agric. For. Meteorol.*, *128*(1–2), 81–92, doi:10.1016/j.agrformet.2004.08.006.

Kume, T., H. Takizawa, N. Yoshifuji, K. Tanaka, C. Tantasirin, N. Tanaka, and M. Suzuki (2007), Impact of soil drought on sap flow and water status of evergreen trees in a tropical monsoon forest in northern Thailand, *For. Ecol. Manage.*, *238*(1–3), 220–230, doi:10.1016/j.foreco.2006.10.019.

Kundzewicz, Z. W., L. J. Mata, N. W. Arnell, P. Döll, P. Kabat, B. Jiménez, K. A. Miller, T. Oki, Z. Şen, and I. A. Shiklomanov (2007), Freshwater resources and their management, in *Climate Change 2007: Impacts, Adaptation and Vulnerability—Contribution of Working Group II to the Fourth Assessment Report of the Intergovernmental Panel on Climate Change*, edited by M. L.

Parry et al., pp. 173–210, Cambridge Univ. Press, Cambridge, U. K. [Available at http://www.ipcc.ch/pdf/assessment-report/ar4/wg2/ar4-wg2-chapter3.pdf site.]

Kustas, W., and M. Anderson (2009), Advances in thermal infrared remote sensing for land surface modeling, *Agric. For. Meteorol.*, *149*(12), 2071–2081, doi:10.1016/j.agrformet.2009.05.016.

Kustas, W. P., and W. Brutsaert (1987), Budgets of water vapor in the unstable boundary layer over rugged terrain, *J. Clim. Appl. Meteorol.*, *26*(5), 607–620, doi:10.1175/1520-0450(1987)026<0607:BOWVIT>2.0.CO;2.

Kustas, W. P., and C. S. T. Daughtry (1990), Estimation of the soil heat-flux net-radiation ratio from spectral data, *Agric. For. Meteorol.*, *49*(3), 205–223, doi:10.1016/0168-1923(90)90033-3.

Kustas, W. P., and J. M. Norman (1996), Use of remote sensing for evapotranspiration monitoring over land surfaces, *Hydrol. Sci. J.*, *41*(4), 495–516, doi:10.1080/02626669609491522.

Kustas, W. P., and J. M. Norman (1999), Evaluation of soil and vegetation heat flux predictions using a simple two-source model with radiometric temperatures for partial canopy cover, *Agric. For. Meteorol.*, *94*(1), 13–29, doi:10.1016/S0168-1923(99)00005-2.

Kustas, W. P., C. S. T. Daughtry, and P. J. Van Oevelen (1993), Analytical treatment of the relationships between soil heat flux/net radiation ratio and vegetation indices, *Remote Sens. Environ.*, *46*(3), 319–330, doi:10.1016/0034-4257(93)90052-Y.

Kustas, W. P., J. H. Blanford, D. I. Stannard, C. S. T. Daughtry, W. D. Nichols, and M. A. Weltz (1994), Local energy flux estimates for unstable conditions using variance data in semiarid rangelands, *Water Resour. Res.*, *30*(5), 1351–1361, doi:10.1029/93WR03084.

Kustas, W. P., R. Bindlish, A. N. French, and T. J. Schmugge (2003), Comparison of energy balance modeling schemes using microwave-derived soil moisture and radiometric surface temperature, *Water Resour. Res.*, *39*(2), 1039, doi:10.1029/2002WR001361.

Kustas, W. P., F. Li, T. J. Jackson, J. H. Prueger, J. I. MacPherson, and M. Wolde (2004), Effects of remote sensing pixel resolution on modeled energy flux variability of croplands in Iowa, *Remote Sens. Environ.*, *92*(4), 535–547, doi:10.1016/j.rse.2004.02.020.

Kustas, W. P., M. C. Anderson, A. N. French, and D. Vickers (2006), Using a remote sensing field experiment to investigate flux-footprint relations and flux sampling distributions for tower and aircraft-based observations, *Adv. Water Resour.*, *29*(2), 355–368, doi:10.1016/j.advwatres.2005.05.003.

Kustas, W. P., M. C. Anderson, J. M. Norman, and F. Q. Li (2007), Utility of radiometric-aerodynamic temperature relations for heat flux estimation, *Boundary Layer Meteorol.*, *122*(1), 167–187, doi:10.1007/s10546-006-9093-1.

Labat, D., Y. Godderis, J. L. Probst, and J. L. Guyot (2004), Evidence for global runoff increase related to climate warming, *Adv. Water Resour.*, *27*(6), 631–642.

Lafleur, P. M., R. A. Hember, S. W. Admiral, and N. T. Roulet (2005), Annual and seasonal variability in evapotranspiration and water table at a shrub-covered bog in southern Ontario, Canada, *Hydrol. Processes*, *19*(18), 3533–3550, doi:10.1002/hyp.5842.

Lagouarde, J. P., J. M. Bonnefond, Y. H. Kerr, K. J. McAneney, and M. Irvine (2002), Integrated sensible heat flux measurements of a two-surface composite landscape using scintillometry, *Boundary Layer Meteorol.*, *105*(1), 5–35, doi:10.1023/A:1019631428921.

Langley, J. A., and J. P. Megonigal (2010), Ecosystem response to elevated CO_2 levels limited by nitrogen-induced plant species shift, *Nature*, *466*(7302), 96–99, doi:10.1038/nature09176.

Law, B. E., et al. (2002), Environmental controls over carbon dioxide and water vapor exchange of terrestrial vegetation, *Agric. For. Meteorol.*, *113*(1–4), 97–120, doi:10.1016/S0168-1923(02)00104-1.

Lawrence, D. M., P. E. Thornton, K. W. Oleson, and G. B. Bonan (2007), The partitioning of evapotranspiration into transpiration, soil evaporation, and canopy evaporation in a GCM: Impacts on land-atmosphere interaction, *J. Hydrometeorol.*, *8*(4), 862–880, doi:10.1175/JHM596.1.

Lawrence, D. M., et al. (2011), Parameterization improvements and functional and structural advances in version 4 of the Community Land Model, *J. Adv. Model. Earth Syst.*, *3*, M03001, doi:10.1029/2011MS000045.

Lawrence, P. J., and T. N. Chase (2009), Climate impacts of making evapotranspiration in the Community Land Model (CLM3) consistent with the simple biosphere model (SiB), *J. Hydrometeorol.*, *10*(2), 374–394, doi:10.1175/2008JHM987.1.

Lee, D., J. Kim, K. S. Lee, and S. Kim (2010), Partitioning of catchment water budget and its implications for ecosystem carbon exchange, *Biogeosciences*, *7*(6), 1903–1914, doi:10.5194/bg-7-1903-2010.

Legates, D. R., and C. J. Willmott (1990), Mean seasonal and spatial variability in gauge-corrected, global precipitation, *Int. J. Climatol.*, *10*(2), 111–127, doi:10.1002/joc.3370100202.

Legates, D. R., H. F. Lins, and G. J. McCabe (2005), Comments on "Evidence for global runoff increase related to climate warming" by Labat et al., *Adv. Water Resour.*, *28*(12), 1310–1315, doi:10.1016/j.advwatres.2005.04.006.

Lei, H. M., and D. W. Yang (2010), Interannual and seasonal variability in evapotranspiration and energy partitioning over an irrigated cropland in the North China Plain, *Agric. For. Meteorol.*, *150*(4), 581–589, doi:10.1016/j.agrformet.2010.01.022.

Lenters, J. D., M. T. Coe, and J. A. Foley (2000), Surface water balance of the continental United States, 1963–1995: Regional evaluation of a terrestrial biosphere model and the NCEP/NCAR reanalysis, *J. Geophys. Res.*, *105*(D17), 22,393–22,425, doi:10.1029/2000JD900277.

Lettenmaier, D. P., and J. S. Famiglietti (2006), Hydrology—Water from on high, *Nature*, *444*(7119), 562–563, doi:10.1038/444562a.

Leuning, R. (1995), A critical appraisal of a combined stomatal-photosynthesis model for C-3 plants, *Plant Cell Environ.*, *18*(4), 339–355, doi:10.1111/j.1365-3040.1995.tb00370.x.

Leuning, R., H. A. Cleugh, S. J. Zegelin, and D. Hughes (2005), Carbon and water fluxes over a temperate Eucalyptus forest and a tropical wet/dry savanna in Australia: Measurements and comparison with MODIS remote sensing estimates, *Agric. For. Meteorol.*, *129*(3–4), 151–173, doi:10.1016/j.agrformet.2004.12.004.

Leuning, R., Y. Q. Zhang, A. Rajaud, H. Cleugh, and K. Tu (2008), A simple surface conductance model to estimate regional evaporation using MODIS leaf area index and the Penman-Monteith equation, *Water Resour. Res.*, *44*, W10419, doi:10.1029/2007WR006562.

Lhomme, J. P., and A. Chehbouni (1999), Comments on dual-source vegetation-atmosphere transfer models, *Agric. For. Meteorol.*, *94*(3–4), 269–273, doi:10.1016/S0168-1923(98)00109-9.

Lhomme, J. P., and L. Guilioni (2006), Comments on some articles about the complementary relationship, *J. Hydrol.*, *323*(1–4), 1–3, doi:10.1016/j.jhydrol.2005.08.014.

Lhomme, J. P., A. Chehbouni, and B. Monteny (2000), Sensible heat flux-radiometric surface temperature relationship over sparse vegetation: Parameterizing B-1, *Boundary Layer Meteorol.*, *97*(3), 431–457, doi:10.1023/A:1002786402695.

Li, R., Q. L. Min, and B. Lin (2009), Estimation of evapotranspiration in a mid-latitude forest using the Microwave Emissivity Difference Vegetation Index (EDVI), *Remote Sens. Environ.*, *113*(9), 2011–2018, doi:10.1016/j.rse.2009.05.007.

Li, S., S. Z. Kang, L. Zhang, F. S. Li, Z. L. Zhu, and B. Z. Zhang (2008), A comparison of three methods for determining vineyard evapotranspiration in the arid desert regions of northwest China, *Hydrol. Processes*, *22*(23), 4554–4564, doi:10.1002/hyp.7059.

Li, Z. L., R. L. Tang, Z. M. Wan, Y. Y. Bi, C. H. Zhou, B. H. Tang, G. J. Yan, and X. Y. Zhang (2009), A review of current methodologies for regional evapotranspiration estimation from remotely sensed data, *Sensors*, *9*(5), 3801–3853, doi:10.3390/s90503801.

Liang, N., K. Maruyama, and Y. Huang (1995), Interactions of elevated CO_2 and drought stress in gas-exchange and water-use efficiency in 3 temperate deciduous tree species, *Photosynthetica*, *31*(4), 529–539.

Liang, N., K. Maruyama, and Y. Huang (1996), Effects of CO_2 concentration on the photosynthetic and carboxylation efficiencies of Fagus crenata and Quercus crispula, *Photosynthetica*, *32*(3), 355–365.

Liepert, B. G., and M. Previdi (2009), Do models and observations disagree on the rainfall response to global warming?, *J. Clim.*, *22*(11), 3156–3166, doi:10.1175/2008JCLI2472.1.

Lima, T. T. S., I. S. Miranda, and S. S. Vasconcelos (2010), Effects of water and nutrient availability on fine root growth in eastern Amazonian forest regrowth, Brazil, *New Phytol.*, *187*(3), 622–630, doi:10.1111/j.1469-8137.2010.03299.x.

Lindroth, A., M. Molder, and F. Lagergren (2010), Heat storage in forest biomass improves energy balance closure, *Biogeosciences*, *7*(1), 301–313, doi:10.5194/bg-7-301-2010.

Liu, W., W. Liu, P. Li, W. Duan, and H. Li (2010), Dry season water uptake by two dominant canopy tree species in a tropical seasonal rainforest of Xishuangbanna, SW China, *Agric. For. Meteorol.*, *150*(3), 380–388, doi:10.1016/j.agrformet.2009.12.006.

Loescher, H. W., J. M. Jacobs, O. Wendroth, D. A. Robinson, G. S. Poulos, K. McGuire, P. Reed, B. P. Mohanty, J. B. Shanley, and W. Krajewski (2007), Enhancing water cycle measurements for future hydrologic research, *Bull. Am. Meteorol. Soc.*, *88*(5), 669–676, doi:10.1175/BAMS-88-5-669.

Lohmann, D., et al. (2004), Streamflow and water balance intercomparisons of four land surface models in the North American Land Data Assimilation System project, *J. Geophys. Res.*, *109*, D07S91, doi:10.1029/2003JD003517.

Lott, R. B., and R. J. Hunt (2001), Estimating evapotranspiration in natural and constructed wetlands, *Wetlands*, *21*(4), 614–628, doi:10.1672/0277-5212(2001)021[0614:EEINAC]2.0.CO;2.

Lu, H., M. R. Raupach, T. R. McVicar, and D. J. Barrett (2003), Decomposition of vegetation cover into woody and herbaceous components using AVHRR NDVI time series, *Remote Sens. Environ.*, *86*(1), 1–18, doi:10.1016/S0034-4257(03)00054-3.

Lu, X. L., and Q. L. Zhuang (2010), Evaluating evapotranspiration and water-use efficiency of terrestrial ecosystems in the conterminous United States using MODIS and AmeriFlux data, *Remote Sens. Environ.*, *114*(9), 1924–1939, doi:10.1016/j.rse.2010.04.001.

Lucht, W., I. C. Prentice, R. B. Myneni, S. Sitch, P. Friedlingstein, W. Cramer, P. Bousquet, W. Buermann, and B. Smith (2002), Climatic control of the high-latitude vegetation greening trend and Pinatubo effect, *Science*, *296*(5573), 1687–1689, doi:10.1126/science.1071828.

Lumley, J. L., and A. M. Yaglom (2001), A century of turbulence, *Flow Turbul. Combus.*, *66*(3), 241–286, doi:10.1023/A:1012437421667.

Mackay, D. S., B. E. Ewers, B. D. Cook, and K. J. Davis (2007), Environmental drivers of evapotranspiration in a shrub wetland and an upland forest in northern Wisconsin, *Water Resour. Res.*, *43*, W03442, doi:10.1029/2006WR005149.

Mahrt, L. (2010), Computing turbulent fluxes near the surface: Needed improvements, *Agric. For. Meteorol.*, *150*(4), 501–509, doi:10.1016/j.agrformet.2010.01.015.

Malek, E. (1993), Comparison of the Bowen ratio–energy balance and stability-corrected aerodynamic methods for measurement of evapotranspiration, *Theor. Appl. Climatol.*, *48*(2–3), 167–178, doi:10.1007/BF00864923.

Malek, E., and G. E. Bingham (1993), Comparison of the Bowen ratio–energy balance and the water balance methods for the measurement of evapotranspiration, *J. Hydrol.*, *146*(1–4), 209–220, doi:10.1016/0022-1694(93)90276-F.

Mallick, K., B. K. Bhattacharya, and N. K. Patel (2009), Estimating volumetric surface moisture content for cropped soils using a soil wetness index based on surface temperature and NDVI, *Agric. For. Meteorol.*, *149*(8), 1327–1342, doi:10.1016/j.agrformet.2009.03.004.

Manabe, S. (1969), Climate and ocean circulation: Part I. The atmospheric circulation and the hydrology of the Earth's surface, *Mon. Weather Rev.*, *97*(11), 739–774, doi:10.1175/1520-0493(1969)097<0739:CATOC>2.3.CO;2.

Mao, L. M., M. J. Bergman, and C. C. Tai (2002), Evapotranspiration measurement and estimation of three wetland environments in the Upper St. Johns River Basin, Florida, *J. Am. Water Resour. Assoc.*, *38*(5), 1271–1285, doi:10.1111/j.1752-1688.2002.tb04347.x.

Margolis, H. A., and M. G. Ryan (1997), A physiological basis for biosphere-atmosphere interactions in the boreal forest: An overview, *Tree Physiol.*, *17*(8–9), 491–499.

Markewitz, D., S. Devine, E. A. Davidson, P. Brando, and D. C. Nepstad (2010), Soil moisture depletion under simulated drought in the Amazon: Impacts on deep root uptake, *New Phytol.*, *187*(3), 592–607, doi:10.1111/j.1469-8137.2010.03391.x.

Marx, A., H. Kunstmann, D. Schuttemeyer, and A. F. Moene (2008), Uncertainty analysis for satellite derived sensible heat fluxes and scintillometer measurements over Savannah environment and comparison to mesoscale meteorological simulation results, *Agric. For. Meteorol.*, *148*(4), 656–667, doi:10.1016/j.agrformet.2007.11.009.

Massman, W. J., and X. Lee (2002), Eddy covariance flux corrections and uncertainties in long-term studies of carbon and energy exchanges, *Agric. For. Meteorol.*, *113*(1–4), 121–144, doi:10.1016/S0168-1923(02)00105-3.

Mauder, M., T. Foken, R. Clement, J. A. Elbers, W. Eugster, T. Grunwald, B. Heusinkveld, and O. Kolle (2008), Quality control of CarboEurope flux data: Part 2. Inter-comparison of eddy-covariance software, *Biogeosciences*, *5*(2), 451–462, doi:10.5194/bg-5-451-2008.

Maurer, E. P., A. W. Wood, J. C. Adam, D. P. Lettenmaier, and B. Nijssen (2002), A Long-term hydrologically based dataset of land surface fluxes and states for the conterminous United States, *J. Clim.*, *15*(22), 3237–3251, doi:10.1175/1520-0442(2002)015<3237:ALTHBD>2.0.CO;2.

Maximov, T., T. Ohta, and A. J. Dolman (2008), Water and energy exchange in East Siberian forest: A synthesis, *Agric. For. Meteorol.*, *148*(12), 2013–2018, doi:10.1016/j.agrformet.2008.10.004.

McAneney, K. J., A. E. Green, and M. S. Astill (1995), Large-aperture scintillometry: The homogeneous case, *Agric. For. Meteorol.*, *76*(3–4), 149–162, doi:10.1016/0168-1923(95)02227-O.

McCabe, M. F., and E. F. Wood (2006), Scale influences on the remote estimation of evapotranspiration using multiple satellite sensors, *Remote Sens. Environ.*, *105*(4), 271–285, doi:10.1016/j.rse.2006.07.006.

McCabe, M. F., E. F. Wood, R. Wicik, M. Pan, J. Sheffield, H. Gao, and H. Su (2008), Hydrological consistency using multi-sensor remote sensing data for water and energy cycle studies, *Remote Sens. Environ.*, *112*(2), 430–444, doi:10.1016/j.rse.2007.03.027.

McCaughey, J. H., M. R. Pejam, M. A. Arain, and D. A. Cameron (2006), Carbon dioxide and energy fluxes from a boreal mixedwood forest ecosystem in Ontario, Canada, *Agric. For. Meteorol.*, *140*(1–4), 79–96, doi:10.1016/j.agrformet.2006.08.010.

McGuffie, K., and A. Henderson-Sellers (2001), Forty years of numerical climate modelling, *Int. J. Climatol.*, *21*(9), 1067–1109, doi:10.1002/joc.632.

McNaughton, K. G., and T. W. Spriggs (1986), A mixed-layer model for regional evaporation, *Boundary Layer Meteorol.*, *34*(3), 243–262, doi:10.1007/BF00122381.

Mecikalski, J. R., G. R. Diak, M. C. Anderson, and J. M. Norman (1999), Estimating fluxes on continental scales using remotely sensed data in an atmospheric and exchange model, *J. Appl. Meteorol.*, *38*(9), 1352–1369, doi:10.1175/1520-0450(1999)038<1352:EFOCSU>2.0.CO;2.

Medlyn, B. E., et al. (1999), Effects of elevated [CO_2] on photosynthesis in European forest species: A meta-analysis of model parameters, *Plant Cell Environ.*, *22*(12), 1475–1495, doi:10.1046/j.1365-3040.1999.00523.x.

Meijninger, W. M. L., O. K. Hartogensis, W. Kohsiek, J. C. B. Hoedjes, R. M. Zuurbier, and H. A. R. De Bruin (2002), Determination of area-averaged sensible heat fluxes with a large aperture scintillometer over a heterogeneous surface: Flevoland field experiment, *Boundary Layer Meteorol.*, *105*(1), 37–62, doi:10.1023/A:1019647732027.

Meir, P., and F. I. Woodward (2010), Amazonian rain forests and drought: Response and vulnerability, *New Phytol.*, *187*(3), 553–557, doi:10.1111/j.1469-8137.2010.03390.x.

Meng, C. L., Z. L. Li, X. Zhan, J. C. Shi, and C. Y. Liu (2009), Land surface temperature data assimilation and its impact on evapotranspiration estimates from the Common Land Model, *Water Resour. Res.*, *45*, W02421, doi:10.1029/2008WR006971.

Mercado, L. M., N. Bellouin, S. Sitch, O. Boucher, C. Huntingford, M. Wild, and P. M. Cox (2009), Impact of changes in diffuse radiation on the global land carbon sink, *Nature*, *458*(7241), 1014–1017, doi:10.1038/nature07949.

Meyers, T. P., and S. E. Hollinger (2004), An assessment of storage terms in the surface energy balance of maize and soybean, *Agric. For. Meteorol.*, *125*(1–2), 105–115, doi:10.1016/j.agrformet.2004.03.001.

Miao, H., S. Chen, J. Chen, W. Zhang, P. Zhang, L. Wei, X. Han, and G. Lin (2009), Cultivation and grazing altered evapotranspiration and dynamics in Inner Mongolia steppes, *Agric. For. Meteorol.*, *149*(11), 1810–1819, doi:10.1016/j.agrformet.2009.06.011.

Michael, H. A., A. E. Mulligan, and C. F. Harvey (2005), Seasonal oscillations in water exchange between aquifers and the coastal ocean, *Nature*, *436*(7054), 1145–1148, doi:10.1038/nature03935.

Michaelides, S., V. Levizzani, E. Anagnostou, P. Bauer, T. Kasparis, and J. E. Lane (2009), Precipitation: Measurement, remote sensing, climatology and modeling, *Atmos. Res.*, *94*(4), 512–533, doi:10.1016/j.atmosres.2009.08.017.

Michiles, A. A. D., and R. Gielow (2008), Above-ground thermal energy storage rates, trunk heat fluxes and surface energy balance in a central Amazonian rainforest, *Agric. For. Meteorol.*, *148*(6–7), 917–930, doi:10.1016/j.agrformet.2008.01.001.

Mieruch, S., S. Noel, H. Bovensmann, and J. P. Burrows (2008), Analysis of global water vapour trends from satellite measurements in the visible spectral range, *Atmos. Chem. Phys.*, *8*(3), 491–504, doi:10.5194/acp-8-491-2008.

Migliavacca, M., et al. (2009), Seasonal and interannual patterns of carbon and water fluxes of a poplar plantation under peculiar eco-climatic conditions, *Agric. For. Meteorol.*, *149*(9), 1460–1476, doi:10.1016/j.agrformet.2009.04.003.

Milliman, J. D., K. L. Farnsworth, P. D. Jones, K. H. Xu, and L. C. Smith (2008), Climatic and anthropogenic factors affecting river discharge to the global ocean, 1951–2000, *Global Planet. Change*, *62*(3–4), 187–194, doi:10.1016/j.gloplacha.2008.03.001.

Min, Q. L., and B. Lin (2006), Remote sensing of evapotranspiration and carbon uptake at Harvard Forest, *Remote Sens. Environ.*, *100*(3), 379–387, doi:10.1016/j.rse.2005.10.020.

Mishra, R. S., M. Z. Abdin, and D. C. Uprety (1999), Interactive effects of elevated CO_2 and moisture stress on the photosynthesis, water relation and growth of *Brassica* species, *J. Agron. Crop Sci.*, *182*(4), 223–230, doi:10.1046/j.1439-037x.1999.00294.x.

Mitchell, K. E., et al. (2004), The multi-institution North American Land Data Assimilation System (NLDAS): Utilizing multiple GCIP products and partners in a continental distributed hydrological modeling system, *J. Geophys. Res.*, *109*, D07S90, doi:10.1029/2003JD003823.

Mitchell, T. D., and P. D. Jones (2005), An improved method of constructing a database of monthly climate observations and associated high-resolution grids, *Int. J. Climatol.*, *25*(6), 693–712, doi:10.1002/joc.1181.

Moderow, U., M. Aubinet, C. Feigenwinter, O. Kolle, A. Lindroth, M. Molder, L. Montagnani, C. Rebmann, and C. Bernhofer (2009), Available energy and energy balance closure at four coniferous forest sites across Europe, *Theor. Appl. Climatol.*, *98*(3–4), 397–412, doi:10.1007/s00704-009-0175-0.

Moene, A. F., F. Beyrich, and O. K. Hartogensis (2009), Developments in scintillometry, *Bull. Am. Meteorol. Soc.*, *90*(5), 694–698, doi:10.1175/2008BAMS2672.1.

Moffat, A. M., et al. (2007), Comprehensive comparison of gap-filling techniques for eddy covariance net carbon fluxes, *Agric. For. Meteorol.*, *147*(3–4), 209–232, doi:10.1016/j.agrformet.2007.08.011.

Monin, A. S., and A. M. Obukhov (1954), Basic laws of turbulent mixing in the ground layer of the atmosphere (in Russian), *Tr. Akad. Nauk SSSR Geophiz. Inst.*, *24*(151), 163–187.

Monteith, J. L. (1965), Evaporation and environment, *Symp. Soc. Exp. Biol.*, *19*, 205–224.

Moran, M. S., and R. D. Jackson (1991), Assessing the spatial distribution of evapotranspiration using remotely sensed inputs, *J. Environ. Qual.*, *20*(4), 725–737, doi:10.2134/jeq1991.00472425002000040003x.

Mu, Q., F. A. Heinsch, M. Zhao, and S. W. Running (2007a), Development of a global evapotranspiration algorithm based on MODIS and global meteorology data, *Remote Sens. Environ.*, *111*(4), 519–536, doi:10.1016/j.rse.2007.04.015.

Mu, Q., M. Zhao, F. A. Heinsch, M. Liu, H. Tian, and S. W. Running (2007b), Evaluating water stress controls on primary production in biogeochemical and remote sensing based models, *J. Geophys. Res.*, *112*, G01012, doi:10.1029/2006JG000179.

Mu, Q., M. Zhao, and S. W. Running (2011), Improvements to a MODIS global terrestrial evapotranspiration algorithm, *Remote Sens. Environ.*, *115*(8), 1781–1800, doi:10.1016/j.rse.2011.02.019.

Mueller, B., M. Hirschi, and S. I. Seneviratne (2011a), New diagnostic estimates of variations in terrestrial water storage based on ERA-Interim data, *Hydrol. Processes*, *25*, 996–1008, doi:10.1002/hyp.7652.

Mueller, B., et al. (2011b), Evaluation of global observations-based evapotranspiration datasets and IPCC AR4 simulations, *Geophys. Res. Lett.*, *38*, L06402, doi:10.1029/2010GL046230.

Mukherji, A., T. Facon, J. Burke, C. de Fraiture, J. Faures, B. Fuleki, M. Glordano, D. Molden, and T. Shah (2009), Revitalizing Asia's irrigation: To sustainably meet tomorrow's food needs, 48 pp., Food and Agric. Organ. of the United Nations, Rome.

Murray, S. J., P. N. Foster, and I. C. Prentice (2011), Evaluation of global continental hydrology as simulated by the Land-surface Processes and eXchanges Dynamic Global Vegetation Model, *Hydrol. Earth Syst. Sci.*, *15*(1), 91–105, doi:10.5194/hess-15-91-2011.

Murray, T., and A. Verhoef (2007), Moving towards a more mechanistic approach in the determination of soil heat flux from remote measurements: II. Diurnal shape of soil heat flux, *Agric. For. Meteorol.*, *147*(1–2), 88–97, doi:10.1016/j.agrformet.2007.06.009.

Myneni, R. B., C. D. Keeling, C. J. Tucker, G. Asrar, and R. R. Nemani (1997), Increased plant growth in the northern high latitudes from 1981 to 1991, *Nature*, *386*(6626), 698–702, doi:10.1038/386698a0.

Myneni, R. B., et al. (2007), Large seasonal swings in leaf area of Amazon rainforests, *Proc. Natl. Acad. Sci. U. S. A.*, *104*(12), 4820–4823, doi:10.1073/pnas.0611338104.

Nemani, R., and S. Running (1997), Land cover characterization using multitemporal red, near-IR, and thermal-IR data from NOAA/AVHRR, *Ecol. Appl.*, *7*(1), 79–90, doi:10.1890/1051-0761(1997)007[0079:LCCUMR]2.0.CO;2.

Nemani, R. R., C. D. Keeling, H. Hashimoto, W. M. Jolly, S. C. Piper, C. J. Tucker, R. B. Myneni, and S. W. Running (2003), Climate-driven increases in global terrestrial net primary production from 1982 to 1999, *Science*, *300*(5625), 1560–1563, doi:10.1126/science.1082750.

Nepstad, D. C., C. R. de Carvalho, E. A. Davidson, P. H. Jipp, P. A. Lefebvre, G. H. Negreiros, E. D. da Silva, T. A. Stone, S. E. Trumbore, and S. Vieira (1994), The role of deep roots in the hydrological and carbon cycles of Amazonian forests and pastures, *Nature*, *372*(6507), 666–669, doi:10.1038/372666a0.

New, M., M. Hulme, and P. Jones (2000), Representing twentieth-century space-time climate variability: Part II. Development of 1901–96 monthly grids of terrestrial surface climate, *J. Clim.*, *13*(13), 2217–2238, doi:10.1175/1520-0442(2000)013<2217:RTCSTC>2.0.CO;2.

New, M., M. Todd, M. Hulme, and P. Jones (2001), Precipitation measurements and trends in the twentieth century, *Int. J. Climatol.*, *21*(15), 1889–1922, doi:10.1002/joc.680.

Nicholson, S. (2000), Land surface processes and Sahel climate, *Rev. Geophys.*, *38*(1), 117–139, doi:10.1029/1999RG900014.

Nishida, K., R. R. Nemani, S. W. Running, and J. M. Glassy (2003a), An operational remote sensing algorithm of land surface evaporation, *J. Geophys. Res.*, *108*(D9), 4270, doi:10.1029/2002JD002062.

Nishida, K., R. R. Nemani, J. M. Glassy, and S. W. Running (2003b), Development of an evapotranspiration index from aqua/MODIS for monitoring surface moisture status, *IEEE Trans. Geosci. Remote Sens.*, *41*(2), 493–501, doi:10.1109/TGRS.2003.811744.

Niu, G. Y., Z. L. Yang, R. E. Dickinson, L. E. Gulden, and H. Su (2007), Development of a simple groundwater model for use in climate models and evaluation with Gravity Recovery and Climate Experiment data, *J. Geophys. Res.*, *112*, D07103, doi:10/1029/2006JD007522.

Niyogi, D. S., and S. Raman (1997), Comparison of four different stomatal resistance schemes using FIFE observations, *J. Appl. Meteorol.*, *36*(7), 903–917, doi:10.1175/1520-0450(1997)036<0903:COFDSR>2.0.CO;2.

Niyogi, D., K. Alapaty, S. Raman, and F. Chen (2009), Development and evaluation of a coupled photosynthesis-based gas exchange evapotranspiration model (GEM) for mesoscale weather forecasting applications, *J. Appl. Meteorol. Climatol.*, *48*(2), 349–368, doi:10.1175/2008JAMC1662.1.

Noormets, A., A. Sôber, E. J. Pell, R. E. Dickson, G. K. Podila, J. Sôber, J. G. Isebrands, and D. F. Karnosky (2001), Stomatal and non-stomatal limitation to photosynthesis in two trembling aspen (Populus tremuloides Michx.) clones exposed to elevated CO_2 and/or O_3, *Plant Cell Environ.*, *24*(3), 327–336, doi:10.1046/j.1365-3040.2001.00678.x.

Norman, J. M., and F. Becker (1995), Terminology in thermal infrared remote sensing of natural surfaces, *Agric. For. Meteorol.*, *77*(3–4), 153–166, doi:10.1016/0168-1923(95)02259-Z.

Norman, J. M., W. P. Kustas, and K. S. Humes (1995), Source approach for estimating soil and vegetation energy fluxes in observations of directional radiometric surface temperature, *Agric. For. Meteorol.*, *77*(3–4), 263–293, doi:10.1016/0168-1923(95)02265-Y.

Norman, J. M., W. P. Kustas, J. H. Prueger, and G. R. Diak (2000), Surface flux estimation using radiometric temperature: A dual-temperature-difference method to minimize measurement errors, *Water Resour. Res.*, *36*(8), 2263–2274, doi:10.1029/2000WR900033.

Norman, J. M., M. C. Anderson, W. P. Kustas, A. N. French, J. Mecikalski, R. Torn, G. R. Diak, T. J. Schmugge, and B. C. W. Tanner (2003), Remote sensing of surface energy fluxes at 10^1-m pixel resolutions, *Water Resour. Res.*, *39*(8), 1221, doi:10.1029/2002WR001775.

Novick, K. A., R. Oren, P. C. Stoy, M. B. S. Siqueira, and G. G. Katul (2009), Nocturnal evapotranspiration in eddy-covariance records from three co-located ecosystems in the southeastern U.S.: Implications for annual fluxes, *Agric. For. Meteorol.*, *149*(9), 1491–1504, doi:10.1016/j.agrformet.2009.04.005.

O'Grady, A. P., D. Eamus, and L. B. Hutley (1999), Transpiration increases during the dry season: Patterns of tree water use in eucalypt open-forests of northern Australia, *Tree Physiol.*, *19*(9), 591–597.

Ohta, T., et al. (2008), Interannual variation of water balance and summer evapotranspiration in an eastern Siberian larch forest over a 7-year period (1998–2006), *Agric. For. Meteorol.*, *148*(12), 1941–1953, doi:10.1016/j.agrformet.2008.04.012.

Oki, T., and S. Kanae (2006), Global hydrological cycles and world water resources, *Science*, *313*(5790), 1068–1072, doi:10.1126/science.1128845.

Oki, T., K. Musiake, H. Matsuyama, and K. Masuda (1995), Global atmospheric water balance and runoff from large river basins, *Hydrol. Processes*, *9*(5–6), 655–678, doi:10.1002/hyp.3360090513.

Oleson, K. W., D. M. Lawrence, G. B. Bonan, M. G. Flanner, and E. Kluzek (2010), Technical description of version 4.0 of the Community Land Model (CLM), *Tech. Note NCAR/TN-478+STR*, 257 pp., Natl. Cent. for Atmos. Res., Boulder, Colo.

Oncley, S. P., et al. (2007), The Energy Balance Experiment EBEX-2000: Part I. Overview and energy balance, *Boundary Layer Meteorol.*, *123*(1), 1–28, doi:10.1007/s10546-007-9161-1.

Overgaard, J., D. Rosbjerg, and M. B. Butts (2006), Land-surface modelling in hydrological perspective—A review, *Biogeosciences*, *3*(2), 229–241, doi:10.5194/bg-3-229-2006.

Parlange, M. B., and G. G. Katul (1992), An advection-aridity evaporation model, *Water Resour. Res.*, *28*(1), 127–132, doi:10.1029/91WR02482.

Parlange, M. B., W. E. Eichinger, and J. D. Albertson (1995), Regional-scale evaporation and the atmospheric boundary layer, *Rev. Geophys.*, *33*(1), 99–124, doi:10.1029/94RG03112.

Parmentier, F. J. W., M. K. van der Molen, R. A. M. de Jeu, D. M. D. Hendriks, and A. J. Dolman (2009), CO_2 fluxes and evaporation on a peatland in the Netherlands appear not affected by water table fluctuations, *Agric. For. Meteorol.*, *149*(6–7), 1201–1208, doi:10.1016/j.agrformet.2008.11.007.

Pauliukonis, N., and R. Schneider (2001), Temporal patterns in evapotranspiration from lysimeters with three common wetland plant species in the eastern United States, *Aquat. Bot.*, *71*(1), 35–46, doi:10.1016/S0304-3770(01)00168-1.

Pauwels, V. R. N., and R. Samson (2006), Comparison of different methods to measure and model actual evapotranspiration rates for a wet sloping grassland, *Agric. Water Manage.*, *82*(1–2), 1–24, doi:10.1016/j.agwat.2005.06.001.

Pauwels, V. R. N., W. Timmermans, and A. Loew (2008), Comparison of the estimated water and energy budgets of a large winter wheat field during AgriSAR 2006 by multiple sensors and models, *J. Hydrol.*, *349*(3–4), 425–440, doi:10.1016/j.jhydrol.2007.11.016.

Peel, M. C., and T. A. McMahon (2006), Continental runoff: A quality-controlled global runoff data set, *Nature*, *444*(7120), E14–E15, doi:10.1038/nature05480.

Pejam, M. R., M. A. Arain, and J. H. McCaughey (2006), Energy and water vapour exchanges over a mixedwood boreal forest in Ontario, Canada, *Hydrol. Processes*, *20*(17), 3709–3724, doi:10.1002/hyp.6384.

Penman, H. L. (1948), Natural evaporation from open water, bare soil and grass, *Proc. R. Soc. London A*, *193*(1032), 120–145, doi:10.1098/rspa.1948.0037.

Peñuelas, J., T. Rutishauser, and I. Filella (2009), Phenology feedbacks on climate change, *Science*, *324*(5929), 887–888, doi:10.1126/science.1173004.

Peterson, T. C., V. S. Golubev, and P. Y. Groisman (1995), Evaporation losing its strength, *Nature*, *377*(6551), 687–688, doi:10.1038/377687b0.

Petropoulos, G., T. N. Carlson, M. J. Wooster, and S. Islam (2009), A review of Ts/VI remote sensing based methods for the retrieval of land surface energy fluxes and soil surface moisture, *Prog. Phys. Geogr.*, *33*(2), 224–250, doi:10.1177/0309133309338997.

Pettijohn, J. C., and G. D. Salvucci (2009), A new two-dimensional physical basis for the complementary relation between terrestrial and pan evaporation, *J. Hydrometeorol.*, *10*(2), 565–574, doi:10.1175/2008JHM1026.1.

Phillips, N., R. Oren, and R. Zimmermann (1996), Radial patterns of xylem sap flow in non-, diffuse- and ring-porous tree species, *Plant Cell Environ.*, *19*(8), 983–990, doi:10.1111/j.1365-3040.1996.tb00463.x.

Phillips, O. L., et al. (2009), Drought sensitivity of the Amazon rainforest, *Science*, *323*(5919), 1344–1347, doi:10.1126/science.1164033.

Piao, S., P. Friedlingstein, and P. Ciais, N. de Noblet-Ducoudré, D. Labat, and S. Zaehle (2007), Changes in climate and land use have a larger direct impact than rising CO_2 on global river runoff trends, *Proc. Natl. Acad. Sci. U. S. A.*, *104*(39), 15,242–15,247.

Pielke, R. A., Sr. (2001), Influence of the spatial distribution of vegetation and soils on the prediction of cumulus convective rainfall, *Rev. Geophys.*, *39*(2), 151–177, doi:10.1029/1999RG000072.

Pielke, R. A., R. Avissar, M. Raupach, A. J. Dolman, X. B. Zeng, and A. S. Denning (1998), Interactions between the atmosphere and terrestrial ecosystems: Influence on weather and climate, *Global Change Biol.*, *4*(5), 461–475, doi:10.1046/j.1365-2486.1998.t01-1-00176.x.

Pitman, A. J. (2003), The evolution of, and revolution in, land surface schemes designed for climate models, *Int. J. Climatol.*, *23*(5), 479–510, doi:10.1002/joc.893.

Pitman, A. J., and A. Henderson-Sellers (1998), Recent progress and results from the project for the intercomparison of landsurface parameterization schemes, *J. Hydrol.*, *212–213*, 128–135, doi:10.1016/S0022-1694(98)00206-6.

Price, J. C. (1990), Using spatial context in satellite data to infer regional scale evapotranspiration, *IEEE Trans. Geosci. Remote Sens.*, *28*(5), 940–948, doi:10.1109/36.58983.

Priestley, C. H. B., and R. J. Taylor (1972), On the assessment of surface heat flux and evaporation using large-scale parameters, *Mon. Weather Rev.*, *100*(2), 81–92, doi:10.1175/1520-0493(1972)100<0081:OTAOSH>2.3.CO;2.

Prince, S. D., S. J. Goetz, R. O. Dubayah, K. P. Czajkowski, and M. Thawley (1998), Inference of surface and air temperature, atmospheric precipitable water and vapor pressure deficit using Advanced Very High-Resolution Radiometer satellite observations: Comparison with field observations, *J. Hydrol.*, *212-213*, 230–249, doi:10.1016/S0022-1694(98)00210-8.

Prueger, J. H., J. L. Hatfield, J. K. Aase, and J. L. Pikul (1997), Bowen-ratio comparisons with lysimeter evapotranspiration, *Agron. J.*, *89*(5), 730–736, doi:10.2134/agronj1997.00021962008900050004x.

Prueger, J. H., J. L. Hatfield, W. P. Kustas, L. E. Hipps, J. I. MacPherson, C. M. U. Neale, W. E. Eichinger, D. I. Cooper, and T. B. Parkin (2005), Tower and aircraft eddy covariance measurements of water vapor, energy, and carbon dioxide fluxes during SMACEX, *J. Hydrometeorol.*, *6*(6), 954–960, doi:10.1175/JHM457.1.

Quattrochi, D. A., and J. C. Luvall (1999), Thermal infrared remote sensing for analysis of landscape ecological processes: Methods and applications, *Landscape Ecol.*, *14*(6), 577–598, doi:10.1023/A:1008168910634.

Ramillien, G., F. Frappart, A. Cazenave, and A. Guntner (2005), Time variations of land water storage from an inversion of 2 years of GRACE geoids, *Earth Planet. Sci. Lett.*, *235*(1–2), 283–301, doi:10.1016/j.epsl.2005.04.005.

Ramírez, J. A., M. T. Hobbins, and T. C. Brown (2005), Observational evidence of the complementary relationship in regional evaporation lends strong support for Bouchet's hypothesis, *Geophys. Res. Lett.*, *32*, L15401, doi:10.1029/2005GL023549.

Rana, G., and N. Katerji (1996), Evapotranspiration measurement for tall plant canopies: The sweet sorghum case, *Theor. Appl. Climatol.*, *54*(3–4), 187–200, doi:10.1007/BF00865161.

Rana, G., and N. Katerji (1998), A measurement based sensitivity analysis of the Penman-Monteith actual evapotranspiration model for crops of different height and in contrasting water status, *Theor. Appl. Climatol.*, *60*(1–4), 141–149, doi:10.1007/s007040050039.

Rana, G., and N. Katerji (2000), Measurement and estimation of actual evapotranspiration in the field under Mediterranean climate: A review, *Eur. J. Agron.*, *13*(2–3), 125–153, doi:10.1016/S1161-0301(00)00070-8.

Rasmusson, E. M. (1967), Atmospheric water vapor transport and the water balance of North America: Part I. Characteristics of the water vapor flux field, *Mon. Weather Rev.*, *95*(7), 403–426, doi:10.1175/1520-0493(1967)095<0403:AWVTAT>2.3.CO;2.

Rasmusson, E. M. (1968), Atmospheric water vapor transport and the water balance of North America, *Mon. Weather Rev.*, *96*(10), 720–734, doi:10.1175/1520-0493(1968)096<0720:AWVTAT>2.0.CO;2.

Rayner, D. P. (2007), Wind run changes: The dominant factor affecting pan evaporation trends in Australia, *J. Clim.*, *20*(14), 3379–3394, doi:10.1175/JCLI4181.1.

Reichle, R. H. (2008), Data assimilation methods in the Earth sciences, *Adv. Water Resour.*, *31*(11), 1411–1418, doi:10.1016/j.advwatres.2008.01.001.

Reichstein, M., et al. (2005), On the separation of net ecosystem exchange into assimilation and ecosystem respiration: Review and improved algorithm, *Global Change Biol.*, *11*(9), 1424–1439, doi:10.1111/j.1365-2486.2005.001002.x.

Richter, I., and S.-P. Xie (2008), Muted precipitation increase in global warming simulations: A surface evaporation perspective, *J. Geophys. Res.*, *113*, D24118, doi:10.1029/2008JD010561.

Rind, D., C. Rosenzweig, and R. Goldberg (1992), Modelling the hydrological cycle in assessments of climate change, *Nature*, *358*(6382), 119–122, doi:10.1038/358119a0.

Roads, J. (2003), The NCEP-NCAR, NCEP-DOE, and TRMM tropical atmosphere hydrologic cycles, *J. Hydrometeorol.*, *4*(5), 826–840, doi:10.1175/1525-7541(2003)004<0826:TNNATT>2.0.CO;2.

Roads, J., and A. Betts (2000), NCEP-NCAR and ECMWF reanalysis surface water and energy budgets for the Mississippi River basin, *J. Hydrometeorol.*, *1*(1), 88–94, doi:10.1175/1525-7541(2000)001<0088:NNAERS>2.0.CO;2.

Robock, A., and H. Li (2006), Solar dimming and CO_2 effects on soil moisture trends, *Geophys. Res. Lett.*, *33*, L20708, doi:10.1029/2006GL027585.

Robock, A., et al. (2003), Evaluation of the North American land data assimilation system over the southern Great Plains during the warm season, *J. Geophys. Res.*, *108*(D22), 8846, doi:10.1029/2002JD003245.

Rodell, M., et al. (2004), The global land data assimilation system, *Bull. Am. Meteorol. Soc.*, *85*(3), 381–394, doi:10.1175/BAMS-85-3-381.

Rodell, M., I. Velicogna, and J. S. Famiglietti (2009), Satellite-based estimates of groundwater depletion in India, *Nature*, *460*(7258), 999–1002, doi:10.1038/nature08238.

Roderick, M. L., and G. D. Farquhar (2002), The cause of decreased pan evaporation over the past 50 years, *Science*, *298*(5597), 1410–1411.

Roderick, M. L., L. D. Rotstayn, G. D. Farquhar, and M. T. Hobbins (2007), On the attribution of changing pan evaporation, *Geophys. Res. Lett.*, *34*, L17403, doi:10.1029/2007GL031166.

Roderick, M. L., M. T. Hobbins, and G. D. Farquhar (2009a), Pan evaporation trends and the terrestrial water balance: II. Energy balance and interpretation, *Geogr. Compass*, *3*(2), 761–780, doi:10.1111/j.1749-8198.2008.00214.x.

Roderick, M. L., M. T. Hobbins, and G. D. Farquhar (2009b), Pan evaporation trends and the terrestrial water balance: I. Principles and observations, *Geogr. Compass*, *3*(2), 746–760, doi:10.1111/j.1749-8198.2008.00213.x.

Rodriguez-Iturbe, I., P. D'Odorico, F. Laio, L. Ridolfi, and S. Tamea (2007), Challenges in humid land ecohydrology: Interactions of water table and unsaturated zone with climate, soil, and vegetation, *Water Resour. Res.*, *43*, W09301, doi:10.1029/2007WR006073.

Rothfuss, Y., P. Biron, I. Braud, L. Canale, J. L. Durand, J. P. Gaudet, P. Richard, M. Vauclin, and T. Bariac (2010), Partitioning evapotranspiration fluxes into soil evaporation and plant transpiration using water stable isotopes under controlled conditions, *Hydrol. Processes*, *24*(22), 3177–3194, doi:10.1002/hyp.7743.

Rudolf, B., et al. (1994), Terrestrial precipitation analysis: Operational method and required density of point measurements, in *Global Precipitations and Climate Change*, *NATO ASI Ser. I*, vol. 26, edited by M. Bubois and F. Désalmand, pp. 173–186, Springer, Berlin.

Sakai, R. K., D. R. Fitzjarrald, and K. E. Moore (2001), Importance of low-frequency contributions to eddy fluxes observed over rough surfaces, *J. Appl. Meteorol.*, *40*(12), 2178–2192, doi:10.1175/1520-0450(2001)040<2178:IOLFCT>2.0.CO;2.

Saleska, S. R., K. Didan, A. R. Huete, and H. R. da Rocha (2007), Amazon forests green-up during 2005 drought, *Science*, *318*(5850), 612, doi:10.1126/science.1146663.

Samanta, A., S. Ganguly, H. Hashimoto, S. Devadiga, E. Vermote, Y. Knyazikhin, R. R. Nemani, and R. B. Myneni (2010), Amazon forests did not green-up during the 2005 drought, *Geophys. Res. Lett.*, *37*, L05401, doi:10.1029/2009GL042154.

Samanta, A., S. Ganguly, and R. B. Myneni (2011), MODIS Enhanced Vegetation Index data do not show greening of Amazon forests during the 2005 drought, *New Phytol.*, *189*(1), 11–15, doi:10.1111/j.1469-8137.2010.03516.x.

Sánchez, J. M., V. Caselles, and E. M. Rubio (2010), Analysis of the energy balance closure over a FLUXNET boreal forest in Finland, *Hydrol. Earth Syst. Sci.*, *14*(8), 1487–1497, doi:10.5194/hess-14-1487-2010.

San José, J., R. Montes, and N. Nikonova (2007), Seasonal patterns of carbon dioxide, water vapour and energy fluxes in pineapple, *Agric. For. Meteorol.*, *147*(1–2), 16–34, doi:10.1016/j.agrformet.2007.06.003.

Santanello, J. A., C. D. Peters-Lidard, S. V. Kumar, C. Alonge, and W.-K. Tao (2009), A modeling and observational framework for diagnosing local land-atmosphere coupling on diurnal time scales, *J. Hydrometeorol.*, *10*(3), 577–599, doi:10.1175/2009JHM1066.1.

Sauer, T. J., J. W. Singer, J. H. Prueger, T. M. DeSutter, and J. L. Hatfield (2007), Radiation balance and evaporation partitioning in a narrow-row soybean canopy, *Agric. For. Meteorol.*, *145*(3–4), 206–214, doi:10.1016/j.agrformet.2007.04.015.

Saugier, B., A. Granier, J. Y. Pontailler, E. Dufrene, and D. D. Baldocchi (1997), Transpiration of a boreal pine forest measured by branch bag, sap flow and micrometeorological methods, *Tree Physiol.*, *17*(8–9), 511–519.

Savage, M. J. (2009), Estimation of evaporation using a dual-beam surface layer scintillometer and component energy balance measurements, *Agric. For. Meteorol.*, *149*(3–4), 501–517, doi:10.1016/j.agrformet.2008.09.012.

Scanlon, B. R., S. W. Tyler, and P. J. Wierenga (1997), Hydrologic issues in arid, unsaturated systems and implications for contaminant transport, *Rev. Geophys.*, *35*(4), 461–490, doi:10.1029/97RG01172.

Schaake, J. C., et al. (2004), An intercomparison of soil moisture fields in the North American Land Data Assimilation System (NLDAS), *J. Geophys. Res.*, *109*, D01S90, doi:10.1029/2002JD003309.

Schapendonk, A. H. C. M., P. Dijkstra, J. Groenwold, C. S. Pot, and S. C. Van De Geijn (1997), Carbon balance and water use efficiency of frequently cut Lolium perenne L. swards at elevated carbon dioxide, *Global Change Biol.*, *3*(3), 207–216, doi:10.1046/j.1365-2486.1997.00099.x.

Schenk, H. J., and R. B. Jackson (2002), The global biography of roots, *Ecol. Monogr.*, *72*(3), 311–328, doi:10.1890/0012-9615(2002)072[0311:TGBOR]2.0.CO;2.

Schenk, H. J., and R. B. Jackson (2005), Mapping the global distribution of deep roots in relation to climate and soil characteristics, *Geoderma*, *126*(1–2), 129–140, doi:10.1016/j.geoderma.2004.11.018.

Schlosser, C. A., and X. Gao (2010), Assessing evapotranspiration estimates from the second Global Soil Wetness Project (GSWP-2) simulations, *J. Hydrometeorol.*, *11*(4), 880–897, doi:10.1175/2010JHM1203.1.

Schmidt, R., et al. (2006), GRACE observations of changes in continental water storage, *Global Planet. Change*, *50*(1–2), 112–126, doi:10.1016/j.gloplacha.2004.11.018.

Schneider, T., P. A. O'Gorman, and X. J. Levine (2010), Water vapor and the dynamics of climate changes, *Rev. Geophys.*, *48*, RG3001, doi:10.1029/2009RG000302.

Schumann, G., P. D. Bates, M. S. Horritt, P. Matgen, and F. Pappenberger (2009), Progress in integration of remote sensing–derived flood extent and stage data and hydraulic models, *Rev. Geophys.*, *47*, RG4001, doi:10.1029/2008RG000274.

Schüttemeyer, D., C. Schillings, A. F. Moene, and H. A. R. De Bruin (2007), Satellite-based actual evapotranspiration over drying semiarid terrain in West Africa, *J. Appl. Meteorol. Climatol.*, *46*(1), 97–111, doi:10.1175/JAM2444.1.

Schwalm, C. R., et al. (2010), A model-data intercomparison of CO_2 exchange across North America: Results from the North American Carbon Program site synthesis, *J. Geophys. Res.*, *115*, G00H05, doi:10.1029/2009JG001229.

Scott, R., D. Entekhabi, R. Koster, and M. Suarez (1997), Timescales of land surface evapotranspiration response, *J. Clim.*, *10*(4), 559–566, doi:10.1175/1520-0442(1997)010<0559:TOLSER>2.0.CO;2.

Scott, R. L., E. A. Edwards, W. J. Shuttleworth, T. E. Huxman, C. Watts, and D. C. Goodrich (2004), Interannual and seasonal variation in fluxes of water and carbon dioxide from a riparian woodland ecosystem, *Agric. For. Meteorol.*, *122*(1–2), 65–84, doi:10.1016/j.agrformet.2003.09.001.

Sellers, P., et al. (1995), The Boreal Ecosystem-Atmosphere Study (Boreas): An overview and early results from the 1994 field year, *Bull. Am. Meteorol. Soc.*, *76*(9), 1549–1577, doi:10.1175/1520-0477(1995)076<1549:TBESAO>2.0.CO;2.

Sellers, P. J., C. J. Tucker, G. J. Collatz, S. O. Los, C. O. Justice, D. A. Dazlich, and D. A. Randall (1996a), A revised land surface parameterization (SiB2) for atmospheric GCMS: Part II. The generation of global fields of terrestrial biophysical parameters from satellite data, *J. Clim.*, *9*(4), 706–737, doi:10.1175/1520-0442(1996)009<0706:ARLSPF>2.0.CO;2.

Sellers, P. J., D. A. Randall, G. J. Collatz, J. A. Berry, C. B. Field, D. A. Dazlich, C. Zhang, G. D. Collelo, and L. Bounoua (1996b), A revised land surface parameterization (SiB2) for atmospheric GCMS: Part I. Model formulation, *J. Clim.*, *9*(4), 676–705, doi:10.1175/1520-0442(1996)009<0676:ARLSPF>2.0.CO;2.

Sellers, P. J., et al. (1997), Modeling the exchanges of energy, water, and carbon between continents and the atmosphere, *Science*, *275*(5299), 502–509, doi:10.1126/science.275.5299.502.

Sen, O. L., W. J. Shuttleworth, and Z.-L. Yang (2000), Comparative evaluation of BATS2, BATS, and SiB2 with Amazon data, *J. Hydrometeorol.*, *1*(2), 135–153, doi:10.1175/1525-7541(2000)001<0135:CEOBBA>2.0.CO;2.

Seneviratne, S. I., D. Luthi, M. Litschi, and C. Schar (2006), Land-atmosphere coupling and climate change in Europe, *Nature*, *443*(7108), 205–209, doi:10.1038/nature05095.

Seneviratne, S. I., T. Corti, E. L. Davin, M. Hirschi, E. B. Jaeger, I. Lehner, B. Orlowsky, and A. J. Teuling (2010), Investigating soil moisture-climate interactions in a changing climate: A review, *Earth Sci. Rev.*, *99*(3–4), 125–161, doi:10.1016/j.earscirev.2010.02.004.

Serraj, R., L. H. Allen, and T. R. Sinclair (1999), Soybean leaf growth and gas exchange response to drought under carbon dioxide enrichment, *Global Change Biol.*, *5*(3), 283–291, doi:10.1046/j.1365-2486.1999.00222.x.

Sheffield, J., E. F. Wood, and F. Munoz-Arriola (2010), Long-term regional estimates of evapotranspiration for Mexico based on downscaled ISCCP data, *J. Hydrometeorol.*, *11*(2), 253–275, doi:10.1175/2009JHM1176.1.

Sherwood, S. C., R. Roca, T. M. Weckwerth, and N. G. Andronova (2010), Tropospheric water vapor, convection, and climate, *Rev. Geophys.*, *48*, RG2001, doi:10.1029/2009RG000301.

Shmakin, A. B., P. C. D. Milly, and K. A. Dunne (2002), Global modeling of land water and energy balances: Part III. Interannual variability, *J. Hydrometeorol.*, *3*(3), 311–321, doi:10.1175/1525-7541(2002)003<0311:GMOLWA>2.0.CO;2.

Shukla, J., and Y. Mintz (1982), Influence of land-surface evapotranspiration on the Earth's climate, *Science*, *215*(4539), 1498–1501, doi:10.1126/science.215.4539.1498.

Shuttleworth, W. J. (1991), Insight from large-scale observational studies of land/atmosphere interactions, *Surv. Geophys.*, *12*(1–3), 3–30, doi:10.1007/BF01903410.

Shuttleworth, W. J. (2007), Putting the "vap" into evaporation, *Hydrol. Earth Syst. Sci.*, *11*(1), 210–244, doi:10.5194/hess-11-210-2007.

Shuttleworth, W. J., and J. S. Wallace (1985), Evaporation from sparse crops—An energy combination theory, *Q. J. R. Meteorol. Soc.*, *111*(469), 839–855, doi:10.1256/smsqj.46909.

Si, J.-H., Q. Feng, X.-Y. Zhang, Z.-Q. Chang, Y.-H. Su, and H.-Y. Xi (2007), Sap flow of *Populus euphratica* in a desert riparian forest in an extreme arid region during the growing season, *J. Integrative Plant Biol.*, *49*(4), 425–436, doi:10.1111/j.1744-7909.2007.00388.x.

Simmons, A. J., K. M. Willett, P. D. Jones, P. W. Thorne, and D. P. Dee (2010), Low-frequency variations in surface atmospheric humidity, temperature, and precipitation: Inferences from reanalyses and monthly gridded observational data sets, *J. Geophys. Res.*, *115*, D01110, doi:10.1029/2009JD012442.

Singh, B., and R. Taillefer (1986), The effect of synoptic-scale advection on the performance of the Priestley-Taylor evaporation formula, *Boundary Layer Meteorol.*, *36*(3), 267–282, doi:10.1007/BF00118664.

Smith, D. M., and S. J. Allen (1996), Measurement of sap flow in plant stems, *J. Exp. Bot.*, *47*(12), 1833–1844, doi:10.1093/jxb/47.12.1833.

Snyder, K. A., J. H. Richards, and L. A. Donovan (2003), Night-time conductance in C_3 and C_4 species: Do plants lose water at night?, *J. Exp. Bot.*, *54*(383), 861–865, doi:10.1093/jxb/erg082.

Sobrino, J. A., M. Gomez, C. Jimenez-Munoz, and A. Olioso (2007), Application of a simple algorithm to estimate daily evapotranspiration from NOAA-AVHRR images for the Iberian Peninsula, *Remote Sens. Environ.*, *110*(2), 139–148, doi:10.1016/j.rse.2007.02.017.

Solignac, P. A., A. Brut, J. L. Selves, J. P. Beteille, J. P. Gastellu-Etchegorry, P. Keravec, P. Beziat, and E. Ceschia (2009), Uncertainty analysis of computational methods for deriving sensible heat flux values from scintillometer measurements, *Atmos. Meas. Tech.*, *2*(2), 741–753, doi:10.5194/amt-2-741-2009.

Sommer, R., T. D. D. Sa, K. Vielhauer, A. C. de Araujo, H. Folster, and P. L. G. Vlek (2002), Transpiration and canopy conductance of secondary vegetation in the eastern Amazon, *Agric. For. Meteorol.*, *112*(2), 103–121, doi:10.1016/S0168-1923(02)00044-8.

Sottocornola, M., and G. Kiely (2010), Energy fluxes and evaporation mechanisms in an Atlantic blanket bog in southwestern Ireland, *Water Resour. Res.*, *46*, W11524, doi:10.1029/2010WR009078.

Stephens, G. L., and T. D. Ellis (2008), Controls of global-mean precipitation increases in global warming GCM experiments, *J. Clim.*, *21*(23), 6141–6155, doi:10.1175/2008JCLI2144.1.

Stewart, J. B. (1988), Modelling surface conductance of pine forest, *Agric. For. Meteorol.*, *43*(1), 19–35, doi:10.1016/0168-1923(88)90003-2.

Stöckli, R., P. L. Vidale, A. Boone, and C. Schär (2007), Impact of scale and aggregation on the terrestrial water exchange: Integrating land surface models and Rhône catchment observations, *J. Hydrometeorol.*, *8*(5), 1002–1015, doi:10.1175/JHM613.1.

Stone, E. L., and P. J. Kalisz (1991), On the maximum extent of tree roots, *For. Ecol. Manage.*, *46*(1–2), 59–102, doi:10.1016/0378-1127(91)90245-Q.

Su, H., M. F. McCabe, E. F. Wood, Z. Su, and J. H. Prueger (2005), Modeling evapotranspiration during SMACEX: Comparing two approaches for local- and regional-scale prediction, *J. Hydrometeorol.*, *6*(6), 910–922, doi:10.1175/JHM466.1.

Su, Z. (2002), The Surface Energy Balance System (SEBS) for estimation of turbulent heat fluxes, *Hydrol. Earth Syst. Sci.*, *6*(1), 85–100, doi:10.5194/hess-6-85-2002.

Su, Z., T. Schmugge, W. P. Kustas, and W. J. Massman (2001), An evaluation of two models for estimation of the roughness height for heat transfer between the land surface and the atmosphere, *J. Appl. Meteorol.*, *40*(11), 1933–1951, doi:10.1175/1520-0450(2001)040<1933:AEOTMF>2.0.CO;2.

Sun, J. L., W. Massman, and D. A. Grantz (1999), Aerodynamic variables in the bulk formulation of turbulent fluxes, *Boundary Layer Meteorol.*, *91*(1), 109–125, doi:10.1023/A:1001838832436.

Sun, L., and C. C. Song (2008), Evapotranspiration from a freshwater marsh in the Sanjiang Plain, northeast China, *J. Hydrol.*, *352*(1–2), 202–210, doi:10.1016/j.jhydrol.2008.01.010.

Sun, X. M., Z. L. Zhu, X. F. Wen, G. F. Yuan, and G. R. Yu (2006), The impact of averaging period on eddy fluxes observed at ChinaFLUX sites, *Agric. For. Meteorol.*, *137*(3–4), 188–193, doi:10.1016/j.agrformet.2006.02.012.

Suyker, A. E., and S. B. Verma (2008), Interannual water vapor and energy exchange in an irrigated maize-based agroecosystem, *Agric. For. Meteorol.*, *148*(3), 417–427, doi:10.1016/j.agrformet.2007.10.005.

Suyker, A. E., and S. B. Verma (2010), Coupling of carbon dioxide and water vapor exchanges of irrigated and rainfed maize-soybean cropping systems and water productivity, *Agric. For. Meteorol.*, *150*(4), 553–563, doi:10.1016/j.agrformet.2010.01.020.

Suzuki, R., K. Masuda, and D. G. Dye (2007), Interannual covariability between actual evapotranspiration and PAL and GIMMS NDVIs of northern Asia, *Remote Sens. Environ.*, *106*(3), 387–398, doi:10.1016/j.rse.2006.10.016.

Swanson, R. H. (1994), Significant historical developments in thermal methods for measuring sap flow in trees, *Agric. For. Meteorol.*, *72*(1–2), 113–132, doi:10.1016/0168-1923(94)90094-9.

Swenson, S. C., and P. C. D. Milly (2006), Climate model biases in seasonality of continental water storage revealed by satellite gravimetry, *Water Resour. Res.*, *42*, W03201, doi:10.1029/2005WR004628.

Swenson, S., and J. Wahr (2002), Methods for inferring regional surface-mass anomalies from Gravity Recovery and Climate Experiment (GRACE) measurements of time-variable gravity, *J. Geophys. Res.*, *107*(B9), 2193, doi:10.1029/2001JB000576.

Syed, T. H., J. S. Famiglietti, J. Chen, M. Rodell, S. I. Seneviratne, P. Viterbo, and C. R. Wilson (2005), Total basin discharge for the Amazon and Mississippi River basins from GRACE and a land-atmosphere water balance, *Geophys. Res. Lett.*, *32*, L24404, doi:10.1029/2005GL024851.

Szilagyi, J. (2001), Modeled areal evaporation trends over the conterminous United States, *J. Irrig. Drain. Eng.*, *127*(4), 196–200, doi:10.1061/(ASCE)0733-9437(2001)127:4(196).

Szilagyi, J., and J. Jozsa (2008), New findings about the complementary relationship-based evaporation estimation methods, *J. Hydrol.*, *354*(1–4), 171–186, doi:10.1016/j.jhydrol.2008.03.008.

Tanaka, N., T. Kume, N. Yoshifuji, K. Tanaka, H. Takizawa, K. Shiraki, C. Tantasirin, N. Tangtham, and M. Suzuki (2008), A review of evapotranspiration estimates from tropical forests in Thailand and adjacent regions, *Agric. For. Meteorol.*, *148*(5), 807–819, doi:10.1016/j.agrformet.2008.01.011.

Tang, R., Z.-L. Li, and B. Tang (2010), An application of the T_s-VI triangle method with enhanced edges determination for evapotranspiration estimation from MODIS data in arid and semi-arid regions: Implementation and validation, *Remote Sens. Environ.*, *114*(3), 540–551, doi:10.1016/j.rse.2009.10.012.

Tanner, C. B. (1960), Energy balance approach to evapotranspiration from crops, *Soil Sci. Soc. Am. Proc.*, *24*, 1–9, doi:10.2136/sssaj1960.03615995002400010012x.

Tapley, B. D., S. Bettadpur, M. Watkins, and C. Reigber (2004a), The Gravity Recovery and Climate Experiment: Mission overview and early results, *Geophys. Res. Lett.*, *31*, L09607, doi:10.1029/2004GL019920.

Tapley, B. D., S. Bettadpur, J. C. Ries, P. F. Thompson, and M. M. Watkins (2004b), GRACE measurements of mass variability in the Earth system, *Science*, *305*(5683), 503–505, doi:10.1126/science.1099192.

Teixeira, A., W. G. M. Bastiaanssen, M. D. Ahmad, and M. G. Bos (2009a), Reviewing SEBAL input parameters for assessing evapotranspiration and water productivity for the Low-Middle São Francisco River basin, Brazil: Part A. Calibration and validation, *Agric. For. Meteorol.*, *149*(3–4), 462–476, doi:10.1016/j.agrformet.2008.09.016.

Teixeira, A., W. G. M. Bastiaanssen, M. D. Ahmad, and M. G. Bos (2009b), Reviewing SEBAL input parameters for assessing evapotranspiration and water productivity for the Low-Middle São Francisco River basin, Brazil: Part B. Application to the regional scale, *Agric. For. Meteorol.*, *149*(3–4), 477–490, doi:10.1016/j.agrformet.2008.09.014.

Teuling, A. J., et al. (2009), A regional perspective on trends in continental evaporation, *Geophys. Res. Lett.*, *36*, L02404, doi:10.1029/2008GL036584.

Timmermans, W. J., W. P. Kustas, M. C. Anderson, and A. N. French (2007), An intercomparison of the surface energy balance algorithm for land (SEBAL) and the two-source energy balance (TSEB) modeling schemes, *Remote Sens. Environ.*, *108*(4), 369–384, doi:10.1016/j.rse.2006.11.028.

Tittebrand, A., A. Schwiebus, and F. H. Berger (2005), The influence of land surface parameters on energy flux densities derived from remote sensing data, *Meteorol. Z.*, *14*(2), 227–236, doi:10.1127/0941-2948/2005/0026.

Tiwari, V. M., J. Wahr, and S. Swenson (2009), Dwindling groundwater resources in northern India, from satellite gravity observations, *Geophys. Res. Lett.*, *36*, L18401, doi:10.1029/2009GL039401.

Todd, R. W., S. R. Evett, and T. A. Howell (2000), The Bowen ratio–energy balance method for estimating latent heat flux of irrigated alfalfa evaluated in a semi-arid, advective environment, *Agric. For. Meteorol.*, *103*(4), 335–348, doi:10.1016/S0168-1923(00)00139-8.

Tognetti, R., A. Giovannelli, A. Lavini, G. Morelli, F. Fragnito, and R. d'Andria (2009), Assessing environmental controls over conductances through the soil-plant-atmosphere continuum in an experimental olive tree plantation of southern Italy, *Agric. For. Meteorol.*, *149*(8), 1229–1243, doi:10.1016/j.agrformet.2009.02.008.

Tolk, J. A., T. A. Howell, and S. R. Evett (2006), Nighttime evapotranspiration from alfalfa and cotton in a semiarid climate, *Agron. J.*, *98*(3), 730–736, doi:10.2134/agronj2005.0276.

Tollefson, F. (2010), Amazon drought raises research doubts, *Nature*, *466*, 423, doi:10.1038/466423a.

Trenberth, K. E., and L. Smith (2005), The mass of the atmosphere: A constraint on global analyses, *J. Clim.*, *18*(6), 864–875, doi:10.1175/JCLI-3299.1.

Trenberth, K. E., J. Fasullo, and L. Smith (2005), Trends and variability in column-integrated atmospheric water vapor, *Clim. Dyn.*, *24*(7–8), 741–758, doi:10.1007/s00382-005-0017-4.

Trenberth, K. E., L. Smith, T. Qian, A. Dai, and J. Fasullo (2007a), Estimates of the global water budget and its annual cycle using observational and model data, *J. Hydrometeorol.*, *8*(4), 758–769, doi:10.1175/JHM600.1.

Trenberth, K. E., et al. (2007b), Observations: Surface and atmospheric climate change, in *Climate Change 2007: The Physical Science Basis—Contribution of Working Group I to the Fourth Assessment Report of the Intergovernmental Panel on Climate Change*, edited by S. Solomon et al., pp. 236–247, Cambridge Univ. Press, Cambridge, U. K.

Trenberth, K. E., J. T. Fasullo, and J. Kiehl (2009), Earth's global energy budget, *Bull. Am. Meteorol. Soc.*, *90*(3), 311–323, doi:10.1175/2008BAMS2634.1.

Tsuang, B.-J., C.-Y. Tu, J.-L. Tsai, J. Dracup, K. Arpe, and T. Meyers (2009), A more accurate scheme for calculating Earth's skin temperature, *Clim. Dyn.*, *32*(2–3), 251–272, doi:10.1007/s00382-008-0479-2.

Twine, T. E., W. P. Kustas, J. M. Norman, D. R. Cook, P. R. Houser, T. P. Meyers, J. H. Prueger, P. J. Starks, and M. L. Wesely (2000), Correcting eddy-covariance flux underestimates over a grassland, *Agric. For. Meteorol.*, *103*(3), 279–300, doi:10.1016/S0168-1923(00)00123-4.

Vano, J. A., J. A. Foley, C. J. Kucharik, and M. T. Coe (2006), Evaluating the seasonal and interannual variations in water balance in northern Wisconsin using a land surface model, *J. Geophys. Res.*, *111*, G02025, doi:10.1029/2005JG000112.

Vaughan, P. J., T. J. Trout, and J. E. Ayars (2007), A processing method for weighing lysimeter data and comparison to micrometeorological ETo predictions, *Agric. Water Manage.*, *88*(1–3), 141–146, doi:10.1016/j.agwat.2006.10.008.

Verhoef, A., B. J. J. M. van den Hurk, A. F. G. Jacobs, and B. G. Heusinkveld (1996), Thermal soil properties for vineyard (EFEDA-I) and savanna (HAPEX-Sahel) sites, *Agric. For. Meteorol.*, *78*(1–2), 1–18, doi:10.1016/0168-1923(95)02254-6.

Verhoef, A., H. A. R. De Bruin, and B. J. J. M. Van Den Hurk (1997), Some practical notes on the parameter kB^{-1} for sparse vegetation, *J. Appl. Meteorol.*, *36*(5), 560–572, doi:10.1175/1520-0450(1997)036<0560:SPNOTP>2.0.CO;2.

Verstraeten, W. W., F. Veroustraete, and J. Feyen (2008), Assessment of evapotranspiration and soil moisture content across different scales of observation, *Sensors*, *8*(1), 70–117, doi:10.3390/s8010070.

Vesala, T., T. Ahonen, P. Hari, E. Krissinel, and N. Shokhirev (1996), Analysis of stomatal CO_2 uptake by a three-dimensional cylindrically symmetric model, *New Phytol.*, *132*(2), 235–245, doi:10.1111/j.1469-8137.1996.tb01843.x.

Vickers, D., M. Gockede, and B. E. Law (2010), Uncertainty estimates for 1-h averaged turbulence fluxes of carbon dioxide, latent heat and sensible heat, *Tellus, Ser. B*, *62*(2), 87–99, doi:10.1111/j.1600-0889.2009.00449.x.

Villarini, G., P. V. Mandapaka, W. F. Krajewski, and R. J. Moore (2008), Rainfall and sampling uncertainties: A rain gauge perspective, *J. Geophys. Res.*, *113*, D11102, doi:10.1029/2007JD009214.

Vonder Haar, T. H., J. M. Forsythe, J. Luo, D. L. Randel, and S. Woo (2005), Water vapor trends and variability from the global NVAP dataset, paper presented at the 16th Symposium on Global Change and Climate Variations, Am. Meteorol. Soc., San Diego, Calif., Jan.

Von Randow, C., B. Kruijt, A. A. M. Holtslag, and M. B. L. de Oliveira (2008), Exploring eddy-covariance and large-aperture scintillometer measurements in an Amazonian rain forest, *Agric. For. Meteorol.*, *148*(4), 680–690, doi:10.1016/j.agrformet.2007.11.011.

Vörösmarty, C. J., and D. Sahagian (2000), Anthropogenic disturbance of the terrestrial water cycle, *BioScience*, *50*(9), 753–765, doi:10.1641/0006-3568(2000)050[0753:ADOTTW]2.0.CO;2.

Vörösmarty, C. J., K. P. Sharma, B. M. Fekete, A. H. Copeland, J. Holden, J. Marble, and J. A. Lough (1997), The storage and aging of continental runoff in large reservoir systems of the world, *Ambio*, *26*(4), 210–219.

Vose, R. S., R. L. Schmoyer, P. M. Steurer, T. C. Peterson, R. Heim, T. R. Karl, and J. K. Eischeid (1992), The Global Historical Climatology Network: Long-term monthly temperature, precipitation, sea level pressure, and station pressure data, *Rep. ORNL/CDIAC-53, NDP-041*, 325 pp., Carbon Dioxide Inf. Anal. Cent., Oak Ridge Natl. Lab., Oak Ridge, Tenn., doi:10.3334/CDIAC/cli.ndp041.

Vourlitis, G. L., N. Priante, M. M. S. Hayashi, J. D. Nogueira, F. T. Caseiro, and J. H. Campelo (2002), Seasonal variations in the evapotranspiration of a transitional tropical forest of Mato Grosso, Brazil, *Water Resour. Res.*, *38*(6), 1094, doi:10.1029/2000WR000122.

Wahr, J., S. Swenson, V. Zlotnicki, and I. Velicogna (2004), Time-variable gravity from GRACE: First results, *Geophys. Res. Lett.*, *31*, L11501, doi:10.1029/2004GL019779.

Wallace, J. S. (1997), Evaporation and radiation interception by neighbouring plants, *Q. J. R. Meteorol. Soc.*, *123*(543), 1885–1905, doi:10.1002/qj.49712354306.

Walter, M. T., D. S. Wilks, J. Y. Parlange, and R. L. Schneider (2004), Increasing evapotranspiration from the conterminous United States, *J. Hydrometeorol.*, *5*(3), 405–408, doi:10.1175/1525-7541(2004)005<0405:IEFTCU>2.0.CO;2.

Wang, A., X. Zeng, S. S. P. Shen, Q.-C. Zeng, and R. E. Dickinson (2006), Time scales of land surface hydrology, *J. Hydrometeorol.*, *7*(5), 868–879, doi:10.1175/JHM527.1.

Wang, G., J. Huang, W. Guo, J. Zuo, J. Wang, J. Bi, Z. Huang, and J. Shi (2010), Observation analysis of land-atmosphere interactions over the Loess Plateau of northwest China, *J. Geophys. Res.*, *115*, D00K17, doi:10.1029/2009JD013372.

Wang, K., and S. Liang (2008), An improved method for estimating global evapotranspiration based on satellite estimation of surface net radiation, vegetation index, temperature, and soil moisture, *J. Hydrometeorol.*, *9*(4), 712–727, doi:10.1175/2007JHM911.1.

Wang, K., and S. L. Liang (2009), Evaluation of ASTER and MODIS land surface temperature and emissivity products using long-term surface longwave radiation observations at SURFRAD sites, *Remote Sens. Environ.*, *113*(7), 1556–1565, doi:10.1016/j.rse.2009.03.009.

Wang, K., Z. Q. Li, and M. Cribb (2006), Estimation of evaporative fraction from a combination of day and night land surface temperatures and NDVI: A new method to determine the Priestley-Taylor parameter, *Remote Sens. Environ.*, *102*(3–4), 293–305, doi:10.1016/j.rse.2006.02.007.

Wang, K., Z. Wan, P. Wang, M. Sparrow, J. Liu, and S. Haginoya (2007a), Evaluation and improvement of the MODIS land surface temperature/emissivity products using ground-based measurements at a semi-desert site on the western Tibetan Plateau, *Int. J. Remote Sens.*, *28*(11), 2549–2565, doi:10.1080/01431160600702665.

Wang, K., P. Wang, Z. Q. Li, M. Cribb, and M. Sparrow (2007b), A simple method to estimate actual evapotranspiration from a combination of net radiation, vegetation index, and temperature, *J. Geophys. Res.*, *112*, D15107, doi:10.1029/2006JD008351.

Wang, K., R. E. Dickinson, and S. L. Liang (2008), Observational evidence on the effects of clouds and aerosols on net ecosystem exchange and evapotranspiration, *Geophys. Res. Lett.*, *35*, L10401, doi:10.1029/2008GL034167.

Wang, K., R. E. Dickinson, M. Wild, and S. Liang (2010a), Evidence for decadal variation in global terrestrial evapotranspiration between 1982 and 2002: 2. Results, *J. Geophys. Res.*, *115*, D20113, doi:10.1029/2010JD013847.

Wang, K., R. E. Dickinson, M. Wild, and S. Liang (2010b), Evidence for decadal variation in global terrestrial evapotranspiration between 1982 and 2002: 1. Model development, *J. Geophys. Res.*, *115*, D20112, doi:10.1029/2009JD013671.

Wang, L. X., K. K. Caylor, J. C. Villegas, G. A. Barron-Gafford, D. D. Breshears, and T. E. Huxman (2010), Partitioning evapotranspiration across gradients of woody plant cover: Assessment of a stable isotope technique, *Geophys. Res. Lett.*, *37*, L09401, doi:10.1029/2010GL043228.

Wang, S. S., Y. Yang, A. P. Trishchenko, A. G. Barr, T. A. Black, and H. McCaughey (2009), Modeling the response of canopy stomatal conductance to humidity, *J. Hydrometeorol.*, *10*(2), 521–532, doi:10.1175/2008JHM1050.1.

Wang, Y.-P., and B. Z. Houlton (2009), Nitrogen constraints on terrestrial carbon uptake: Implications for the global carbon-climate feedback, *Geophys. Res. Lett.*, *36*, L24403, doi:10.1029/2009GL041009.

Way, D. A., R. Oren, H.-S. Kim, and G. G. Katul (2011), How well do stomatal conductance models perform on closing plant carbon budgets? A test using seedlings grown under current and elevated air temperatures, *J. Geophys. Res.*, *116*, G04031, doi:10.1029/2011JG001808.

Wayne, P. M., E. G. Reekie, and F. A. Bazzaz (1998), Elevated CO_2 ameliorates birch response to high temperature and frost stress: Implications for modeling climate-induced geographic range shifts, *Oecologia*, *114*(3), 335–342, doi:10.1007/s004420050455.

Wentz, F. J., and M. Schabel (2000), Precise climate monitoring using complementary satellite data sets, *Nature*, *403*(6768), 414–416, doi:10.1038/35000184.

Wentz, F. J., L. Ricciardulli, K. Hilburn, and C. Mears (2007), How much more rain will global warming bring?, *Science*, *317*(5835), 233–235.

Were, A., L. Villagarcia, F. Domingo, L. Alados-Arboledas, and J. Puigdefabregas (2007), Analysis of effective resistance calculation methods and their effect on modelling evapotranspiration in two different patches of vegetation in semi-arid SE Spain, *Hydrol. Earth Syst. Sci.*, *11*(5), 1529–1542, doi:10.5194/hess-11-1529-2007.

Werth, D., and R. Avissar (2004), The regional evapotranspiration of the Amazon, *J. Hydrometeorol.*, *5*(1), 100–109, doi:10.1175/1525-7541(2004)005<0100:TREOTA>2.0.CO;2.

Werth, S., and A. Güntner (2010), Calibration analysis for water storage variability of the global hydrological model WGHM, *Hydrol. Earth Syst. Sci.*, *14*(1), 59–78, doi:10.5194/hess-14-59-2010.

Werth, S., A. Guntner, R. Schmidt, and J. Kusche (2009), Evaluation of GRACE filter tools from a hydrological perspective, *Geophys. J. Int.*, *179*(3), 1499–1515, doi:10.1111/j.1365-246X.2009.04355.x.

Wieringa, J. (1980), A revaluation of the Kansas mast influence on measurements of stress and cup anemometer overspeeding, *Boundary Layer Meteorol.*, *18*(4), 411–430, doi:10.1007/BF00119497.

Wiernga, J. (1993), Representative roughness parameters for homogeneous terrain, *Boundary Layer Meteorol.*, *63*(4), 323–363, doi:10.1007/BF00705357.

Wild, M., and B. Liepert (2010), The Earth radiation balance as driver of the global hydrological cycle, *Environ. Res. Lett.*, *5*(2), 025203, doi:10.1088/1748-9326/5/2/025203.

Willett, K. M., N. P. Gillett, P. D. Jones, and P. W. Thorne (2007), Attribution of observed surface humidity changes to human influence, *Nature*, *449*(7163), 710–712, doi:10.1038/nature06207.

Willett, K. M., P. D. Jones, N. P. Gillett, and P. W. Thorne (2008), Recent changes in surface humidity: Development of the HadCRUH dataset, *J. Clim.*, *21*(20), 5364–5383, doi:10.1175/2008JCLI2274.1.

Williams, D. G., et al. (2004), Evapotranspiration components determined by stable isotope, sap flow and eddy covariance techniques, *Agric. For. Meteorol.*, *125*(3–4), 241–258, doi:10.1016/j.agrformet.2004.04.008.

Wilson, K. B., and D. D. Baldocchi (2000), Seasonal and interannual variability of energy fluxes over a broadleaved temperate deciduous forest in North America, *Agric. For. Meteorol.*, *100*(1), 1–18, doi:10.1016/S0168-1923(99)00088-X.

Wilson, K. B., P. J. Hanson, P. J. Mulholland, D. D. Baldocchi, and S. D. Wullschleger (2001), A comparison of methods for determining forest evapotranspiration and its components: Sap-flow, soil water budget, eddy covariance and catchment water balance, *Agric. For. Meteorol.*, *106*(2), 153–168, doi:10.1016/S0168-1923(00)00199-4.

Wilson, K., et al. (2002), Energy balance closure at FLUXNET sites, *Agric. For. Meteorol.*, *113*(1–4), 223–243, doi:10.1016/S0168-1923(02)00109-0.

Witte, J.-P. M., B. Kruijt, and K. Maas (2006), The effects of rising CO_2 levels on evapotranspiration, *Rep. KWR 06.004*, 59 pp., Kiwa Nederland, Nieuwegein, Netherlands.

Wohlfahrt, G., A. Haslwanter, L. Hortnagl, R. L. Jasoni, L. F. Fenstermaker, J. A. Arnone, and A. Hammerle (2009), On the consequences of the energy imbalance for calculating surface conductance to water vapour, *Agric. For. Meteorol.*, *149*(9), 1556–1559, doi:10.1016/j.agrformet.2009.03.015.

Wolf, A., N. Saliendra, K. Akshalov, D. A. Johnson, and E. Laca (2008), Effects of different eddy covariance correction schemes on an energy balance closure and comparisons with the modified Bowen ratio system, *Agric. For. Meteorol.*, *148*(6–7), 942–952, doi:10.1016/j.agrformet.2008.01.005.

World Meteorological Organization (WMO) (2008), Measurement of evaporation, in *WMO Guide to Meteorological Instruments and Methods of Observation*, 7th ed., chap. 10, pp. I10-1–I10-10, Geneva, Switzerland. [Available at http://www.wmo.int/pages/prog/www/IMOP/publications/CIMO-Guide/CIMO_Guide-7th_Edition-2008.html.]

Xie, P., and P. A. Arkin (1996), Analyses of global monthly precipitation using gauge observations, satellite estimates, and numerical model predictions, *J. Clim.*, *9*(4), 840–858, doi:10.1175/1520-0442(1996)009<0840:AOGMPU>2.0.CO;2.

Xu, C. Y., and V. P. Singh (2005), Evaluation of three complementary relationship evapotranspiration models by water balance approach to estimate actual regional evapotranspiration in different climatic regions, *J. Hydrol.*, *308*(1–4), 105–121, doi:10.1016/j.jhydrol.2004.10.024.

Xu, C. Y., L. B. Gong, T. Jiang, D. L. Chen, and V. P. Singh (2006), Analysis of spatial distribution and temporal trend of reference evapotranspiration and pan evaporation in Changjiang (Yangtze River) catchment, *J. Hydrol.*, *327*(1–2), 81–93, doi:10.1016/j.jhydrol.2005.11.029.

Yan, H., and H. H. Shugart (2010), An air relative-humidity-based evapotranspiration model from eddy covariance data, *J. Geophys. Res.*, *115*, D16106, doi:10.1029/2009JD013598.

Yang, D. Q., D. Kane, Z. P. Zhang, D. Legates, and B. Goodison (2005), Bias corrections of long-term (1973–2004) daily precipitation data over the northern regions, *Geophys. Res. Lett.*, *32*, L19501, doi:10.1029/2005GL024057.

Yang, D. W., F. B. Sun, Z. T. Liu, Z. T. Cong, and Z. D. Lei (2006), Interpreting the complementary relationship in non-humid environments based on the Budyko and Penman hypotheses, *Geophys. Res. Lett.*, *33*, L18402, doi:10.1029/2006GL027657.

Yang, F. H., M. A. White, A. R. Michaelis, K. Ichii, H. Hashimoto, P. Votava, A. X. Zhu, and R. R. Nemani (2006), Prediction of continental-scale evapotranspiration by combining MODIS and AmeriFlux data through support vector machine, *IEEE Trans. Geosci. Remote Sens.*, *44*(11), 3452–3461, doi:10.1109/TGRS.2006.876297.

Yang, K., and T. Koike (2005), A general model to estimate hourly and daily solar radiation for hydrological studies, *Water Resour. Res.*, *41*, W10403, doi:10.1029/2005WR003976.

Yang, K., T. Koike, H. Ishikawa, and Y. M. Ma (2004), Analysis of the surface energy budget at a site of GAME/Tibet using a single-source model, *J. Meteorol. Soc. Jpn.*, *82*(1), 131–153, doi:10.2151/jmsj.82.131.

Yang, K., Y. Y. Chen, and J. Qin (2009), Some practical notes on the land surface modeling in the Tibetan Plateau, *Hydrol. Earth Syst. Sci.*, *13*(5), 687–701, doi:10.5194/hess-13-687-2009.

Yang, Z. (2004), Modeling land surface processes in short-term weather and climate studies, in *Observations, Theory, and Modeling of Atmospheric Variability*, edited by X. Zhu, pp. 288–313, World Sci., Singapore.

Yaseef, N. R., D. Yakir, E. Rotenberg, G. Schiller, and S. Cohen (2010), Ecohydrology of a semi-arid forest: Partitioning among water balance components and its implications for predicted precipitation changes, *Ecohydrology*, *3*(2), 143–154.

Ye, B., D. Yang, Y. Ding, T. Han, and T. Koike (2004), A bias-corrected precipitation climatology for China, *J. Hydrometeorol.*, *5*(6), 1147–1160, doi:10.1175/JHM-366.1.

Yeh, P. J. F., and J. S. Famiglietti (2008), Regional terrestrial water storage change and evapotranspiration from terrestrial and atmospheric water balance computations, *J. Geophys. Res.*, *113*, D09108, doi:10.1029/2007JD009045.

Yeh, P. J. F., M. Irizarry, and E. A. B. Eltahir (1998), Hydroclimatology of Illinois: A comparison of monthly evaporation estimates based on atmospheric water balance and soil water balance, *J. Geophys. Res.*, *103*, 19,823–19,837, doi:10.1029/98JD01721.

Young, M. H., P. J. Wierenga, and C. F. Mancino (1996), Large weighing lysimeters for water use and deep percolation studies, *Soil Sci.*, *161*(8), 491–501, doi:10.1097/00010694-199608000-00004.

Yuan, W., S. Liu, H. Liu, J. T. Randerson, G. Yu, and L. L. Tieszen (2010), Impacts of precipitation seasonality and ecosystem types on evapotranspiration in the Yukon River Basin, Alaska, *Water Resour. Res.*, *46*, W02514, doi:10.1029/2009WR008119.

Zaehle, S., P. Friedlingstein, and A. D. Friend (2010), Terrestrial nitrogen feedbacks may accelerate future climate change, *Geophys. Res. Lett.*, *37*, L01401, doi:10.1029/2009GL041345.

Zaitchik, B. F., M. Rodell, and F. Olivera (2010), Evaluation of the Global Land Data Assimilation System using global river discharge data and a source-to-sink routing scheme, *Water Resour. Res.*, *46*, W06507, doi:10.1029/2009WR007811.

Zeggaf, A. T., S. Takeuchi, H. Dehghanisanij, H. Anyoji, and T. Yano (2008), A Bowen ratio technique for partitioning energy fluxes between maize transpiration and soil surface evaporation, *Agron. J.*, *100*(4), 988–996, doi:10.2134/agronj2007.0201.

Zeng, N., J. D. Neelin, K. M. Lau, and C. J. Tucker (1999), Enhancement of interdecadal climate variability in the sahel by vegetation interaction, *Science*, *286*(5444), 1537–1540, doi:10.1126/science.286.5444.1537.

Zeng, X. (2001), Global vegetation root distribution for land modeling, *J. Hydrometeorol.*, *2*(5), 525–530, doi:10.1175/1525-7541(2001)002<0525:GVRDFL>2.0.CO;2.

Zeppel, M., C. Macinnis-Ng, C. Ford, and D. Eamus (2008), The response of sap flow to pulses of rain in a temperate Australian woodland, *Plant Soil*, *305*(1–2), 121–130, doi:10.1007/s11104-007-9349-7.

Zeweldi, D. A., M. Gebremichael, J. M. Wang, T. Sammis, J. Kleissl, and D. Miller (2010), Intercomparison of sensible heat flux from large aperture scintillometer and eddy covariance methods: Field experiment over a homogeneous semi-arid region, *Boundary Layer Meteorol.*, *135*(1), 151–159, doi:10.1007/s10546-009-9460-9.

Zha, T., A. G. Barr, G. van der Kamp, T. A. Black, J. H. McCaughey, and L. B. Flanagan (2010), Interannual variation of evapotranspiration from forest and grassland ecosystems in western Canada in relation to drought, *Agric. For. Meteorol.*, *150*(11), 1476–1484, doi:10.1016/j.agrformet.2010.08.003.

Zhan, X., W. P. Kustas, and K. S. Humes (1996), An intercomparison study on models of sensible heat flux over partial canopy surfaces with remotely sensed surface temperature, *Remote Sens. Environ.*, *58*(3), 242–256, doi:10.1016/S0034-4257(96)00049-1.

Zhang, G., G. M. Zeng, Y. M. Jiang, G. H. Huang, J. B. Li, J. M. Yao, W. Tan, R. Xiang, and X. L. Zhang (2006), Modelling and measurement of two-layer-canopy interception losses in a subtropical evergreen forest of central-south China, *Hydrol. Earth Syst. Sci.*, *10*(1), 65–77, doi:10.5194/hess-10-65-2006.

Zhang, X. D., X. H. Jia, J. Y. Yang, and L. B. Hu (2010), Evaluation of MOST functions and roughness length parameterization on sensible heat flux measured by large aperture scintillometer over a corn field, *Agric. For. Meteorol.*, *150*(9), 1182–1191, doi:10.1016/j.agrformet.2010.05.003.

Zhang, Y., R. Leuning, L. B. Hutley, J. Beringer, I. McHugh, and J. P. Walker (2010), Using long-term water balances to parameterize surface conductances and calculate evaporation at 0.05° spatial resolution, *Water Resour. Res.*, *46*, W05512, doi:10.1029/2009WR008716.

Zhang, Z. Z., B. F. Chao, Y. Lu, and H. T. Hsu (2009), An effective filtering for GRACE time-variable gravity: Fan filter, *Geophys. Res. Lett.*, *36*, L17311, doi:10.1029/2009GL039459.

Zhao, M., and S. W. Running (2010), Drought-induced reduction in global terrestrial net primary production from 2000 through 2009, *Science*, *329*(5994), 940–943, doi:10.1126/science.1192666.

Zhao, M., F. A. Heinsch, R. R. Nemani, and S. W. Running (2005), Improvements of the MODIS terrestrial gross and net primary production global data set, *Remote Sens. Environ.*, *95*(2), 164–176, doi:10.1016/j.rse.2004.12.011.

Zhao, W. Z., X. B. Ji, E. S. Kang, Z. H. Zhang, and B. W. Jin (2010a), Evaluation of Penman-Monteith model applied to a maize field in the arid area of northwest China, *Hydrol. Earth Syst. Sci.*, *14*(7), 1353–1364, doi:10.5194/hess-14-1353-2010.

Zhao, X. S., Y. B. Liu, H. Tanaka, and T. Hiyama (2010b), A comparison of flux variance and surface renewal methods with eddy covariance, *Select. Topics Appl. Earth Observ. Remote Sens.*, *3*(3), 345–350, doi:10.1109/JSTARS.2010.2060473.

Zhou, L. M., C. J. Tucker, R. K. Kaufmann, D. Slayback, N. V. Shabanov, and R. B. Myneni (2001), Variations in northern vegetation activity inferred from satellite data of vegetation index during 1981 to 1999, *J. Geophys. Res.*, *106*(D17), 20,069–20,083, doi:10.1029/2000JD000115.

Zhu, Z., X. Sun, and R. Zhang (2003), Spatial analysis and comparative study of energy balance components estimated using micrometeorological technique during HUBEX/IOP 1998/1999, *Adv. Atmos. Sci.*, *20*, 285–291.

Zveryaev, II, and R. P. Allan (2010), Summertime precipitation variability over Europe and its links to atmospheric dynamics and evaporation, *J. Geophys. Res.*, *115*, D12102, doi:10/1029/2008JD011213.